NOVA SCHOOL OF SCIENCE & TECHNOLOGY

DEPARTAMENT OF CHEMISTRY

CASPR2 AUTOIMMUNE ANTIBODIES MODIFY THE DEVELOPMENTAL TRAJECTORY AND NETWORK ACTIVITY IN HUMAN BRAIN ORGANOIDS

ANA RAFAELA GOMES SOARES OLIVEIRA

Master in Cellular and Molecular Biology

DOCTORATE IN BIOENGINEERING SYSTEMS (MIT-PORTUGAL)

NOVA University Lisbon
March, 2023

DEPARTAMENT OF
CHEMISTRY

NOVA SCHOOL OF
SCIENCE & TECHNOLOGY

CASPR2 AUTOIMMUNE ANTIBODIES MODIFY THE DEVELOPMENTAL TRAJECTORY AND NETWORK ACTIVITY IN HUMAN BRAIN ORGANOIDS

Master in Cellular and Molecular Biology

ANA RAFAELA GOMES SOARES OLIVEIRA

Adviser: João Miguel Peça Lima Novo Silvestre
Assistant Professor, Faculty of Science and Technology, University of Coimbra

Co-advisers: Lino da Silva Ferreira
Full Professor, Faculty of Medicine, University of Coimbra

João Paulo Serejo Goulão Crespo
Full Professor, NOVA University Lisbon

Examination Committee:

Chair: Pedro Miguel Ribeiro Viana Baptista,
Full Professor, Faculty of Science and Technology, NOVA University Lisbon

Rapporteurs: Liliana Simões Mendonça,
Assistant Researcher, Center for Neuroscience and Cell Biology, University of Coimbra

Maria José de Oliveira Diógenes Nogueira,
Associate Professor with Habilitation, Faculty of Medicine, University of Lisbon

Adviser: João Miguel Peça Lima Novo Silvestre,
Assistant Professor, Faculty of Science and Technology, University of Coimbra

Members: Luís Fernando Morgado Pereira de Almeida,
Associate Professor, Faculty of Pharmacy, University of Coimbra

DOCTORATE IN BIOENGINEERING SYSTEMS (MIT-PORTUGAL)

NOVA University Lisbon
March, 2023

CASPR2 autoimmune antibodies modify the developmental trajectory and network activity in human brain organoids.

This work was conducted at the Center for Neuroscience and Cell Biology (CNC) of University of Coimbra, under the scientific supervision of Doctor João Miguel Peça Lima Novo Silvestre, Principal Investigator at the Center for Neuroscience and Cell Biology and Assistant Professor at the Department for Life Sciences, Faculty of Science and Technology, University of Coimbra, and Doctor Lino da Silva Ferreira, Principal Investigator at the UC-Biotech and Full Professor at the Faculty of Medicine, University of Coimbra.

Ana Rafaela Gomes Soares Oliveira was supported by a fellowship (PD/BD/139074/2018) awarded by the MIT-Portugal PhD Program in Bioengineering Systems and funded by the Portuguese Foundation of Science and Technology (FCT).

This project has received funding from the European Union's Horizon 2020 research and innovation programme under grant agreement 799164 and 813986 and by the European Regional Development Fund (ERDF), through the Centro 2020 and through the COMPETE 2020 - Operational Programme for Competitiveness and Internationalisation and Portuguese national funds via FCT – Fundação para a Ciência e a Tecnologia, under project UIDB/04539/2020. This work was further supported by Pfizer Award 2019 and a 2020 IBRO Early Career Award.

Aos meus pais.

Ao João.

ACKNOWLEDGMENTS

Primeiramente um agradecimento ao meu orientador, Professor João Peça, que acreditou em mim para o desenvolvimento deste projeto. Um projeto ambicioso, com culturas ambiciosas e em início de implementação no laboratório. Obrigada pelo apoio nestes anos e pela transmissão de conhecimento, que irá certamente acompanhar-me ao longo da minha carreira.

Um agradecimento aos meus coorientadores, Professor Lino Ferreira e Professor João Paulo Crespo, por se terem mostrado sempre disponíveis e dispostos a ajudar no que fosse preciso, agilizando e facilitando todos os processos.

À Bárbara, que foi incansável e uma grande ajuda na agilização de todos os processos. A sua ajuda foi preciosa!

Um agradecimento a TODOS os membros do Grupo de Circuitos Neuronais e Comportamento! Somos todos tão diferentes, mas se houve coisa que notei nos últimos anos é que se for preciso algo, vocês estão ali para ajudar. Um agradecimento especial à Ana Luísa Cardoso, que já me acompanha a alguns anos e por quem tenho um carinho especial. Continua a ser bom aprender contigo! Um grande obrigada à Catarina Seabra, pela ajuda e motivação ao longo destes anos, por ser uma ótima comunicadora de ciência, uma ótima ouvinte, e por perceber os mil e um lados da mesma moeda. Quero também agradecer à Joana Guedes por toda a ajuda ao longo deste percurso, por ser tão crítica, por estar disposta a pensar connosco e nos ajudar a questionar coisas que não questionaríamos. *Thank you ephys mom!* Obrigada ao Giuseppe por toda a ajuda nas experiências de cálcio e pela partilha de dores conjuntas. *I wish you the best, Giuseppe!* Obrigada à Ana Maria Cardoso pela grande ajuda nos qPCRs e pelo seu apoio nos últimos anos deste meu doutoramento. Obrigada à Mariana Martins por ser um amor de pessoa, sempre disposta a ajudar e a lamentar por o que de mal nos possa ter acontecido. Obrigada à Solange pelo apoio nos últimos tempos e pelo entusiasmo com estes nossos organoides. Reis, Mário, Marcos, Pedro, Marta, Carolina, Sara obrigada pelos bons momentos e pelas partilhas de outras tantas angústias. Minha Jess e minha Marianinha, agora bem que podia passar aqui o dia a escrever...vocês são incríveis! São as amigas que qualquer pessoa pode querer e eu quero muito manter-vos na minha vida. Venham os brunches, venham almoços, lanches ou jantares, mas a verdade é que nunca terei palavras para vos agradecer todo o apoio, ajuda e amizade.

Um agradecimento muito especial à Dominique por todo o conhecimento que me passou sobre a CASPR2 e por ser uma companheira de secretária à altura. À Ângela pela disponibilidade e ajuda na eletrofisiologia. À Gladys, ao Moh, tenho uma estima

gigante por vocês. E um agradecimento a todos os elementos do Grupo da Professora Ana Luísa e Professor Carlos Duarte. Foram, sem dúvida, anos de boas partilhas e boas caminhadas!

Obrigado Gonçalo Teixeira e Rita Sá Ferreira por me terem ajudado com todas as questões relacionadas com o processo de submissão, desde as reuniões da CAT, à própria submissão da tese. Foram incríveis!

Às minhas princesas lindas. Andreia, Beatriz, Carina, Inês Gomes, Joana, Laetitia, Madalena, Marina, Marta, Rafa 2 e Raquel, obrigada por terem aparecido na minha vida e terem continuado. Obrigado por me ouvirem e por me apoiarem sempre, por saberem o que dizer e quando dizer. Obrigada por me mostrarem que os amigos a sério existem mesmo e que estão presentes nos bons e maus momentos. Obrigada à Ju, à Filipa e à Rita, por mesmo longe estarem sempre perto. Obrigada, Inês Santos e João Nunes por me aturarem há tantos anos e por me continuarem a ouvir falar de ciência. A todos, um mega obrigado pela vossa amizade.

Quero agradecer aos meus pais, e também ao meu irmão, pelo voto de confiança que me dão todos os dias, por me deixarem sempre à vontade nas minhas decisões e por me apoiarem em TUDO. Por se orgulharem de mim todos os dias, tanto como me orgulho da educação que me deram. Adoro-vos!

Ao João! O meu João que tanto se irrita comigo pela minha obsessão com o trabalho, mas que tanto me apoia e tanto me ajuda a crescer. Estar aqui hoje é muito graças ao teu incentivo e à tua motivação. Obrigada pelos teus constantes empurrões, chamadas de atenção, para que eu perceba que sou capaz de muito. Um obrigada não chega!

A todos estes, e àqueles que não mencionei mas que sabem o quão foram e são importantes, mil obrigadas por me ajudarem a concretizar mais um projeto desafiante e muito enriquecedor.

"Research is seeing what everybody else has seen and thinking what nobody else has thought."
Albert Szent-Györgyi

ABSTRACT

Recent decades have seen great expansion on our understanding on how neurons communicate and process information, however, limited access to human brain samples is a critical aspect preventing a greater understanding on the cellular and molecular mechanisms underlying brain diseases. Additionally, animal models and *in vitro* two-dimensional (2D) cell cultures fail to mimic the unique cellular and molecular physiology of the human brain. Recently, the development of human brain organoids has presented a new tool that may facilitate the study of functional human synapses and neuronal networks, that may further our understanding of disease mechanisms.

Gestational transfer of brain-reactive antibodies is an important environmental risk factor triggering neurodevelopmental disorders. CASPR2 is encoded by *CNTNAP2*, an autism susceptibility gene and is a known target for pathogenic maternal autoantibodies that can interfere with fetal neurodevelopment. CASPR2 was originally described to be involved in the stabilization of voltage-gated potassium channels (Kv1.1 and Kv1.2) in myelinated axons, and later to have a role in earlier phases of rodent brain development. However, the effects induced by the presence of anti-CASPR2 antibodies (anti-CASPR2-Ab) during human brain development have not yet been addressed.

To tackle this gap in knowledge we cultured human brain organoids for a period of up to 6-months in media containing human anti-CASPR2-Ab. We found that this challenge produced a decrease in CASPR2 and Contactin-2 protein levels, altered spontaneous synaptic activity, and led to an increase in the frequency of action potential firing upon current injection. These alterations were consistent with change in action potential kinetics, suggestive of altered function in voltage-gated potassium channels. In line with these observations, we also observed an overall increase in network activity in acute brain organoid slices.

In parallel with this work, we also produced brain organoids from human induced pluripotent stem cells (hiPSCs) generated *de novo* from individuals carrying a genetic mutation associated with a neurological disease. The resulting mutated organoids recapitulated the genetic and molecular features of the original patients' cells and offer a platform for further studying the mechanisms associated with the disease.

Therefore, our data highlights the value of using brain organoids as robust models to study brain development and neurological disorders. These models may ultimately allow us to interpret the underlying neurobiological mechanisms associated with several disorders and lay the groundwork for identifying and testing novel therapeutic approaches.

Keywords: neurodevelopmental disorders, hiPSCs, reprogramming, human brain models, brain organoids, anti-CASPR2 antibodies, Kv1 channel dysfunction, neuronal excitability.

RESUMO

Nas últimas décadas temos visto uma grande expansão na nossa compreensão sobre como os neurónios comunicam e processam informação, no entanto, o acesso limitado a amostras de cérebro humano é um aspeto crítico que impede uma maior compreensão sobre os mecanismos celulares e moleculares subjacente às doenças cerebrais. Adicionalmente, modelos animais e culturas celulares bidimensionais (2D) *in vitro* não conseguem mimetizar a fisiologia celular e molecular única do cérebro humano. Recentemente, o desenvolvimento de organoides cerebrais humanos tem apresentado uma nova ferramenta que pode facilitar o estudo de sinapses humanas funcionais e redes neuronais, o que pode aprofundar a nossa compreensão dos mecanismos da doença.

A transferência gestacional de anticorpos cerebrais reativos é um importante fator de risco ambiental que pode desencadear doenças do neurodesenvolvimento. CASPR2 é codificada por *CNTNAP2*, um gene de suscetibilidade ao autismo, e é um alvo conhecido de autoanticorpos maternos patogénicos que podem interferir com o neurodesenvolvimento do feto. CASPR2 foi inicialmente descrita como estando envolvida na estabilização dos canais de potássio sensíveis à voltagem (Kv1.1 e Kv1.2) nos axónios mielinizados e, mais tarde, por ter um papel em fases mais precoces do desenvolvimento do cérebro de ratinhos. No entanto, os efeitos induzidos pela presença de anticorpos anti-CASPR2 (anti-CASPR2-Ab) durante o desenvolvimento do cérebro humano ainda não foram estudados.

Para resolver esta lacuna no conhecimento, cultivámos organoides cerebrais humanos por um período de até 6 meses em meio contendo anti-CASPR2-Ab humanos. Descobrimos que este desafio levou a uma diminuição nos níveis de proteína CASPR2 e Contactin-2, alterou a atividade sináptica espontânea e levou a um aumento na frequência de disparo de potenciais de ação após injeção de corrente. Estas alterações foram consistentes com alteração na cinética dos potenciais de ação, sugestivo de alteração na função dos canais de potássio sensíveis à voltagem. Em linha com estas observações, também observámos um aumento geral na atividade de rede em fatias de organoides cerebrais.

Em paralelo a este trabalho, também produzimos organoides cerebrais humanos a partir de células estaminais pluripotentes induzidas (hiPSCs) obtidas *de novo* de indivíduos portadores de uma mutação genética associada a uma doença neurológica. Os organoides resultantes recapitularam as características genéticas e moleculares das

células originais dos doentes e oferecem uma plataforma para estudar mais aprofundadamente os mecanismos associados à doença.

Deste modo, os nossos resultados destacam o valor do uso de organoides cerebrais como modelos robustos para estudar o desenvolvimento cerebral e distúrbios neurológicos. Estes modelos podem, em última análise, permitir-nos interpretar os mecanismos neurobiológicos subjacentes associados a várias doenças e fundamentar para a identificação e testagem de novas abordagens terapêuticas.

Palavras-chave: doenças do neurodesenvolvimento, hiPSCs, reprogramação, modelos de cérebro humano, organoides cerebrais, anticorpos anti-CASPR2, disfunção de canais Kv1, excitabilidade neuronal.

CONTENTS

LIST OF FIGURES

Chapter 5

LIST OF TABLES

ABBREVIATIONS

2D – Two-dimensional

3D – Three-dimensional

aCSF – Artificial cerebrospinal fluid

ADAM – Disintegrin and Metalloproteinase domain-containing protein

ADHD – Attention deficit hyperactivity disorder

AIS – Axon initial segment

ALI-Cos – Air-liquid interface cerebral organoids

AMPARs – α-amino-3-hydroxy-5-methylisoxazole-4-propionic acid (AMPA) receptors

Anti-CASPR2-Ab – Anti-CASPR2 antibodies

AP – Action potential

ASD – Autism spectrum disorder

BENOs – Bioengineered neuronal organoids

CASPR2 – Contactin-associated protein 2

cDNA – Complementary DNA

Cm – Capacitance

CNTNAP2 - Contactin-associated protein-like 2

CNQX – 6-cyano-7-nitroquinoxaline-2,3-dione

CNS – Central nervous system

CSF – Cerebrospinal fluid

CTR – Control

DIV – Days *in vitro*

DMEM – Dulbecco's modified Eagle's medium

E/I – Excitatory/inhibitory

EBs – Embryoid bodies

EEG – Electroencephalogram

EGF – Epidermal growth factor

EGFP – Enhanced green fluorescent protein

EPSCs – Excitatory postsynaptic currents

fAHP – Fast-afterhyperpolarization

FTLD – Frontotemporal lobar dementia

GABARs – Gamma-amino-butyric acid receptors

GDP – Giant depolarizing potential

GNP – Glycophorin-Neurexin IV-Paranodin

GRN – Granulin
HBS – HEPES Buffered Saline
hCSs – Human cortical spheroids
HEK293T – Human embryonic kidney 293T cell line
hESCs – Human embryonic stem cells
hiPSCs – Human induced pluripotent stem cells
hSkM – Human skeletal muscle spheroid
hSpS – Human spinal spheroid
hStrS – Human striatal neurons
hThCOs – Human thalamocortical organoids
hThOs – Human thalamus organoids
IgG – Immunoglobulin
IPSCs – Inhibitory postsynaptic currents
JXP – Juxtaparanodal
KO – Knock-out
LGI1 – Leucine-rich glioma-inactivated 1 protein
LTD – Long-term depression
LTP – Long-term potentiation
MEA – Multielectrode arrays
mEPSCs – Miniature excitatory postsynaptic currents
MGE – Medial ganglionic eminence
Mo – Month-old
NCL – Neuronal ceroid lipofuscinosis
NMDG-aCSF – N-Methyl-D-Glucamine-enriched artificial cerebrospinal fluid
OCD – Obsessive-compulsive disorder
PBS – Phosphate Buffered Saline
PFA – Paraformaldehyde
PGRN – Progranulin
PSD – Postsynaptic density protein
Ra – Access resistance
Rm – Membrane resistance
RMP – Resting membrane potential
ROIs – Regions of interest
RT – Room temperature
SEM – Standard error of the mean
sEPSCs – Spontaneous excitatory postsynaptic currents

SFEB – Serum-free floating culture of embryoid bodies

SFEBq – Serum-free floating culture of embryoid bodies with quick aggregation

sIPSCs – Spontaneous inhibitory postsynaptic currents

SNPs – Single nucleotide polymorphisms

sPSCs – Spontaneous postsynaptic currents

STD – Short-term depression

STP – Short-term potentiation

TAG-1 – Transient axonal glycoprotein-1

TTX – Tetrodotoxin

VGKCs – Voltage-gated potassium channels

WIV – Weeks *in vitro*

CHAPTER 1
INTRODUCTION

Part of this chapter is under preparation for submission as a review:

Oliveira, AR.; Cammarata, G.; Cardoso, AL.; Seabra, CM.; Peça, J. Cellular and electrophysiological landmarks in organoids for neurodevelopmental research: pitfalls and opportunities. *(in preparation)*.

1. Contactin-associated protein 2 (CASPR2) – general introduction

Contactin-associated protein 2 (CASPR2) was identified by Poliak and colleagues in 1999 as a new member of the neurexin superfamily (Poliak et al., 1999), a group of transmembrane proteins that mediate cell-cell interactions in the central nervous system. Initially, CASPR2, which is coded by the contactin-associated protein-like 2 (*CNTNAP2*) gene was described to have a crucial role in the stabilization of voltage-gated potassium channels (VGKCs) at the juxtaparanodal (JXP) regions of the nodes of Ranvier (Poliak et al., 1999). Throughout the years, CASPR2 has been associated with several roles, including regulation of the excitation/inhibition balance (Jurgensen and Castillo, 2015; Peñagarikano et al., 2011; Vogt et al., 2018), neuronal networks and neuronal migration (Peñagarikano et al., 2011), neurite outgrowth (Anderson et al., 2012; Canali et al., 2018; Varea et al., 2015) and synapse development and maintenance (Anderson et al., 2012; Fernandes et al., 2019; Gdalyahu et al., 2015; Jurgensen and Castillo, 2015; Varea et al., 2015). Moreover, since 2003, mutations in the *CNTNAP2* gene have been associated with several neurodevelopmental and neuropsychiatric disorders, including obsessive-compulsive disorder (OCD) (Verkerk et al., 2003), epilepsy, intellectual disability, autism spectrum disorders (ASD), schizophrenia, speech disorders and attention deficit and hyperactivity disorder (ADHD) (Rodenas-Cuadrado et al., 2014). CASPR2 was also identified as an antigen in autoimmune synaptic encephalitis (Irani et al., 2010; Lancaster et al., 2011), a rare central nervous system (CNS) syndrome characterized by memory dysfunction, temporal lobe seizures and frontal lobe impairments. More recently, anti-CASPR2-Ab have been linked to neurodevelopmental disorders due to the gestational transfer of those antibodies from the mother to the fetus (Brimberg et al., 2016, 2013; Coutinho et al., 2017b).

1.1. Expression and structure of CASPR2

CASPR2 is expressed during embryonic stages, but its expression significantly increases over development. In humans, it is mainly expressed in the CNS, including the spinal cord and the brain, though lower mRNA levels are also detected in ovaries and prostate (Poliak et al., 1999). During the early stages of development, CASPR2 is enriched in the human anterior temporal and prefrontal cortex (Abrahams et al., 2007). In rodents, embryonic expression of CASPR2 is detected near embryonic day 14 and is mostly expressed in the ganglionic eminences and the ventricular proliferative zones (Peñagarikano et al., 2011). In adult rodents, CASPR2 is strongly expressed in the cortex.

Additionally, it is also broadly expressed in other brain regions, including the hippocampus, striatum, dorsal thalamus, amygdala, basal ganglia and substantia nigra (Gordon et al., 2016; Peñagarikano et al., 2011). It was also reported an enrichment of CASPR2 in sensory system, including the olfactory, visual, auditory, gustatory and somatosensory regions (Gordon et al., 2016).

At the cellular level, CASPR2 was primarily detected in neurons, namely in the soma and dendrites of cortex pyramidal neurons and in pyramidal neurons of the CA3 region of the hippocampus (Poliak et al., 1999). It is also expressed in the axons, specifically at the distal part of the axon initial segment (AIS) and in myelinated axons in the JXP region of nodes of Ranvier (Inda et al., 2006; Ogawa et al., 2008; Poliak et al., 1999; Scott et al., 2019) (**Fig. 1.1A, C**).

In cultured hippocampal neurons, it was observed that at early stages, CASPR2 was expressed in the soma, dendrites and axons, and at later stages, it was preferentially distributed along axons (Pinatel et al., 2015). CASPR2 was also found in the synaptic membrane (Bakkaloglu et al., 2008; Chen et al., 2015), being expressed in both presynaptic and postsynaptic compartments (Fernandes et al., 2019; Pinatel et al., 2015; Varea et al., 2015). However, a strong colocalization of CASPR2 with presynaptic compartments was observed (Pinatel et al., 2015). Additionally, a higher expression of CASPR2 in inhibitory neurons, relative to excitatory neurons, has also been reported (Pinatel et al., 2015) (**Fig. 1.1D**). Moreover, disruption of the inhibitory system development and function was observed in some *CNTNAP2* mutant mouse models (Jurgensen and Castillo, 2015; Peñagarikano et al., 2011).

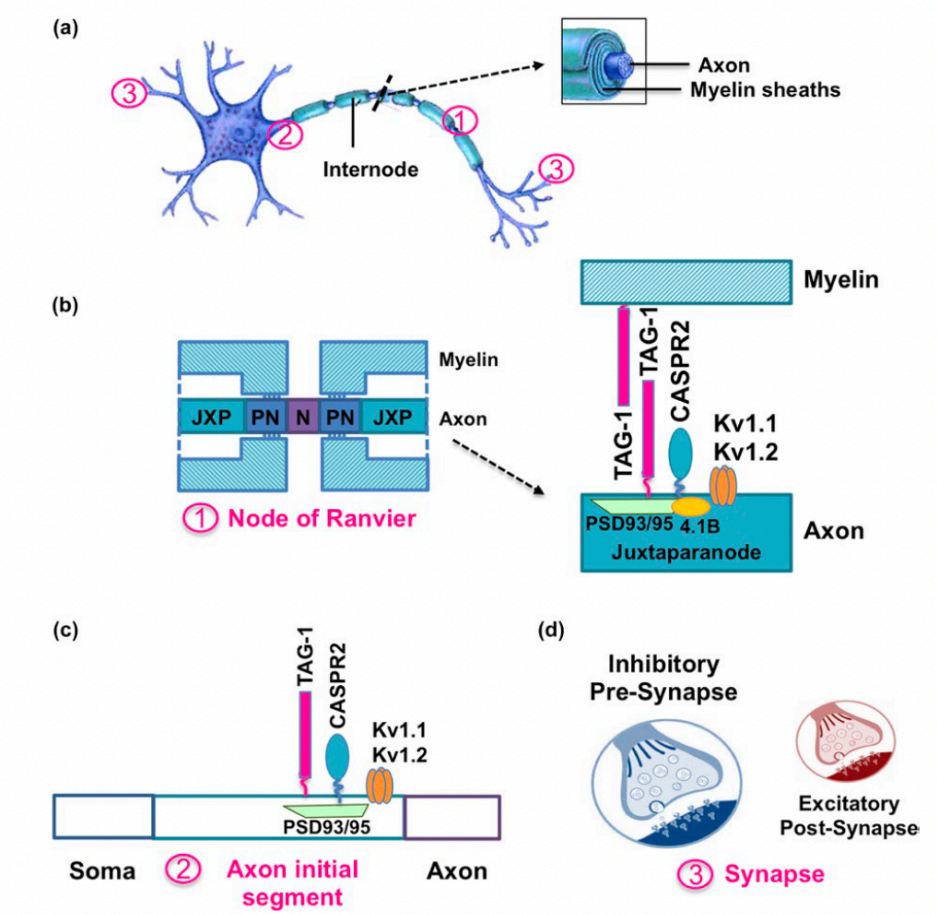

Figure 1.1. CASPR2 expression in neurons. (**A)** CASPR2 can be expressed in different compartments of a neuron, including the nodes of Ranvier (1), the axon initial segment (2) and the synapse (3). (**B)** At the node of Ranvier, CASPR2 is expressed in the JXP region and it is involved in the clustering of TAG-1 (also known as Contactin-2) and recruitment of Kv1.1 and Kv1.2 channels through its binding to the 4.1B-binding motif. (**C)** At the axon initial segment, CASPR2 is mainly found in the distal part and it also involved in the clustering of TAG-1, Kv1.1 and Kv1.2 channels, but it does not seem crucial for their correct localization. **(D)** At the synapse, CASPR2 is mainly found in inhibitory pre-synaptic compartment. N: node, PN: paranode, JXP: juxtaparanodal. *(Saint-Martin et al., 2018)* – License number: 5515401103324.

Regarding its structure, CASPR2 is composed of several domains, containing a long extracellular and a short cytoplasmic region (**Fig. 1.2**). Its extracellular region is composed of a signal peptide near the N-terminal, a discoidin homology domain, four laminin G neurexin-like motifs (L1-L4), two epidermal growth factor-like (EGF) repeats (E1-E2) and a fibrinogen-like domain (F) (Poliak et al., 1999). The C-terminal intracellular region contains a juxtamembrane GNP (Glycophorin, Neurexin IV, Paranodin) motif, also known as 4.1B-binding motif, and a type II PDZ-binding domain (Poliak et al., 1999). CASPR2 is organized into three flexible lobes, giving it a vertical or horizontal orientation, which could be responsible for its binding capacity to different binding partners and for its subcellular localizations within neuronal regions (Lu et al., 2016).

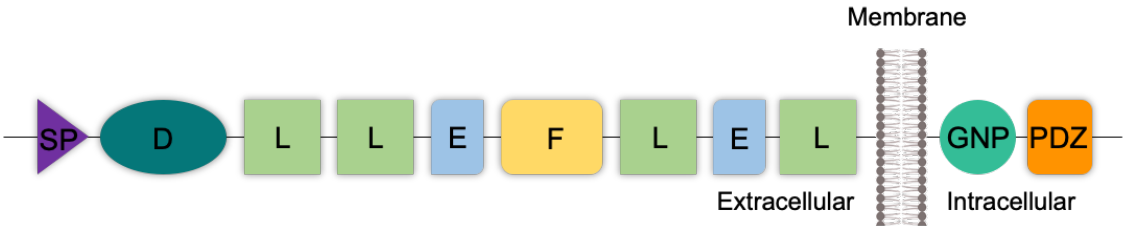

Figure 1.2. CASPR2 domains organization. CASPR2 contains a long extracellular and a short cytoplasmic region. The extracellular region contains a signal peptide (SP), a discoidin homology domain (D; F58C), four laminin G neurexin-like motifs (L), two EGF-like repeats (E) and one fibrinogen-like domain (F). The intracellular region contains a GNP motif and a PDZ-binding domain (PDZ).

Extracellular CASPR2 is known to complex with the cell surface protein Contactin-2, also called TAG-1 (transient axonal glycoprotein-1) or Axonin-1 that is present on both axonal and glial membrane. This arrangement allows axon-glia interactions that are essential for the recruitment and stabilization of VGKCs (Kv1.1 and Kv1.2) in the axonal membrane (Poliak et al., 2003) (**Fig. 1.1B**).

Intracellular CASPR2 binds through the GNP motif to cytoskeleton-associated proteins containing FERM (Four-point-one, Ezrin, Radixin, Moesin) domains, such as β1 integrins, cytoskeleton adaptor protein 4.1 and schwannomin, to anchor CASPR2 to the actin-based cytoskeleton (Denisenko-Nehrbass et al., 2003a, 2003b). Also through its GNP motif, CASPR2 interacts with Kv1.1 and Kv1.2 channels, playing an important role in their stabilization at the JXP (Horresh et al., 2008). It also interacts with the G protein-coupled receptor 37 (GPR37) (Tanabe et al., 2015) and ADAM (Disintegrin and Metalloproteinase domain-containing protein) members, specifically with ADAM22 complexed with soluble LGI1 (Leucine-rich glioma-inactivated 1) protein (Chen et al., 2015). Additionally, via its PDZ-binding domain, CASPR2 interacts with MAGUKS (membrane-associated guanylate kinases), such as PSD93, PSD95, SAP97 (synapse-associated protein 97) and CASK (calcium/calmodulin-dependent serine protein kinase) (Chen et al., 2015; Ogawa et al., 2008; Poliak et al., 1999). Furthermore, it was also shown to interact with carboxypeptidase E, allowing CASPR2 trafficking to the dendritic membrane via a Golgi-dependent pathway (Oiso et al., 2009). Recently, it was observed an interaction between the GluA1 subunit of AMPARs (AMPA-type glutamate receptors) and CASPR2 (Fernandes et al., 2019).

1.2. Biological functions of CASPR2

The first described role of CASPR2 was its involvement in the recruitment of VGKCs to the membrane. Over time, other biological roles have been proposed, including a potential role in axonal organization and action potential propagation, in cellular development and network activity and more recently, its role in synaptic plasticity.

1.2.1. CASPR2 functions in axonal organization and action potential propagation

CASPR2 may play a role in the axonal growth, since in *CNTNAP2* KO mouse embryos, a reduction in axonal growth was observed (Canali et al., 2018; Varea et al., 2015). Moreover, CASPR2 may play a critical role in axonal organization at the nodes of Ranvier, particularly in myelin sheathing and correct propagation of action potentials (Poliak et al., 2003; Simons and Trajkovic, 2006).

Nodes of Ranvier are characterized by the presence of a high density of voltage-dependent sodium channels linked to the cytoskeleton by ankyrinG (Bennett and Lambert, 1999; Jenkins and Bennett, 2001; Rasband and Peles, 2015). On the other hand, the JXP regions comprise high density clusters of Kv1 channels that colocalize with CASPR2 and Contactin-2 (Poliak et al., 2003; Rasband et al., 2002; Traka et al., 2003). Kv1 channels are crucial for axonal excitability regulation, due to their role in the repolarization of neuronal membranes after an action potential (Debanne et al., 1997; Lai and Jan, 2006). In the JXP region, CASPR2 is essential to cluster Kv channels in the membrane (Pinatel et al., 2017; Poliak et al., 1999), but it is not responsible for Kv channel clustering at the AIS, which in turn is mediated by PSD93/95 PDZ-binding domains. (Ogawa et al., 2008). Conversely, CASPR2 and Contactin-2 are necessary for PSD93/95 accumulation at the JXP region (Horresh et al., 2008). In CASPR2 knock-out (KO) mice, depletion of Kv1 and Contactin-2 was observed at the JXPs, with Kv1 channels seen to diffuse along the internode region (Poliak et al., 2003). Surprisingly, no gross alterations were detected in axonal myelination, neither in axonal excitability (Poliak et al., 2003), probably due to a compensation by other potassium channels (Devaux et al., 2003). Contrarily, others demonstrated, by functional magnetic resonance imaging, reduced local and long range prefrontal functional connectivity, with no gross changes in myelination, in *CNTNAP2*-lacking mice (Liska et al., 2018). Additionally, Dawes and colleagues observed a reduction in Kv1 surface expression and smaller Kv1-mediated currents (Dawes et al., 2018). More recently, also due to alterations in Kv1 clustering in the JXP region, defects in nodal formation and delay in myelin sheaths were reported,

together with alterations in action potential propagation, which included a decrease in action potential repolarization velocity and an increase in excitatory postsynaptic potentials (Scott et al., 2019). Accordingly, in the auditory cortex, loss of *CNTNAP2* gene also contribute to a hyperexcitability phenotype, most probably due to changes in VGKCs (Scott et al., 2022).

Overall, these results strongly point to an important role of CASPR2 in VGKC organization in the JXP and in axonal myelination.

1.2.2. CASPR2 functions in cellular development and network activity

In addition to the role of CASPR2 in the structural organization of axons, recent evidence has also suggested an involvement in cellular development and migration. In both animal models and neuronal cultures from human induced pluripotent stem cells (hiPSCs), the presence of CASPR2 mutations was shown to impact neuronal migration (Flaherty et al., 2017; Lee et al., 2015; Peñagarikano et al., 2011). Moreover, a reduction in subpopulations of GABAergic interneurons was also identified, which was shown to result in impaired GABAergic inhibitory transmission and increased excitability in adult mice (Anderson et al., 2012; Bridi et al., 2017; Jurgensen and Castillo, 2015; Lauber et al., 2018; Lu et al., 2021; Peñagarikano et al., 2011; Vogt et al., 2018). Likewise, inhibitory neurons' defects were also observed in mouse cortical organoids (Hali et al., 2020). Interestingly, using optogenetics, Selimbeyoglu and colleagues reverted the alteration in excitatory/inhibitory (E/I) balance in *CNTNAP2* KO mice and rescued the hyperactivity phenotype (Selimbeyoglu et al., 2017). However, depending on the brain region probed, the effect of CASPR2 disruption have been reported to be distinct. For instance, Scott and colleagues reported no changes in neocortical inhibitory circuits in developing and adult *CNTNAP2* deletion models (Scott et al., 2019). Whereas, more broadly, the excitatory transmission is either normal (Jurgensen and Castillo, 2015) or decreased across different *CNTNAP2* deletion models (Anderson et al., 2012; Kim et al., 2019; Lazaro et al., 2019; Lu et al., 2021; Vogt et al., 2018).

As previously indicated, CASPR2 is expressed also in the somatodendritic compartment (Fernandes et al., 2019; Inda et al., 2006; Ogawa et al., 2008; Poliak et al., 1999; Scott et al., 2019; Varea et al., 2015). Additionally, downregulation of CASPR2 also led to a reduction in dendritic arborization (Anderson et al., 2012; Gao et al., 2018; Lu et al., 2021), probably due to impairments in CASPR2 binding to the cytoskeleton adaptor protein 4.1 that is necessary to recruit relevant elements for dendrite growth (Anderson et al., 2012). In these studies, a decrease in both excitatory and inhibitory synaptic density

and changes in spine morphology and dynamics were observed (Anderson et al., 2012; Lazaro et al., 2019).

These findings suggest that altered CASPR2 expression induced changes in E/I regulation.

1.2.3. CASPR2 functions in synaptic plasticity

The impact of CASPR2 mutation on network activity may be linked to altered axonal conductivity, but also to alterations in synaptic transmission. In fact, CASPR2 has been involved in the establishment and stabilization of newly formed synapses (Anderson et al., 2012; Gdalyahu et al., 2015). Additionally, CASPR2 deletion caused a decrease in both excitatory postsynaptic currents (EPSCs) mediated by AMPA- and NMDA-receptors and inhibitory postsynaptic currents (IPSCs) mediated by GABARs, in primary cortical neurons and in the prefrontal cortex (Anderson et al., 2012; Sacai et al., 2020). These results are consistent with a significant decrease in the frequency, but not in the amplitude of both miniature EPSCs (mEPSCs) and miniature IPSCs (mIPSCs), implicated in a reduction of excitatory synapses in these neurons (Anderson et al., 2012; Sacai et al., 2020). However, others also reported decreased amplitude (Fernandes et al., 2019; Kim et al., 2019; Lazaro et al., 2019), but no differences in the frequency of mEPSCs (Fernandes et al., 2019; Kim et al., 2019). Moreover, a decrease in spontaneous excitatory and inhibitory postsynaptic currents (sEPSCs and sIPSCs) in *CNTNAP2* mutant cortical neurons was observed (Lu et al., 2021). Consequently, synaptic transmission is affected by *CNTNAP2* deletion with no reported alterations in the membrane properties of the neurons (Anderson et al., 2012). Several studies have suggested the involvement of CASPR2 in AMPAR trafficking (Anderson et al., 2012; Fernandes et al., 2019; Kim et al., 2019; Varea et al., 2015). Absence of CASPR2 results in a decrease of synaptic GluA1 – a AMPAR subunit – and an increase in GluA1 cytoplasmic aggregates in excitatory neurons (Anderson et al., 2012; Fernandes et al., 2019; Varea et al., 2015). Conversely, interneurons showed an increase in synaptic GluA1 (Kim et al., 2019). Furthermore, it was demonstrated a relevant role for CASPR2 in synaptic scaling, specifically in homeostatic plasticity since its deletion impeded the correct trafficking of AMPARs, perturbing the excitatory transmission (Fernandes et al., 2019).

Altogether, these results suggest deficits in synaptic transmission which impact homeostatic plasticity. Nevertheless, careful exploration of cell autonomous and non-cell autonomous effects should be performed before drawing firm conclusions on the effects of *CNTNAP2* mutations.

1.3. CASPR2 in the pathogenesis of neurodevelopmental and neuropsychiatric disorders

Considering the biological roles of CASPR2, it is not surprising that alterations in CASPR2 or in its gene – *CNTNAP2* – may lead to neurological or neuropsychiatric disorders.

The first described mutation in the *CNTNAP2* gene was observed in a family with Gilles de la Tourette syndrome, accompanied by OCD and ADHD (Belloso et al., 2007; Verkerk et al., 2003). Over the years, other mutations in the *CNTNAP2* gene have been implicated in other neurodevelopmental and neuropsychiatric disorders, including ASD (Alarcón et al., 2008; Arking et al., 2008; Bakkaloglu et al., 2008; Chien et al., 2021), intellectual disability (Mikhail et al., 2011), schizophrenia (Friedman et al., 2008; O'Dushlaine et al., 2011), bipolar disorder (O'Dushlaine et al., 2011), language impairments (Sehested et al., 2010; Vernes et al., 2008), epilepsy (Friedman et al., 2008) and cortical dysplasia focal epilepsy syndrome (Strauss et al., 2006), among others (**Fig. 1.3**). Some of these phenotypes were also observed in *CNTNAP2* mutation animal models, such as

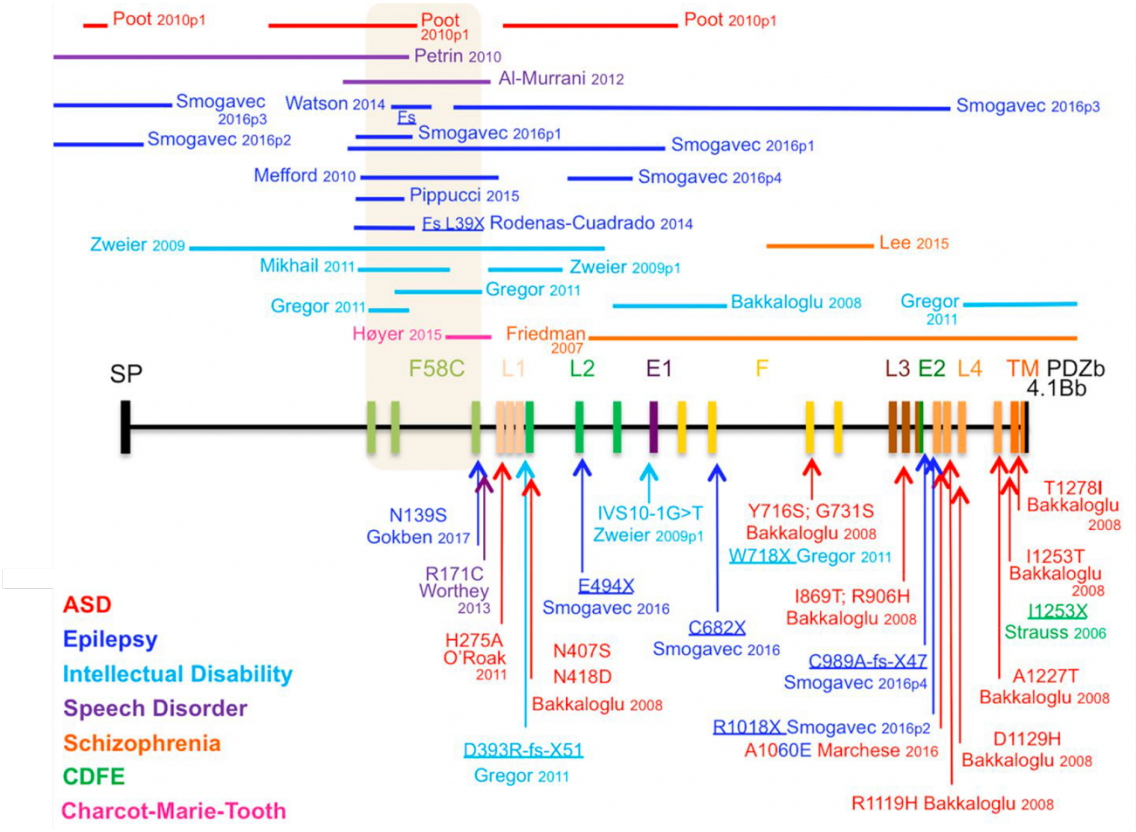

Figure 1.3. CASPR2-associated genetic diseases. Representation of the *CNTNAP2* gene (black line) and its 24 exons (colored vertical lines) coding for the different domains of CASPR2. The colored horizontal lines above the *CNTNAP2* gene indicate copy number variations (CNVs). The arrows under the *CNTNAP2* gene indicate point mutations, and stop mutations are underlined. The clinical condition associated with each mutation is presented in the left side of the image. Adapted from *(Saint-Martin et al., 2018)*.

hyperactivity and memory impairments, epileptic seizures and ASD-like symptoms (Peñagarikano et al., 2011; Sacai et al., 2020; Scott et al., 2019).

More recently, CASPR2 was also identified as an antigen in autoimmune synaptic encephalitis (Irani et al., 2010; Lancaster et al., 2011). Neuropsychiatric symptoms are evident in patients that produce exacerbated levels of antibodies targeting CASPR2 (Irani et al., 2010; Lancaster et al., 2011; Liu et al., 2021; Schou et al., 2019). Additionally, anti-CASPR2-Ab were also detected, during pregnancy, in mothers of children with ASD (Brimberg et al., 2013) and intellectual disability (Coutinho et al., 2017a). This phenotype was translated to the offspring of pregnant mice exposed to anti-CASPR2-Ab via maternal-transfer of antibodies to the fetus (Brimberg et al., 2016; Coutinho et al., 2017b).

1.4. Autoimmune synaptic encephalitis: anti-CASPR2 antibodies

Autoimmune synaptic encephalitis is characterized by an exacerbated production of antibodies that target specific neuronal cell-surface or synaptic epitopes. The major antigens associated to autoimmune encephalitis are NMDARs (Dalmau et al., 2007), AMPARs (Lai et al., 2009), GABARs (Lancaster et al., 2010; Petit-Pedrol et al., 2014), LGI1 (Lai et al., 2010) and CASPR2 (Irani et al., 2010), each of them with syndromes that include memory deficits, cognitive impairment, mood and behavior disorders and variable presence of seizure in the CNS and peripheral nerve hyperexcitability, movement disorders and neuropathic pain in the peripheral nervous system (PNS) (Dalmau et al., 2017).

Autoantibodies targeting CASPR2 were identified not only in the serum but also in the cerebrospinal fluid (CSF) of patients with severe neurological syndromes that included neuromyotonia, Morvan's syndrome and limbic encephalitis (Irani et al., 2010). Autoimmune synaptic encephalitis is diagnosed based on a cell-based assay with serum titers $\geq$ 1:200, complemented with brain magnetic resonance imaging (MRI) (Bien et al., 2017). Immunoglobulin G4 (IgG4) is the most abundant IgG in the serum of these patients, although the more severe cognitive and psychiatric symptoms are associated with high levels of the IgG1 subclass (Binks et al., 2018; Joubert et al., 2016). The treatment of this condition is usually based on immunotherapies, with positive clinical outcomes but recurrent relapse, implicating the need for chronic immunosuppression that is associated with permanent cognitive problems in some cases (Bastiaansen et al., 2017; Liu et al., 2021). Considering that symptoms are mostly reversible upon treatment, this indicates a direct pathogenic role of CASPR2 antibodies. Hence, it is important to unveil additional mechanisms underlying these disorders to provide more targeted and efficient therapies to these patients.

1.4.1. Pathogenic mechanisms associated with anti-CASPR2 antibodies

The vast majority of anti-CASPR2-Ab found in patients serum and CSF include the IgG4 subclass (Binks et al., 2018; Joubert et al., 2016). IgG4 subclass undergoes the Fab-arm exchange process, allowing the bispecificity of some IgG4 antibodies, suggesting that the antibody may target more than one epitope, namely both laminin G1 and discoidin domains that seem to be obligatory epitopes to bind (Joubert et al., 2016; Olsen et al., 2015; van Sonderen et al., 2016). Furthermore, the binding of IgG4 subclass to the Fc-γ receptors is weak, consequently it does not activate the complement and immune responses efficiently (van Sonderen et al., 2016). Therefore, it has been proposed that IgG4 anti-CASPR2-Ab pathogenicity may be related to changes in protein-protein interactions (van Sonderen et al., 2016). Indeed, it was shown that IgG4 anti-CASPR2-Ab failed to internalize CASPR2 and inhibited the interaction between CASPR2 and Contactin-2 in a sample-dependent manner (Patterson et al., 2018). Since CASPR2-Contactin-2 interaction is essential for VGKCs recruitment at the JXP region, stabilizing the conduction at nodes of Ranvier and preventing hyperexcitability (Poliak et al., 2003; Traka et al., 2003), these antibodies can disrupt this process. This was validated by Dawes and colleagues showing that, after injection of human anti-CASPR2-Ab into wild-type mice, a downregulation of both CASPR2 and Kv1 expression resulted in a pain-related hypersensitivity phenotype and increased excitability of dorsal root ganglia neurons (Dawes et al., 2018). Moreover, in cultured hippocampal neurons, patient-IgGs strongly targeted inhibitory neurons, and led to changes in inhibitory synapses, which may contribute to the hyperexcitability observed in patients with autoimmune encephalitis (Pinatel et al., 2015). Alternatively, despite observing decreased interaction between CASPR2 and Contactin-2, Saint-Martin reported an increase in the expression of Kv1.2 in both HEK cells and hippocampal neurons and an increase in surface CASPR2 in CASPR2-transfected neurons upon antibodies addition (Saint-Martin et al., 2019). A trend towards higher levels of CASPR2 was also observed in brain extracts of CASPR2-injected mice and again in hippocampal neurons and HEK cells (Giannoccaro et al., 2019). The increased expression of CASPR2 and Kv1.2 might be due to compensatory mechanisms. The observed discrepancies may also be due to distinct patient samples with different anti-CASPR2-Ab concentrations, varying IgG subclasses targeting different epitopes, and also due to different cell types used in each experiment.

Importantly, although most of the patients present IgG4 subclasses, there are cases containing a mixture of different subclasses. Therefore, it was reported that non-IgG4-

CASPR2-Abs also influence microglia and astrocytes activation (Giannoccaro et al., 2019; Körtvelyessy et al., 2015). Behavioral impairments in CASPR2-injected mice (whose blood brain barrier is temporarily destabilized) show higher levels of c-fos expression which correlates with increased excitability, as observed by Dawes (Dawes et al., 2018; Giannoccaro et al., 2019). Moreover, synaptic CASPR2 distribution was shown to be decreased in neuronal cultures exposed to anti-CASPR2-Ab, suggesting an internalization of the protein (Fernandes et al., 2019). Additionally, these antibodies also had an impact on AMPARs trafficking with an increase in AMPARs endocytosis and consequently a decrease in its synaptic expression (Fernandes et al., 2019). Along with the previous findings, mice injected with anti-CASPR2-Ab presented a decrease in the amplitude of mEPSCs, suggesting that glutamatergic transmission impairment is another neuronal alteration arising from anti-CASPR2 encephalitis (Fernandes et al., 2019).

1.4.2. Anti-CASPR2 antibodies and neurodevelopmental disorders

It is well-known that maternal immune activation impacts the gestating fetus (Silverstein, 1996). Maternal IgG binds to the neonatal Fc receptor (nFcR), which transposes IgG into fetal circulation, thereby providing adaptive immunity to the newborn before its immune system is fully developed (Simister and Mostov, 1989). IgG antibodies are important to provide immunity against pathogens and toxins, however, this pathway opens the possibility for pathogenic autoantibodies to also be transferred. Therefore, maternal immune activation has been linked to neurodevelopmental disorders, such as ASD and intellectual disability, which may be caused by autoantibody-dependent or -independent mechanism (Estes and McAllister, 2016). For instance, maternal influenza infection (Atladóttir et al., 2012), as well as increased levels of MCP-1 (monocyte chemoattractant protein-1) chemokine in the amniotic fluid (Abdallah et al., 2012) and increased levels of interferon-γ (IFNγ), interleukin-4 and 5 (IL-4 and IL-5) (Goines et al., 2011) were associated with increased risk of infantile autism. Importantly, both genetic and environmental factors determine the severity of the disorder (Mazina et al., 2015). More recently, maternal immune activation driven by viral infection was shown to be mediated by IL-17 (Choi et al., 2016). Regarding instances leading to abnormal antibody impacting the developing fetal brain, these have been shown to lead to neurodevelopmental disorders in the offspring (Braunschweig et al., 2008; Brimberg et al., 2013; Coutinho et al., 2017a; Croen et al., 2008; Singer et al., 2008). Several studies in animal models – where serum or polyclonal antibodies were injected into a pregnant

dams – revealed neurodevelopmental conditions in the animal offspring (Bauman et al., 2013; Dalton et al., 2003; Singer et al., 2009). These studies provide additional support for the “smoking gun” sign that is the presence of anti-CASPR2-Ab in mothers of a subset of children with ASD (Brimberg et al., 2013; Coutinho et al., 2017a). Offspring exposed *in utero* to anti-CASPR2-Ab displayed cellular and behavioral phenotypes with similarities to those found in CASPR2-encephalitis patients and *CNTNAP2*-associated neurodevelopmental/neuropsychiatric disorders (Bagnall-Moreau et al., 2020; Brimberg et al., 2016; Coutinho et al., 2017b). Social interaction deficits and repetitive behaviors were also observed in male offspring, as well as abnormal cortical development, reduced dendritic arborization of excitatory neurons, decreased glutamatergic synapses, reduced levels of GluA1, decreased number of inhibitory neurons and an increase in microglia activation (Bagnall-Moreau et al., 2020; Brimberg et al., 2016; Coutinho et al., 2017b). This phenotype was observed using both serum, total purified IgG or a monoclonal antibody against CASPR2 (Bagnall-Moreau et al., 2020; Brimberg et al., 2016; Coutinho et al., 2017b).

These results strongly suggest that maternal CASPR2 antibodies may directly influence gestating offspring and contribute to the appearance of neurodevelopmental disorders.

1.5. Modelling brain disorders

Despite great advances in modelling human diseases in simpler organisms, from yeast to mice, it has been a challenge for the scientific community and pharmaceutical industry to translate findings and treatments towards the benefit of patients. This is speculated to be due to specific aspects of human cellular physiology and complexity of the human brain. Thus, the limited access to human brain samples and appropriately complex models (i.e. beyond limited 2D cultures), has stymied progress. Mice models, due to the complexity associated with an intact animal, have allowed the study of brain development and behavior, including the impact of specific genetic mutations and the environment on brain function (Lima Caldeira et al., 2019; Peça and Feng, 2012; Ting et al., 2012). However, these models cannot mimic the unique cellular and molecular physiology of the human brain, which has compromised the success for clinical translation into effective treatments (Akhtar, 2015; Seok et al., 2013; Zhao and Bhattacharyya, 2018). Therefore, advanced human models are essential to study brain development, function and disease. With this goal in mind, the reprogramming of human somatic cells into pluripotent stem cells, including human embryonic stem cells (hESCs) and hiPSCs, has allowed the creation of patient- and disease-specific stem cell populations (Takahashi et al., 2007; Thomson et al., 1998). These can then be further differentiated into various cell types, including neurons and glia, allowing for subsequent studies with potential applications for drug discovery and neurological disease research, while preserving the genetic background of each individual (Brennand et al., 2011; Park et al., 2008; Wen et al., 2014). Notwithstanding, the lack of brain cytoarchitecture and of a 3D microenvironment may compromise the reliability of the information on disease phenotypes that can be extracted from patient-derived stem cells. Indeed, core pathogenic deficits may arise only in the context of more complex structures capable of displaying meaningful neuronal architecture and circuitry (Lancaster et al., 2013; Y. Li et al., 2017). To overcome these limitations, in 2013, Lancaster and colleagues generated and described human cerebral organoids (Lancaster et al., 2013). Essentially, cerebral organoids, or brain organoids, arise from stem cell aggregates that self-organize to form a structure that mimics, to a certain degree, the 3D and layer organization of the human brain (Lancaster et al., 2013). At the same time, these models retain genetic and tissue-specific features, such as patterns of cellular migration, transcriptional and epigenomic programs and synaptic and network activity that resemble several aspects of the fetal brain (Camp et al., 2015; Lancaster et al., 2013; Luo et al., 2016; Quadrato et al., 2017; Trujillo et al., 2019).

Thus, brain organoids are now considered emerging models that complement the toolkit available to biomedical researchers and promise a renewed potential for translational applications.

1.6. Brain organoids: from single cells to 3D models

While over the past few years brain organoids have seen an explosion of interest, key discoveries on the organizing principle of cells dates back to Henry Wilson's demonstration that undifferentiated cells can reorganize and differentiate into a new functional organism (Wilson, 1907). In 1960, Weiss and colleagues observed that a single-cell suspension of chick embryos are able to reorganize and re-form the initial organism without external signals (Weiss and Taylor, 1960). Then, due to stem cell advances and generation of mouse embryonic stem cells (mESCs), embryoid bodies (EBs) were generated and differentiated both *in vivo* and *in vitro* (Evans and Kaufman, 1981). Later, EBs were used to differentiate hESCs into neural precursors, within neural rosettes, in the presence of external signals, and into mature neurons and glia (Reubinoff et al., 2000; Zhang et al., 2001). Additionally, Watanabe and colleagues used the serum-free floating culture of embryoid bodies (SFEB) to demonstrate that this method *per se* allows for the autonomous neural differentiation (Watanabe et al., 2007, 2005). However, extracellular patterning factors can be added to the medium to promote the differentiation of distinct regions, fostering the selective neural differentiation of EBs *in vitro* (Watanabe et al., 2007, 2005). In 2008, a 3D version of the latter method was developed – SFEB, with quick aggregation (SFEBq) – to mimic the developing mouse and human cortex (Eiraku et al., 2008). This method was based on a quicker re-aggregation of the cells and the formation of uniform EBs in U-bottom plates, which promoted an efficient differentiation of ESCs into cortical progenitors and functional cortical neurons (Eiraku et al., 2008). Once again, by manipulating extrinsic factors, regional and temporal identities could be influenced and controlled. The same method, improved by the addition of basement-membrane matrix components (Matrigel), was used for the generation of 3D neural retinal tissue (Eiraku et al., 2011). Subsequently, 3D SFEBq-like structures were developed from hiPSCs, with expression profiles similar to the embryonic telencephalon development in humans (Mariani et al., 2012). In 2013, a landmark model of human 3D brain structures, termed cerebral organoids, was developed by Lancaster and colleagues (Lancaster et al., 2013). This approach is devoid of patterning growth factors and takes advantage of Matrigel, used as structural support to promote proper tissue growth. Furthermore, to avoid the lack of oxygen and nutrients, the structures are transferred to a spinning bioreactor (Lancaster et al., 2013).

Brain organoids mimic the whole brain and have been shown to present different and interdependent regions, indicative of cerebral cortex, choroid plexus, retina and meninges, and recapitulate various aspects of human cortical development (Lancaster et al., 2013). In the same year, Matrigel was also used for the generation of neocortex-like tissue using hESCs (Kadoshima et al., 2013). Nonetheless, considering that Matrigel is obtained from tumors and its components depend on cultivation and purification that may display batch to batch variability, Paşca and colleagues established a novel, simpler and reproducible method for 3D cultures, termed 3D human cortical spheroids (hCSs) (Paşca et al., 2015). In this approach, minimal external factors are added to the culture for the patterning into cortex-like structures. These hCSs were shown to contain spontaneously active excitatory neurons (Paşca et al., 2015).

Currently, numerous studies have been performed in order to overcome the limitations and improve available methods, which include region-specific differentiation (Jo et al., 2016; Lancaster et al., 2017; Muguruma et al., 2015; Paşca et al., 2015; Sakaguchi et al., 2015; Xiang et al., 2019), fusion of different type of organoids to create circuit-specific models (Andersen et al., 2020; Bagley et al., 2017; Birey et al., 2017; Miura et al., 2020; Xiang et al., 2019), axially patterned organoids (Cederquist et al., 2019), and co-culture of organoids with other cell types (Cakir et al., 2019; Shi et al., 2020; Song et al., 2019a, 2019b). The history timeline for the development of these models is presented below (**Figure 1.4)**.

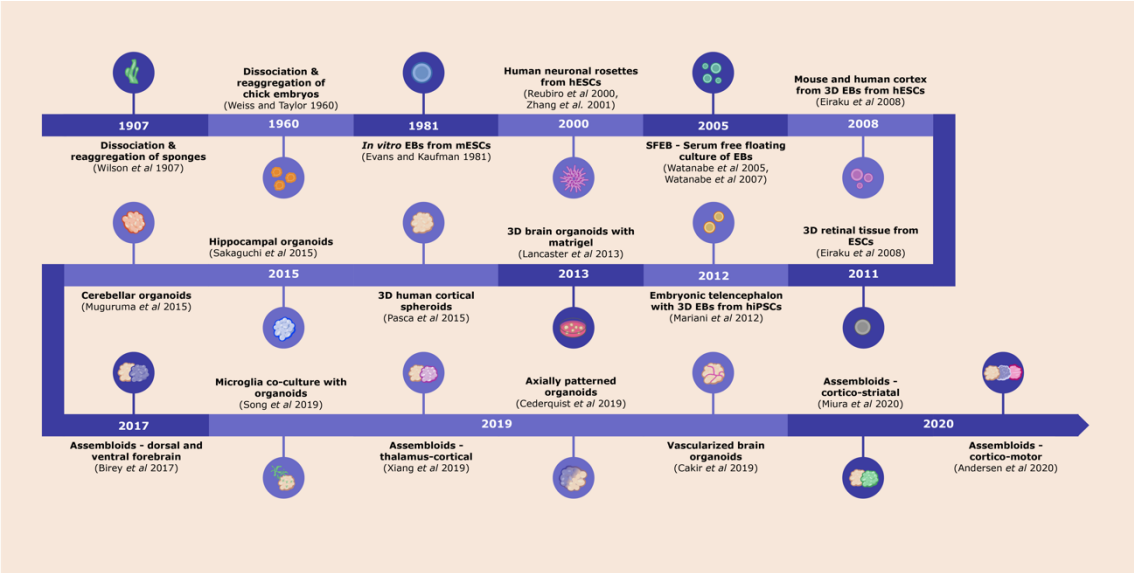

Figure 1.4. Historical timeline for organoids generation. The first discoveries occurred early in the 20th Century with significant improvements over the years.

1.7. Brain organoids 2.0: assembloids

Multi-regional assembloids are now being used to model the interactions between different brain regions, to offer insights on fundamental developmental processes, such as migration of different cell types into another region, synaptogenesis occurring when cells integrate a new neuronal circuit, and the formation of reciprocal and functional projections (Bagley et al., 2017; Birey et al., 2017; Sloan et al., 2018; Xiang et al., 2019, 2017). One of the first attempts to recapitulate migration of different cell types to a different patterned organoid was performed by Bagley and colleagues, who modelled the migration of medial ganglionic eminence (MGE) neurons into cortical organoids by modulating its activity (Bagley et al., 2017). These complex models have also been used to study cellular and molecular mechanisms and circuit assembly associated with brain disorders. For instance, dorsal-ventral assembloids were used to model Timothy syndrome features, a severe neurodevelopmental disorder characterized by ASD and epilepsy and caused by a mutation in the L-type calcium channel (LTCC) $Ca_v1.2$ (Birey et al., 2022, 2017).

Advances have been made and other complex multi-regional assembloids have been developed, including thalamocortical assembloids (Xiang et al., 2019), cortico-striatal assembloids (Miura et al., 2020), cortico-motor assembloids (Andersen et al., 2020) and retina-cortical and retina-thalamic-cortical assembloids (Fligor et al., 2021).

In humans, the development of the thalamocortical circuit is characterized by the formation of extensive reciprocal projections, whose function is to process sensorimotor signals, attention and arousal. Defects in the development of this system have been linked to neurodevelopmental disorders, including ASD, schizophrenia, and epilepsy (Xiang et al., 2019). Xiang et al. established a method that models reciprocal connectivity between thalamus and cortex by fusing regionally specific brain organoids. Using this system, formation of reciprocal connections between the two patterned organoids were observed, followed by synaptogenesis in the respective targeted regions and functional maturation (Xiang et al., 2019).

Regarding cortico-striatal circuits of the forebrain, they are known to modulate the motivated behaviors and movement. The structure of this system features cerebral cortex projections directed towards the GABAergic medium spiny neurons, which connect to the basal ganglia and acquire a physiologically mature state. Dysfunctions of the cortical-striatal pathway may also contribute to neurodevelopmental and psychiatric disorders such as Tourette syndrome, ASD, schizophrenia or OCD. Cortico-striatal assembloids were characterized by cortical glutamatergic projections targeting the striatal side, which was mainly composed of morphologically and functionally mature

striatal neurons (Miura et al., 2020). This directionality in the interaction between cortex and striatum is known to be present *in vivo* (Shepherd, 2013). This specific model allowed the generation of cortico-striatal assembloids derived from patients with 22q13.3 deletion syndrome (Phelan-McDermid syndrome) (Miura et al., 2020).

Andersen and colleagues also developed a cortico-motor circuit, composed of hCSs fused to a human spinal spheroid (hSpS) and a human skeletal muscle spheroid (hSkM). This network involved cortical neurons that controlled the contraction of muscle cells via the motor neuron component (Andersen et al., 2020).

Additionally, the generation of retina-thalamic-cortical assembloids was a great improvement to the previous retina organoid models (Zhong et al., 2014). This model promoted a significant increase in the survival of retinal ganglion cells, due to the signals provided by thalamic organoids (Fligor et al., 2021), allowing the study of developing human retina or retina injuries.

1.8. Limitations in cell diversity in brain organoids

Assessing the regional complexity and cell composition of brain organoids has been crucial to determine the validity of these culture models. Single-cell transcriptomic analysis has been used for the identification of different brain regions and various cell types within brain organoids. For instance, self-patterned whole brain organoids display heterogeneous tissues and regions, such as forebrain, midbrain, and hindbrain, but also choroid plexus, retina and optic vesicles (Gabriel et al., 2021; Lancaster et al., 2013; Quadrato et al., 2017). Moreover, it is also clear the heterogeneity of cellular populations, which include neuronal progenitors at first and mature neurons in later stages, including dopaminergic, glutamatergic and GABAergic neurons (Kanton et al., 2019; Lancaster et al., 2013; Quadrato et al., 2017), with the latter being mainly restricted to older organoids (6 to 10 months), which is in line with *in vivo* development (Trujillo et al., 2019). This model also contains glial cells, such as astrocytes and oligodendrocyte precursor cells, after long-term culture (Kanton et al., 2019; Quadrato et al., 2017), and according to Ormel, microglia-like cells may be also observed within the organoid if mesodermal precursors are present in the initial stages of organoid formation (Ormel et al., 2018). Nevertheless, in most studies, microglial populations are not reported as present in human brain organoids, but can be added by incorporating microglial progenitors into the developing organoid (Abud et al., 2017; Bodnar et al., 2021; Fagerlund et al., 2021; Popova et al., 2021; Sabate-Soler et al., 2022; Song et al., 2019b; Xu et al., 2021). Moreover, endothelial populations may have been reported in organoids, however, with no evidence of vascularization (Tanaka et al., 2020). This has led to efforts in creating

brain organoids with vasculature (Cakir et al., 2019; Daviaud et al., 2018; Mansour et al., 2018; Pham et al., 2018; Shi et al., 2020; Song et al., 2019a).

Despite the fact that self-patterned methods produce more heterogeneous cell populations, with limited spatial organization, similar cell types, gene expression profiles, and developmental trajectories were observed across distinct differentiation methods (Tanaka et al., 2020), with exception of some metabolic genes that are indicative of cell stress caused by *in vitro* culture (Bhaduri et al., 2020; Pollen et al., 2019). Furthermore, studies have been performed to compare brain organoids with other tissues, including non-human primates' brains (chimpanzee and macaque) (Kanton et al., 2019; Pollen et al., 2019) and human fetal brain (Amiri et al., 2018; Camp et al., 2015; Gordon et al., 2021; Nascimento et al., 2019; Tanaka et al., 2020; Velasco et al., 2019). Although some genes were differentially expressed, several gene networks are conserved across human and non-human primates (Pollen et al., 2019), with human organoids showing delayed maturation with respect to other primates (Kanton et al., 2019). On the other hand, gene expression patterns of human brain organoids are preserved comparing to human brain tissue and resemble aspects of *in vivo* human corticogenesis, including the proliferation and self-renewal capacity of neural progenitor cells, production of extracellular matrix, neuronal migration and differentiation (Camp et al., 2015; Kanton et al., 2019). It was also reported that several cell types, such as mature astrocytes, only appear later in organoid development, which is also in accordance with the observed in human development (Gordon et al., 2021). Therefore, despite limitation and lack of important cellular population that exist in the "natural" brain, long-term maturation of brain organoids correlates with *in vivo* development not only at the epigenetic and transcriptomic levels, but also in a chronological manner (Gordon et al., 2021; Tanaka et al., 2020).

1.9. Functional properties of brain organoids

Together with the complexity and cell composition of brain organoids, it is crucial to assess their maturation and the establishment of functional synapses and neural networks. Patch-clamp, optogenetics, calcium (Ca^{2+}) imaging and multielectrode arrays (MEA) have been several of the different and complementary methods used to evaluate the electrophysiological activity in brain organoids (**Table 1 and Table 2**). Patch-clamp can give the most detailed information about an individual cell, including its intrinsic properties, such as the membrane resistance, capacitance, resting membrane potential and ion channel activity and even network connectivity.

To overcome the variability associated with the production of whole-brain organoids, improvements have been made, which included the generation of cell and region-specific models (Andersen et al., 2020; Birey et al., 2017; Miura et al., 2020; Monzel et al., 2017; Paşca et al., 2015; Xiang et al., 2019, 2017). In 2015, Paşca developed the first human region-specific organoids, the hCSs. These cortical spheroids presented spontaneous activity, evaluated by Ca^{2+} imaging, at 130 days of age, and present the capability to fire action potentials upon depolarizing current injection (Paşca et al., 2015). Notably, at earlier ages, using the same amount of depolarizing currents, less firing of action potentials was observed, with lower amplitudes, higher threshold and slower kinetic of repolarization (R. Li et al., 2017). Similarly, sEPSCs were only observed at later stages, following more pronounced neuronal maturation (R. Li et al., 2017).

The assembly of organoids resembling different brain regions allowed to study brain connectivity between multiple regions during brain development and disease. The contribution of the inhibitory system is notorious upon migration of inhibitory neurons from the ventral to the dorsal forebrain, with an overall increase in synaptic inputs and in the frequency of the action potentials generated (Birey et al., 2017). Recently, thalamo-cortical (Xiang et al., 2019), cortico-striatal (Miura et al., 2020), and cortico-motor (Andersen et al., 2020) organoids were developed and in all these cases, functional interactions were observed, as well as improvements in the electrophysiological capability. For example, Xiang and colleagues showed by whole-cell patch clamp that thalamic neurons from thalamocortical organoids (hThCOs) displayed increased firing frequency compared to thalamic neurons from non-fused thalamus organoids (hThOs) (Xiang et al., 2019). Moreover, striatal neurons (hStrS) from cortico-striatal assembloids also showed increased frequency of action potentials and higher frequency of spontaneous activity after fusion (Miura et al., 2020). Likewise, Andersen demonstrated more spontaneous contractions after fusion of human cortical spheroids, human spinal spheroids and human skeletal muscle spheroids (hCSs-hSpS-hSkM) (Andersen et al., 2020). Additionally, in some of these studies, optogenetic stimulation was used to validate the connections between assembloids (Andersen et al., 2020; Miura et al., 2020).

In a recent and elegant study, the neuronal network dynamic was evaluated over several months and compared with a human preterm neonatal electroencephalogram (EEG) (Trujillo et al., 2019). Using whole-cell patch clamp, it was shown that action potential firing activity was inhibited by glutamate receptor antagonists, revealing the presence of functional excitatory synapses. At the mesoscopic level, MEA revealed

increases in electrical activity over the course of 10 months. Additionally, the network activity progressed from periodic but infrequent events to repetitive and regular nested oscillatory networks, reaching a higher spatiotemporal complexity and variability, which resemble self-organized networks. Moreover, using machine learning procedures, the authors demonstrated similarities between the network transitions present in cortical organoids to the EEG of a preterm human newborn (Trujillo et al., 2019).

Bioengineered neuronal organoids (BENOs) were generated to improve the maturation time and functional properties of brain organoids (Zafeiriou et al., 2020). This protocol was implemented using dispersed hiPSCs in collagen type I, followed by controlled differentiation and maturation protocol using defined media and a variety of factors (collagen, small molecules, and growth factors.) in a 1-step culture. Using Ca^{2+} imaging and MEA, the authors reported complex network function after 2 months of culture. These features seem to be similar to the reported ones by Trujillo after 7 months of brain organoids culture (Trujillo et al., 2019; Zafeiriou et al., 2020). BENOs displayed an increase in the frequency of Giant depolarizing potential (GDP)-like events in earlier stages of development and a decrease in later stages, as observed during fetal development, as well as the switch of GABA from excitatory to inhibitory neurotransmission – indicative of neuronal network maturation. Additionally, BENOs showed long- and short-term potentiation (LTP/STP) or depression (LTD/STD), which is a phenomenon associated with neuronal plasticity, validating the network function of this model (Zafeiriou et al., 2020).

Considering the lack of microglia as one of the limitations associated to these models, several authors have been generating microglia from hiPSCs and seeding them into brain organoids (Abud et al., 2017; Bodnar et al., 2021; Fagerlund et al., 2021; Popova et al., 2021; Sabate-Soler et al., 2022; Song et al., 2019b; Xu et al., 2021). Xu et al. showed that neurons from microglia-containing brain organoids were functionally mature, presenting voltage-gated Na^+ and K^+ currents, firing action potentials upon current injection, but also displaying spontaneous action potentials and spontaneous postsynaptic currents (sPSCs) at 90 days (Xu et al., 2021). Nonetheless, the authors did not compare microglia-containing brain organoids with brain organoids without microglia, which would be essential to evaluate the microglia effect on brain organoids development. More recently, hiPSCs differentiated into erythromyeloid progenitors were allowed to mature into microglia-like cells within the organoid environment (Fagerlund et al., 2021). The authors showed larger Na^+ and K^+ currents density, increased sEPSCs, increased firing activity of action potentials and increased neuronal networks in microglia-containing brain organoids than in their counterparts lacking microglia

(Fagerlund et al., 2021). This was observed both at 107-120 days and 150-165 days with a higher intensity in the later stage. However, at 200-213 days the same was not observed, probably due to the excessive time spent in culture and increased cell death (Fagerlund et al., 2021). This is correlated with other studies where the authors also reported increased excitability of neurons in organoids containing microglia (Popova et al., 2021; Sabate-Soler et al., 2022). These observations are in line with the known roles of microglia in neurodevelopment, including synaptic pruning to eliminate extra and inactive synapses, strengthening and supporting active synapses, contributing for neuronal maturation, and support the relevance of introducing microglia into brain organoids (Guedes et al., 2022).

Another drawback of these 3D models is related to the lack of vasculature, which directly influences normal neuronal development, due to the formation of a nutrient and oxygen gradient from the surface to the core of the organoids, leading to a cytotoxic environment in the center of large organoids. Therefore, protocols have been developed to create vascularized organoids (Cakir et al., 2019; Daviaud et al., 2018; Mansour et al., 2018; Pham et al., 2018; Shi et al., 2020; Song et al., 2019a) and the functional properties of the neurons were analyzed (Shi et al., 2020). The authors observed differences in the intrinsic properties of neurons, but also in neuronal networks. Neurons in vascularized organoids presented lower resting membrane potential, increases in outward current amplitudes over time and higher firing frequencies. These results suggest that vascularization supports neuronal maturation.

Overall, brain organoids display neuronal and network activity with signs of increased neuronal maturation over time, resembling the human fetal development. Moreover, microglia and vasculature may be important elements to consider for additional complexity and maturation of the model.

1.10. Reliability of brain organoids

Brain organoids are known to be robust models to study neurodevelopmental disorders as they recapitulate key features of human brain development. However, several concerns have been pointed out in the field regarding the reproducibility of these models, as they are based on cell culture and are subject of similar issues from the traditional cell cultures, such as cell line differences and batch effects. To measure the robustness and efficiency of these models it is important to assess the cell type distribution among different batches of organoids and from different starting cell lines, and whether the developmental and transcriptional timings are similar to those found in the developing human brain.

Variability is an important factor to keep in mind when performing disease modelling studies using brain organoids, as these studies typically rely on comparing multiple patient and control cell lines that have distinct genetic backgrounds. Recent studies have shown that organoids generated from patient-derived cell lines showed higher variability when compared to brain organoids from isogenic cell lines (Hernández et al., 2021). While this allows for the opportunity of having a more diverse and representative cell-type composition, it decreases the predictability of this method in terms of generating homogenous neuronal populations. Quadrato and colleagues used single-cell RNA sequencing to assess 80,000 individual cells from brain organoids and found that radial glia progenitors were present in all organoids samples, whereas cortical interneurons and intermediate progenitors were present in only 50% of the organoids (Quadrato et al., 2017). This variability has been the center point in the optimization of self-patterned and patterned protocols that give rise to a more homogeneous, and thus less diverse, population of cells. For instance, using poly(lactide-co-glycolide) copolymer fiber microfilaments as floating scaffolds, an increase in organoid surface area and facilitation in neuronal induction was observed (Lancaster et al., 2017). Additionally, region-specific protocols have also shown to increase cell homogeneity. Cortical spheroids that recapitulate ventral and dorsal forebrain development have shown to be reproducible, upon differentiation from multiple human pluripotent stem cell lines, as only 8.4% of the variance was due to cell line differences and overall variability was shown to decrease with differentiation (Yoon et al., 2019). A recent study (Bhaduri et al., 2020) has compared the transcriptional profile of brain organoids generated using both self-patterned and patterned protocols and has shown that, although they do not fully recapitulate transcriptional profiles of the fetal brain as they are missing key cell types and extra cortical inputs, they are reproducible in terms of gross, overall cell composition.

Taken together, these observations indicate that brain organoids are promising models that have been improved to better recapitulate several features of the *in vivo* brain development (**Fig. 1.5**). Overall, they present heterogenous populations of cells that contribute for neuronal maturation and development of functional neuronal networks. These models will allow the study of underlying cellular and molecular features of several neurodevelopmental and neuropsychiatric disorders, including the ones caused by anti-CASPR2 autoantibodies.

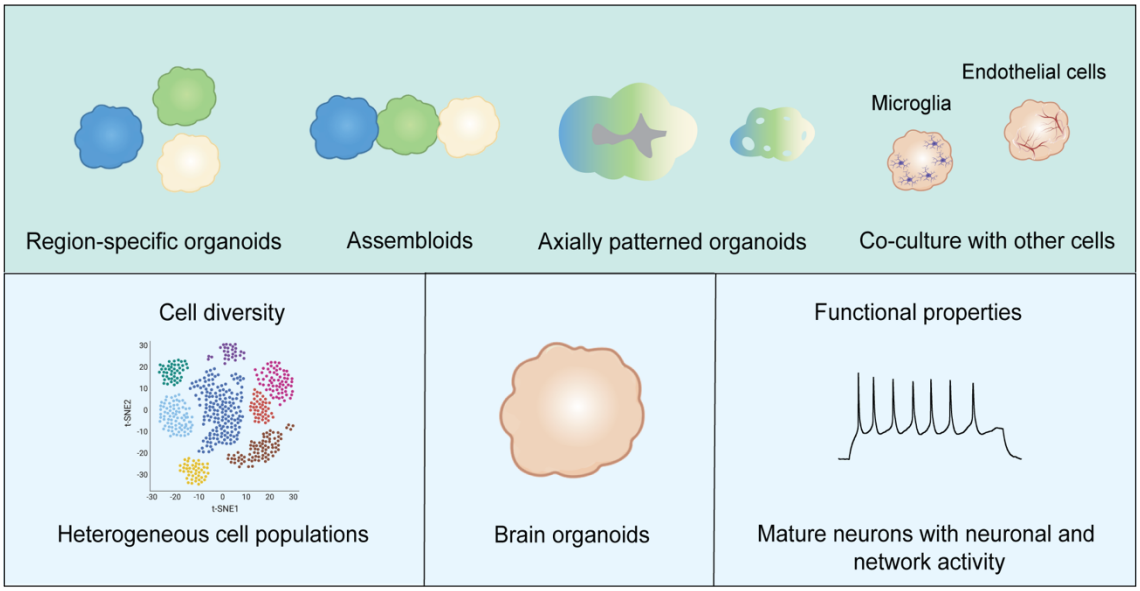

Figure 1.5. Brain organoids features and technologies. Brain organoids present a wide variety of cell populations and display neuronal activity. Different protocols have been generated to improve the field's needs, including the generation of region-specific organoids, assembloids, axially patterned organoids and co-culture of organoids with different cells.

Table 1. Functional properties of human brain organoids assessed by whole-cell patch clamp.

Protocol	Main focus	Electrophysiological technique	Organoid's age	Organoid's preparation	Drugs	Main findings related to functionality	References
Guided (hCSs)	Model validation (cell-subtype specification)	Whole-cell patch clamp	~130 days	Dissociated hCSs (cultured in monolayer for 2 weeks) Slices	TTX, D-AP5, NBQX, Kynurenic acid	Monolayer/slices: APs (20pA) sEPSCs Monolayer: Na^+ and K^+ currents	(Paşca et al., 2015)
Guided (forebrain organoids)	Model validation (regional specification)	Whole-cell patch clamp	~100 days	Slices	Gabazine, DNQX, TTX	APs (10 pA) Rectifying membrane properties Na^+ and K^+ currents sEPSCs and sIPSCs	(Qian et al., 2016)
Guided (midbrain organoids)	Model validation (cell-subtype specification)	Whole-cell patch clamp	33-50 days 65-84 days	Slices	CNQX, AP5, PTX, Quinpirole	↑ Na^+ and K^+ currents over time ↓ Rm and ↑ Cm over time APs (10pA) sEPSCs, sIPSCs, sEPSPs Rhythmic discharged (mDAs)	(Jo et al., 2016)
Guided (assembloid: hCS + hSS)	Regional specification and interaction	Whole-cell patch clamp	96-141 days	Slices	Gabazine, Kynurenic acid	hSS: APs (5pA) sIPSCs hCS+hSS: ↑ AP rate; Dlxi1/2b::eGFP$^+$ cells that migrated into the hCS display EPSCs and iPSCs Glutamatergic cells from hCS display EPSCs and iPSCs Evoked EPSCs and iPSCs (neuronal integration into a functional microcircuit)	(Birey et al., 2017)

Guided (hCOs)	Cell-subtype specification	Whole-cell patch clamp	51, 62, 121 days	Slices	TTX	sEPSCs on day 121 APs with higher amplitude and faster kinetic of repolarization on day 121 than 51	(R. Li et al., 2017)
Guided (assembloid: hCOs + hMGEOs)	Regional specification and interaction	Whole-cell patch clamp	Not defined	Slices	No drugs	hMGEOs: APs (+5pA)	(Xiang et al., 2017)
Unguided (hCOs)	Model validation	Whole-cell patch clamp	11-12 weeks	Slices	TTX	APs Na^+ and K^+ currents Cells with APs: > Na^+/K^+ currents Intrinsic properties similar to slices of human fetal cortex from gestational weeks 16–22	(Watanabe et al., 2017)
Guided (assembloid: hThCOs)	Model validation	Whole-cell patch clamp	90-100 days	Slices	No drugs	hThCOs + hCOs: > frequency than non-fused hThCOs	(Xiang et al., 2019)
Unguided (whole-brain organoids)	Model validation	Whole-cell patch clamp	Not defined	ALI-CO slices	No drugs	Trains of APs	(Giandomenico et al., 2019)
Guided (hCOs)	Model validation	Whole-cell patch clamp	6 months	Intact organoids	TTX, CNQX, AP5	APs Na^+ and K^+ currents sEPSCs	(Trujillo et al., 2019)
Unguided (whole-brain organoids)	Model validation	Whole-cell patch clamp	12, 24 weeks	Slices	No drugs	Developing neurons: APs with slow kinetics and small amplitudes sEPSCs Na^+ and K^+ currents Mature neurons: APs with fast kinetics and high amplitudes sEPSCs Bigger Na^+ and K^+ currents than developing neurons	(Sivitilli et al., 2020)

Guided (BENOs)	Model validation	Whole-cell patch clamp	35-65 days	Slices	TTX	EPSPs Na^+ and K^+ currents	(Zafeiriou et al., 2020)
Guided (assembloid: hCOs + hStrSs)	Regional specification and interaction	Whole-cell patch clamp Optogenetics + whole-cell patch clamp	110-120 days; 160-170 days	Slices	No drugs	<u>Whole-cell patch clamp:</u> hStrS: Inward rectification APs (slow-ramp depolarization) Hyperpolarized RMP (~ -80mV) hCOs + hStrSs: (compared to hStrSs alone) ↑ excitability ↓ spike half-widths ↑ sEPSCs <u>Optogenetics + whole-cell patch clamp:</u> hCOs + hStrSs: oEPSCs (optically evoked) oEPSPs APs	(Miura et al., 2020)
Guided (assembloid: hCS + hSpS + hSkM)	Regional specification and interaction	Whole-cell patch clamp Optogenetics + whole-cell patch clamp	Not defined	Slices	TTX	<u>Whole-cell patch clamp:</u> hSpS: APs <u>Optogenetics + whole-cell patch clamp:</u> hCS + hSpS EPSCs after light stimulation	(Andersen et al., 2020)

Guided (hCOs)	Model validation (vascularization)	Whole-cell patch clamp	60, 80, 90, 210 days	Slices	Bicuculline methiodide	<u>Whole-cell patch clamp:</u> ↑ outward current amplitudes ↑ APs firing frequency More negative RMP ↑ spontaneous activity <u>Dual patch clamp:</u> Electrical synapses	(Shi et al., 2020)
Guided	Model validation (microglia)	Whole-cell patch clamp	90-92 days	Slices	No drugs	Na^+ and K^+ currents APs Spontaneous APs sPSCs	(Xu et al., 2021)
Unguided	Model validation (microglia)	Whole-cell patch clamp	107-120 days 150-165 days	Slices	No drugs	↑ Na^+ and K^+ currents ↑ APs firing frequency ↑ sEPSCs	(Fagerlund et al., 2021)
Guided (midbrain organoids)	Model validation (microglia)	Whole-cell patch clamp	35 days	Intact organoids	No drugs	↑ Na^+ currents ↓ threshold potential ↑ excitability	(Sabate-Soler et al., 2022)

hCSs: human cortical spheroids; **hSS:** human subpallium spheroids; **hCOs:** human cortical organoids; **hMGEOs:** human medial ganglionic eminence organoids; **hThCOs:** human fused thalamus-cortex organoids; **ALI-CO:** air-liquid interface cerebral organoids; **BENOs:** Bioengineered Neuronal Organoids; **hStrSs:** human striatal spheroids; **hSpS:** human spinal spheroids; **hSkM:** human skeletal muscle spheroids; **mDAs:** midbrain dopaminergic neurons.
APs: action potentials; s**PSCs:** spontaneous postsynaptic currents **sEPSCs:** spontaneous excitatory postsynaptic currents; **sIPSCs:** spontaneous inhibitory postsynaptic currents; **sEPSPs:** spontaneous excitatory postsynaptic potentials; **RMP:** resting membrane potential.

Table 2. Functional properties of human brain organoids assessed by calcium imaging and multielectrode arrays.

Protocol	Main focus	Electrophysiological technique	Organoid's age	Organoid's preparation	Drugs	Main findings related to electrophysiology	References
Unguided (whole-brain organoids)	Model validation	Ca^{2+} imaging (Fluo4)	Not defined	-	Glutamate, TTX	Spontaneous Ca^{2+} activity	(Lancaster et al., 2013)
Guided (hCSs)	Model validation (cell-subtype specification)	Ca^{2+} imaging (Fura2/Fluo4)	~130 days	Dissociated hCSs (cultured in monolayer for 2 weeks) hCSs slices	No drugs	Monolayer/slices: Spontaneous Ca^{2+} activity	(Paşca et al., 2015)
Guided (forebrain organoids)	Model validation (regional specification)	Ca^{2+} imaging (Fluo4-AM)	~100 days	Slices	Glutamate, GABA, Bicuculline	Ca^{2+} rise in response to GABA-induced depolarization at earlier ages	(Qian et al., 2016)
Guided (assembloid: hCS + hSS)	Regional specification and interaction	Ca^{2+} imaging (Fura2)	43-52 days	Intact organoids	KCl	hCS/hSS: Ca^{2+} activity after depolarization	(Birey et al., 2017)
Unguided (whole-brain organoids)	Model validation	MEA	4 months 8 months 7-9 months (light stimulation)	Intact organoids	TTX NBQX	APs at 8mo Excitatory monosynaptic connections Non-NMDAR-mediated excitatory synaptic transmission Network activity with self-organized patterns of activity Firing rate after light exposure (4 out of 10 organoids) ↑ cFos after light exposure	(Quadrato et al., 2017)

Guided (midbrain organoids)	Model validation (cell-subtype specification)	Ca^{2+} imaging (Fluo4-AM) MEA	Ca^{2+} imaging: 50-52 days MEA: 82-84 days	Intact organoids	Quinpirole	<u>Ca^{2+} imaging:</u> Spontaneous activity with regular firing patterns, resembling the pacemaker activity of mDNs <u>MEA:</u> Spontaneous activity Neuronal network synchronicity	(Monzel et al., 2017)
Guided (hCOs)	Cell-subtype specification	Ca^{2+} imaging (Fluo4-AM)	85 days	Slices	TTX	Spontaneous activity	(R. Li et al., 2017)
Guided (assembloid: hCOs + hMGEOs)	Regional specification and interaction	Ca^{2+} imaging (AAV1.syn.GCaMP6s.WPRE.SV40)	40-50 days	Intact organoids	TTX, Bicuculline	hMGEOs/hCOs: Spontaneous activity; synchronization (=functional neuronal networks)	(Xiang et al., 2017)
Unguided (hCOs)	Model validation	Ca^{2+} imaging (AAV1-Syn.GCaMP6f.WPRE.SV40)	Not defined	Intact organoids	No drugs	Spontaneous activity with partial synchronization	(Watanabe et al., 2017)
Guided (assembloid: hThCOs)	Model validation	Ca^{2+} imaging (AAV1.syn.GCaMP6s.WPRE.SV40)	48 days	Intact organoids	No drugs	hThOs/hThCOs: Spontaneous synchronized activity	(Xiang et al., 2019)
Guided	Model validation	Ca^{2+} imaging (Fluo4-AM)	76-104 days (intact organoids) 16-30 days after dissociation (dissociation: 70-100 days)	Intact organoids Dissociated cells	Glutamate, Bicuculline, CNQX, D-AP5	Intact organoids: Asynchronous spontaneous activity Cells: 16 days after dissociation: Asynchronous spontaneous activity 30 days after dissociation: Synchronized spontaneous activity Drug-induced dynamic change of the neural networks	(Sakaguchi et al., 2019)

Unguided (whole-brain organoids)	Model validation	MEA	117 days (sliced at 63 days plus 54 days under ALI conditions)	ALI-CO slices	TTX	Spontaneous activity Network bursts Muscle contraction after ALI-CO axon tracts stimulation	(Giandomenico et al., 2019)
Guided (hCOs)	Model validation	MEA	2, 4, 6 and 8 months	Intact organoids	TTX, AP5, CNQX, Bicuculline, Picrotoxin; Baclofen; Muscimol	↑ electrical activity (channel-wise firing rate, burst frequency and synchrony) over time Synchronous activity Network activity data in organoids correlates with EEG data of preterm human infants	(Trujillo et al., 2019)
Guided (BENOs)	Model validation	Ca^{2+} imaging (Flu8-AM) MEA	Ca^{2+} imaging: 20-98 days MEA: 20-57 days	Ca^{2+} imaging: Intact BENOs MEA: Slices	Ca^{2+} imaging: TTX PTX CNQX MK-801 Saclofen	<u>Ca^{2+} imaging:</u> GDP-like events in early and intermediate BENOs stages, but not in later BENOs stages, indicative of a developmental switch of GABA from excitatory to inhibitory activity Paired-pulse depression (PPD) <u>MEA:</u> ↑ individual bursts and network bursts at later stages LTP, LTD, STP and STD observed 1h after HFS	(Zafeiriou et al., 2020)
Unguided (whole-brain organoids)	Model validation	MEA	34, 64, 99, 120, 161 days	Intact organoids	No drugs	↑ number of spikes, bursts and spike rates over time	(Fair et al., 2020)

Guided (assembloid: hCOs + hStrSs)	Regional specification and interaction	Ca^{2+} imaging (AAV.GCaMP6) Optogenetics + Ca^{2+} imaging	90-145 days	Intact organoids	Ca^{2+} imaging: NBQX, AP5, Bicuculline Optogenetics + Ca^{2+} imaging: NBQX, AP5	<u>Ca^{2+} imaging:</u> hStrS: Spontaneous and synchronized activity <u>Optogenetics + Ca^{2+} imaging:</u> hCOs + hStrSs: ↑ activity after light stimulation ↑ signal at later stages Glutamatergic transmission from hCSs to hStrSs	(Miura et al., 2020)
Guided (assembloid: hCS + hSpS + hSkM)	Regional specification and interaction	Ca^{2+} imaging (Cal590-AM, AAV.GCaMP7s) Optogenetics + Ca^{2+} imaging Glutamate uncaging Optogenetics + glutamate uncaging	Ca^{2+} imaging: 29-46 daf (hCS + hSpS) Optogenetics + Ca^{2+} imaging: 4-5 weeks, 7-8weeks Glutamate uncaging: Not defined Optogenetics + glutamate uncaging: Not defined	Intact organoids	Optogenetics + Ca^{2+} imaging: NBQX, AP5 Optogenetics + glutamate uncaging: NBQX, AP5	<u>Optogenetics + Ca^{2+} imaging:</u> hCS + hSpS: ↑ activity after light stimulation Glutamatergic transmission from hCSs to hSpS. hCS + hSpS + hSkM: ↑ Ca^{2+} spikes in hSkM fibers upon light stimulation <u>Glutamate uncaging:</u> hCS+ hSpS + hSkM: ↑ spontaneous contractions compared to hSkM alone or hCS-hSkM assembloids More coordination <u>Optogenetics + glutamate uncaging:</u> hCS+ hSpS + hSkM: hSkM contraction after light stimulation	(Andersen et al., 2020)
Guided (hCOs)	Model validation (vascularization)	Ca^{2+} imaging	50, 85 days	Slices	TTX, CNQX, AP5, bicuculline methiodide, glutamate	Spontaneous Ca^{2+} activity	(Shi et al., 2020)

Unguided	Model validation (microglia)	3D MEA	150-165 days 200-213 days	Slices	NMDA	↑ spontaneously active electrodes ↑ firing and bursting activity	(Fagerlund et al., 2021)
Guided (midbrain organoids)	Model validation (microglia)	MEA	35 days	Intact organoids	No drugs	↓ interspike interval	(Sabate-Soler et al., 2022)

hCSs: human cortical spheroids; **hSS:** human subpallium spheroids; **hCOs:** human cortical organoids; **hMGEOs:** human medial ganglionic eminence organoids; **hThCOs:** human fused thalamus-cortex organoids; **ALI-CO:** air-liquid interface cerebral organoids; **BENOs:** Bioengineered Neuronal Organoids; **hStrSs:** human striatal spheroids; **hSpS:** human spinal spheroids; **hSkM:** human skeletal muscle spheroids; **mDNs:** midbrain dopaminergic neurons; **daf:** days after fusion.
APs: action potentials; **LTP:** long-term potentiation; **LTD:** long-term depression; **STP:** short-term potentiation; **STD:** short-term depression; **GDP:** Giant-depolarizing potential; **EEG:** electroencephalogram.

OBJECTIVES OF THE PRESENT STUDY

Considering the contribution of anti-CASPR2-Ab to neuropsychiatric and neurodevelopmental disorders, our main aim was to evaluate the impact of these antibodies in an earlier phase of human brain development, using human brain organoids. To assess the ability of this new model to recapitulate the early stages of human brain development, we:

1. Generated and characterized hiPSCs-derived whole-brain organoids (**Task 1**).
   1.1. Expression levels of neuronal and glial markers over time in brain organoids
   1.2. Functional neurophysiological properties of brain organoids and key timelines to observe robust neuronal activity

2. Evaluated the effect of anti-CASPR2-Ab on neurodevelopment and characterized hiPSCs-derived whole-brain organoids after exposure to anti-CASPR2-Ab (**Task 2**).
   2.1. Binding specificity of anti-CASPR2-Ab to the CASPR2 protein in cortical neuronal cultures and HEK cells
   2.2. Expression levels of CASPR2-related proteins and genes in brain organoids exposed to anti-CASPR2-Ab
   2.3. Functional neuronal properties changes in brain organoids exposed to anti-CASPR2-Ab

Furthermore, we aimed to assess the potential of whole-brain organoids use as models for genetic-driven frontotemporal lobar degeneration. Specifically, new human disease-specific hiPSCs lines from patients with mutation in the granulin gene (*GRN*) (**Task 3**). In this part of the work, we assessed the pluripotency and trilineage differentiation capacity of the generated lines; characterized these cells and their ability to generate whole-brain organoids for future studies.

CHAPTER 2
METHODS

2.1. Fibroblasts culture from skin biopsy

Skin punch biopsies were collected at Centro Hospitalar e Universitário de Coimbra (CHUC), according to the approval of the Ethics Committee of the Faculty of Medicine, University of Coimbra (Project CE-028/2016) and following the guidelines of the Declaration of Helsinki. Data were treated confidentially according to the General Data Protection (GDPR), Regulation (EU) 2016/679 of the European Parliament and of the Council of 27 April 2016. The dissection of each skin punch biopsy and isolation of fibroblasts were performed following the protocol described by Vangipuram (Vangipuram et al., 2013). In brief, the epidermis was excluded, and the dermis was cut into small pieces and placed into a 6-well plate (Thermo Fisher Scientific) (3 pieces/well). The samples were covered with a coverslip and fibroblasts medium (DMEM – D5648 (Sigma), supplemented with 44 mM $NaHCO_3$ (Fisher Scientific), 1 mM Na-pyruvate (Gibco), 1% penicillin/streptomycin (Gibco) and 10% of heat-inactivated FBS, pH 7.3). The cells were maintained at 37ºC in a humidified atmosphere containing 5% CO_2. Once fibroblasts were confluent, the cells were expanded and subsequently used for reprogramming.

2.2. HEK293T cell line culture and transfection

Human embryonic kidney (HEK) 293T cell line was maintained at 37ºC in a humidified atmosphere containing 5% CO_2 in DMEM D5648 (Sigma), supplemented with 44 mM $NaHCO_3$ (Sigma), 1% penicillin/streptomycin (Gibco) and 10% of heat-inactivated FBS, at pH 7.2.

HEK293T cells were cultured in 12-well plates (Thermo Fisher Scientific) with 18 mm poly-L-lysine-coated glass coverslips at a density of 1×10^5 cells/well. The following day, cells were transfected using the calcium phosphate method. Briefly, 4 μg of pCASPR2-EGFP or pCTR(control)-EGFP diluted in ddH_2O were added dropwise to a 2 M $CaCl_2$ solution. This mixture was then added to a HEPES Buffered Saline solution (HBS: 50 mM HEPES, 280 mM NaCl, 1.5 mM Na_2HPO_4, pH 7.05) and immediately added, dropwise, to the cells. The cells were incubated at 37ºC, 5% CO_2 for 5 h. After 5 h, fresh culture medium was added and the cells were kept in the incubator (37ºC, 5% CO_2) for 48 h.

2.3. Primary culture of rat cortical neurons

Low-density Banker primary cultures of rat cortical neurons were prepared from the cortices of E18 Wistar rat embryos. All procedures were reviewed and approved by the Portuguese National Authority for Animal Health (DGAV). Shortly, the tissue was dissected and treated for 15 min at 37ºC with 0.06% trypsin (Gibco) in Ca^{2+}- and Mg^{2+}-free Hank's balanced salt solution (HBSS: 5.36 mM KCl, 0.44 mM KH_2PO_4, 137 mM NaCl, 4.16 mM $NaHCO_3$, 0.34 mM $Na_2HPO_4.2H_2O$, 5 mM glucose, 1 mM Na-pyruvate, 10 mM HEPES and 0.001% phenol red). Then, cells were washed 6 times in HBSS and mechanically dissociated. Cells were plated in neuronal plating medium (Minimal Essential Medium (MEM) supplemented with 10% horse serum, 0.6% glucose and 1 mM pyruvic acid) onto poly-D-lysine-coated (0.1 mg/mL) coverslips in 60 mm tissue culture plates at a density of 3×10^5 cells/plate. After 2 – 4 h, coverslips were flipped over an astroglial feeder layer in Neurobasal medium (NBM) supplemented with SM1 neuronal supplement (Stem Cell Technologies), 0.5 mM glutamine (Sigma) and 0.12 mg/mL gentamycin (Gibco). Neurons were grown faced down over the feeder layer and wax dots on the neuronal side of the coverslip allowed the physical separation of neurons from glial cells. To further prevent glia overgrowth, neuronal cultures were treated with 10 µM of 5-Fluoro-2'-deoxyuridine (Sigma) after 3 days *in vitro* (DIV). Cortical cultures were maintained at 37°C in a humidified atmosphere containing 5% CO_2, for up to 13 DIV.

2.4. Live cell-based assay

The specificity of binding to CASPR2 was assessed using a live cell-based assay in transfected HEK293T cells and DIV 11-13 cortical neurons, where patient and healthy plasma (20 µg/mL) were diluted and added, for 1h, to live HEK293T cells expressing EGFP-CASPR2 or EGFP-CTR and to live cortical neurons.

To evaluate antibodies depletion in organoids medium over time, brain organoids medium containing patient and healthy plasma was collected and re-incubated in HEK293-transfected cells.

Afterwards, cells were fixed in 4% PFA for 10 min at room temperature (RT) and kept at 4°C in PBS 1x for subsequent immunocytochemistry experiments.

2.5. Clinical history of anti-CASPR2 encephalitis patient

Plasma exchange samples obtained from a 72-year-old male patient with anti-CASPR2 autoimmune encephalitis**,** experiencing periods of disease exacerbation, were collected at the John Radcliffe Hospital, Oxford University. The patient presented high

levels of CASPR2 autoantibodies, developed Morvan's syndrome, progressive neuropathic pain, episodes of lack of perception with goosebumps, and memory complaints (short- and long-term memory, including word-finding difficulties), with no indication of paraneoplastic causes. Written informed consent was obtained from patient and healthy controls.

2.6. Generation and maintenance of human induced pluripotent stem cells (hiPSCs)

Human dermal fibroblasts were reprogrammed by episomal nucleofection of Yamanaka factors as described by Howden et al. with several modifications (Howden et al., 2015). Human dermal fibroblasts were cultured in fibroblast medium at 37ºC in a humidified atmosphere containing 5% CO_2. Cells were harvested and 1 x 10^6 cells per condition were resuspended in 100 μL PBS 1x. The cell suspension containing 1.5 μg of the following reprogramming constructs: pCXLE-hOCT3/4-shp53-F (Addgene, #27077), pCXLE-hUL (Addgene, #27080), pCXLE-hSK (Addgene, #27078) and pSimple-miR302/367 (Addgene, #98748) was added to a 0.2-cm cuvette (Mirus) and electroporated on an Amaxa Nucleofactor II (Lonza) device. Following electroporation, cells were plated on a 10-cm gelatin-coated tissue culture plate with the respective medium and incubated at 37ºC and 5% CO_2. Then, the medium was replaced every day with fresh medium containing 0.5 mM sodium butyrate (Stem Cell Technologies). On day 7, cells were dissociated and plated on 6-well Matrigel-coated plates (Thermo Fisher Scientific) with medium containing 0.5 mM sodium butyrate (Stem Cell Technologies). On day 8, medium was replaced by mTeSR Plus (Stem Cell Technologies) with 0.5 mM sodium butyrate (Stem Cell Technologies) and changed every other day until day 12. From day 12, medium was replaced every other day with mTeSR Plus (Stem Cell Technologies) until iPSCs colonies emerged. Emerging colonies were manually collected for single cell clone expansion. After iPSCs isolation, cells were maintained and expanded in mTeSR Plus (Stem Cell Technologies) with manual passages until around passage 4. Hereafter, the ReLeSR (Stem Cell Technologies) passaging reagent was used for gentle colonies dissociation. After expansion, the cells were used for characterization and further experiments.

31f-r1 hiPSCs were kindly provided by Prof. Dr. Oliver Brüstle from the University of Bonn (iLB-C-31f-r1). These cells were reprogrammed from human dermal fibroblasts by lentiviral infection of Yamanaka factors (Oct3/4, Sox2, c-Myc, Klf4). 31f-r1 hiPSCs were cultured in Matrigel-coated plates (Thermo Scientific) with mTeSR Plus (Stem Cell

Technologies), supplemented with 1% Penicillin/Streptomycin (Gibco), at 37ºC and 5% CO_2. The cells were passaged every 3-5 days using ReLeSR (Stem Cell Technologies) for gentle colonies dissociation.

2.7. Trilineage assay*: in vitro* spontaneous differentiation

iPSCs differentiation into the three germ layers was performed as described by Varga and colleagues (Varga et al., 2017). Firstly, cells were harvested for embryoid body (EB) formation (Lancaster et al., 2013). Five days later, the EBs formed were plated on Matrigel-coated µ-slide 8-well ibiTreat chamber slides (ibidi) in differentiation medium (DMEM/F-12 (Gibco), 20% heat-inactivated FBS, 1% MEM non-essential amino acid solution (Gibco), 0.1 mM β-mercaptoethanol (Sigma) and 1% penicillin/streptomycin (Gibco)). The medium was changed every other day until day 14 of differentiation. On day 14, the cells were fixed with 4% PFA for 20 min at RT and kept at 4ºC in PBS 1x for later validation by immunocytochemistry and qPCR.

2.8. Karyotyping

Karyotype processing and analysis was performed by Laboratórios Germano de Sousa (Lisbon, Portugal). Thirty independent metaphases were counted.

2.9. Sequencing

DNA was extracted from hiPSCs using the NZY Tissue gDNA Isolation kit (Nzytech), following the manufacturer's instructions. The entire coding region of the *GRN* gene (NM_002087.3) was amplified by PCR using specific primer sequences flanking the intron-exon boundaries. Genomic DNA (100 ng) was amplified in a 25 µL reaction volume, using 0.5 µM of each primer, 1.5 mM $MgCl_2$, 0.2 mM dNTPs, and 0.5 unit of Taq polymerase (Promega). The amplicons were purified using a High Pure PCR Product Purification Kit (Roche), according to the manufacturer's protocol. Subsequently, the PCR products were directly sequenced on a capillary automated sequencer CEQ 8000 (Beckman Coulter). The presence of the pathogenic variant and the co-segregation studies were performed on a separate amplification of the exon 9 of the *GRN* gene with subsequent direct sequencing.

2.10. Immunocytochemistry

The binding specificity of CASPR2 plasma was assessed in HEK293T transfected cells and in rat cortical neurons. Briefly, cells were washed 3 times with PBS 1x and permeabilized with 0.25% Triton X-100 in PBS 1x for 5 min at 4ºC and non-specific binding epitopes were blocked by incubating cells with PBS 10% BSA for 30 min at 37ºC.

For the transfected HEK 293T cells, a rabbit anti-GFP primary antibody (1:750; MBL #598) was used and for the cortical neurons a guinea pig anti-MAP2 primary antibody (1:1000, Synaptic Systems #188004). The primary antibodies were incubated in a 3% BSA solution in PBS 1x, overnight, at 4°C. The following day, cells were washed twice with PBS 1x and incubated for 1 h at RT with the secondary antibodies anti-rabbit Alexa Fluor-488 conjugate (Invitrogen A-11008), anti-human Alexa Fluor-568 conjugate (Invitrogen A-21090) and anti-guinea pig Alexa Fluor-647 conjugate (Invitrogen A-21450), diluted 1:500 in PBS 1x 3% BSA in PBS 1x. Finally, nuclei were stained with Hoechst 33342 (1 µg/mL) for 5 min in the dark and cells were again washed twice in PBS 1x and kept in PBS 1x at 4ºC until observation.

Images were acquired using a Zeiss Axiovert 200M microscope with a 40x NA 1.4 oil or 63x NA 1.4 oil objective and processed using Zen Software (Zeiss).

After reprogramming, the expression of pluripotency and three germ layers markers were evaluated. The following primary antibodies were used: anti-OCT4 (1:400, Abcam ab19857), anti-SSEA4 (1:66, Abcam ab16287), anti-TRA-1-60 (1:100, Abcam ab16288), anti-SOX2 (1:1000, Abcam ab97959), anti-NESTIN (1:500, Merck Millipore ABD69), anti-β-III TUBULIN (1:200, Merck Millipore MAB163) anti-SMA (1:200, Dako M0851) and anti-GATA4 (1:500, Santa Cruz Biotechnology sc-25310). Succinctly, after fixation with 4% PFA for 20 min at RT, cells in µ-Slide 8-well ibiTreat chamber slides (ibidi) were washed twice with PBS 1x and permeabilized with 0.2% Triton X-100 in PBS 1x for 2 min at RT. Non-specific binding epitopes were blocked by incubating cells with a 3% BSA solution in PBS 1x for 30 min. Primary antibodies were incubated in a 3% BSA solution in PBS 1x overnight at 4ºC. The following day, cells were washed twice with PBS 1x and incubated for 2 h with the secondary antibodies anti-rabbit Alexa Fluor-488 conjugate (Invitrogen A-11008) and anti-mouse Alexa Fluor-568 conjugate (Invitrogen A-11031), diluted 1:200 in 3% BSA in PBS 1x. The nuclei were stained with Hoechst 33342 (1 µg/mL) for 5 min in the dark and cells were again washed twice in PBS 1x and kept in PBS 1x at 4ºC until observation. Images were acquired using a Zeiss Confocal LSM 710 microscope with a 20x NA 0.8 or 40x NA 1.4 oil objective and processed using Zen Software (Zeiss).

2.11. Generation of whole-brain organoids and plasma incubation

Whole-brain organoids were generated based on the protocol published by Lancaster et al. (Lancaster et al., 2013; Lancaster and Knoblich, 2014), with the modifications presented in the STEMdiff Cerebral Organoid Kit (Stem Cell Technologies). In brief, iPSCs colonies were dissociated using Accutase (Stem Cell Technologies) and 9 000 cells per well were plated on a 96-well cell suspension plate (greiner bio-one) in EBs formation Medium with 10 μM of the ROCK inhibitor Y-27632 (Stem Cell Technologies). Embryoid bodies were fed on day 2 and day 4 with EB Formation Medium and transferred to 24-well cell suspension plates (greiner bio-one) in Induction Medium, on day 5. On day 7, EBs were embedded on droplets of cold Matrigel (corning) on a sheet of Parafilm. The droplets were allowed to polymerize at 37ºC for 30 min and were subsequently removed from the Parafilm and grown in Expansion Medium for 3 days in ultra-low-attachment 6-well plates (Corning). Afterwards, the EBs droplets were kept in suspension in Maturation Medium and placed on an orbital shaker at 65 rpm. Whole-brain organoids were maintained in Maturation Medium for up to 6 months, with media changes every 3-4 days, and were collected each month for further analysis.

For CASPR2-related experiments, brain organoids were exposed to anti-CASPR2 encephalitis patient or healthy control plasma (20 μg/mL), from 2 months of differentiation onwards. The media was changed every 3-4 days with addition of fresh plasma and were collected at different ages for further analysis.

2.12. Immunohistochemistry

Brain organoids were collected at different ages, from 1 to 6 months of differentiation. Upon collection, they were fixed in 4% PFA for 90 min and then transferred to a solution of 30% sucrose in PBS 1x for cryoprotection. Subsequently, they were transferred into OCT embedding matrix (VWR), snap-frozen on dry ice and stored at -80ºC until further use for immunohistochemistry experiments.

Using a cryostat, 20 μm thick sections were obtained and collected directly into adhesive Superfrost Plus slides (Thermo Scientific Menzel). Cryosections were washed twice with PBS 1x and permeabilized with 0.5% Triton X-100 in PBS 1x for 15 min at RT. Sections were then blocked in 3% BSA in PBS 1x for 1 h at RT and incubated with primary antibodies diluted in 3% BSA in PBS 1x, overnight, at 4ºC. In the next day, sections were washed twice with PBS 1x and incubated for 2 h, at RT, with the secondary antibodies anti-rabbit Alexa Fluor-488 conjugate (Invitrogen A-11008), anti-mouse Alexa Fluor-568 conjugate (Invitrogen A-11031) and anti-guinea pig Alexa Fluor-647 conjugate

(Invitrogen A-21450) diluted 1:200 in 3% BSA in PBS 1x. Nuclei were stained with Hoechst 33342 (1 µg/mL) for 5 min in the dark. Sections were washed twice in PBS 1x and mounted for microscopy using Dako Fluorescent Mounting Medium (Dako). Images were acquired using a Zeiss Confocal LSM 710 microscope with a 20x NA 0.8, 40x NA 1.4 oil or 60x NA 1.4 oil objective and processed using Zen Software (Zeiss). The following primary antibodies were used: anti-NESTIN (1:500, Merck Millipore ABD69), anti-NEUN (1:100, Merck Millipore MAB377), anti-MAP2 (1:1000, Synaptic Systems #188004), anti-IBA1 (1:1000, Wako #019-19741), anti-GFAP (1:400, Neuromab #73-240), anti-SOX10 (1:250, Abcam ab155279), anti-OLIG2 (1:200, ab109186), anti-TH (1:500, Merck AB152), anti-VGLUT1 (1:5000, Merck Millipore AB5905), anti-GAD67 (1:100, Merck Millipore MAB5406B), anti-TBR1 (1:300, Abcam ab31940) and anti-SATB2 (1:200, Abcam ab51502).

2.13. Real time quantitative PCR (qPCR)

RNA was extracted from hiPSCs and frozen whole-brain organoids from 1 to 6 months of differentiation using the NucleoSpin RNA Isolation Kit (Macherey-Nagel), according to the manufacturer's recommendations for cultured cells. Complementary DNA (cDNA) was synthesized from 150 ng (chapter 4), 400 ng (chapter 5) and 800 ng (chapter 3) of total extracted RNA using the NZY First-Strand cDNA Synthesis Kit (Nzytech), following the instructions from the supplier. The synthesized cDNA was further diluted 20 times with RNase-free water and stored at -20ºC until required for quantitative PCR analysis.

qPCR was accomplished in a StepOnePlus thermocycler (Applied Biosystems) using 96-well low-profile microtitre plates (Nerbe Plus) and employing the NZYSpeedy qPCR Green Master Mix 2x (Nzytech) for mRNA quantification. Relative mRNA levels were determined following the Pfaffl method (Pfaffl, 2001), taking into consideration the different amplification efficiencies of each primer, obtained from a standard curve of serial sample dilutions, determined according to the formula $E = 10^{[-1/\text{slope}]}$. Values were normalized to the average expression of *GAPDH* and *HPRT*, except in reprogramming characterization experiments, where *HPRT* was the only gene used for normalization. The majority of the primers were designed through the Ensembl and Primer-Blast softwares (primer sequences are listed in **Table 2.1**).

Table 2.1. Primer sequences for qPCR analysis and respective melting temperatures (Tm) and product size.

Primer	*Primer sequence (5'-3')*	*Tm (ºC)*	*Product length (bps)*
FOXG1	FW: AACCTGTGTTGCGCAAATGC RV: AAACACGGGCATATGACCAC	60.9 58.5	95
PAX6	FW: AGGAGGGGGAGAGAATACCA RV: TGGGTTCTCTCAAACTCTTTC	58.6 55.0	156
TBR1	FW: TGCAAAAGGATTTCGGGAT RV: TGCTCACGAACTGGTCCT	55.0 58.0	155
DLX2	FW: ACGGGAAGCCAAAGAAAGTC RV: TTTTGGAAACGCCGCTGAAG	58.3 60.0	82
NKX2.1	FW: AGCACACGACTCCGTTCTC RV: GCCCACTTTCTTGTAGCTTTCC	59.7 59.8	68
NESTIN	FW: CTCAGCTTTCAGGACCCCAA RV: ACAGGTGTCTCAAGGGTAGC	59.6 59.0	134
β-III TUBULIN	FW: CGTCCACAGTTCTGGGAAGT RV: TGTGAGAAGAGGCCTCGTTG	59.6 59.7	124
MAP2	FW: CCACCAGGTCAGAGCCAATT RV: AATAACTTGGTGGGGTGCCA	60.0 59.5	102
SCN1A	FW: TGTGTGAAAGCTGGTAGAAATCCC RV: CAGCAGCACGTAATGTCAGTTGAT	61.0 61.9	136
KCNA1	FW: CATCGTGGAAACGCTGTGTAT RV: AACCCTTACCAAGCGGATGAC	59.0 60.3	232
KCNA2	FW: CTTACCGGTCCCTGTCATTGTG RV: CTTTAGGTCAGGGGAGGATGGG	60.9 61.6	127
SLC17A7	FW: GCAGCCAACAGAGTTTTCGG RV: TGACCCCCTCTACCAACCC	60.0 60.2	133
GAD1	FW: ATGCAACCAGATGTGTGCAG RV: TGCCCTTTGCTTTCCACATC	59.1 59.0	140

SOX6	FW: TGAGGAGCTACCAACACTTGTC RV: CTCTGATTCCATTCTTTGCTGAG	60.0 57.5	88
GFAP	FW: GACCTGACAGACGCTGCTG RV: AGGGACTCGTTCGTGCC	60.7 58.9	131
OLIG2	FW: TCGCCAGAGCCCGATGAC RV: ACACGGTGCCCCCAGT	61.8 60.5	79
CNTNAP2	FW: ATGTGATGAGCCACTTGTCTCTG RV: ATCCCCCAGCACCTCCTCTCTTG	60.6 65.6	119
GRIA1	FW: GGAAGAGACCCAAGTACACCTC RV: GAACAGCTGGGTTAGCCAGAC	59.8 60.8	141
GRIA2	FW: GACAGTGACAGAGGCTTATCAAC RV: GTGATCGGTACATCTCATCTTTCTTG	59.1 59.8	127
SOX2	FW: GCCGAGTGGAAACTTTTGTCG RV: GGCAGCGTGTACTTATCCTTCT	60.3 60.2	155
OCT4	FW: TATTTGGGAAGGTATTCAGCC RV: CTGCTTTGCATATCTCCTGAAG	55.0 57.0	150
NANOG	FW: CGTCACACCATTGCTATTCTTG RV: CTCCAACATCCTGAACCTCAGC	58.0 61.0	115
NCAM1	FW: GACATCACCTGCTACTTCCTG RV: GGCTCCTTGGACTCATCTTTC	58.1 58.4	143
GAPDH	FW: CATGAGAAGTATGACAACAGCCT RV: AGTCCTTCCACGATACCAAAGT	58.5 59.1	113
HPRT	FW: TGACACTGGCAAAACAATGCA RV: GGTCCTTTTCACCAGCAAGCT	60.0 61.0	94

2.14. Tissue/cells collection and biochemical analysis

hiPSCs pellets and 6-months whole-brain organoids were collected and stored, individually, at -80ºC. Subsequently, samples were homogenized at 4ºC in RIPA lysis buffer (150 mM NaCl, 1% Triton X-100, 0.5% sodium deoxycholate, 0.1% sodium dodecyl sulfate (SDS), 25 mM Tris pH 7.4), supplemented with 10% CLAP, 0.5 mM dithiothreitol (DTT) and 1 mM Phenylmethylsulfonyl fluoride (PMSF). Freeze and thaw cycles were complemented with sonication to improve cell membrane disruption. Then, samples were centrifuged at 14 800 rpm, for 20 min at 4ºC. The supernatant was collected, and protein content was determined using the DC Biorad protein assay kit (Bio-Rad), following the manufacturer's instructions. Protein samples (30 and 50 μg – chapter 5 and 4, respectively) were denatured with 4x Laemmli buffer (Bio-Rad) and 10% β-mercaptoethanol and boiled at 95 ºC for 5 min. Samples were frozen at -20ºC until further use in western blots.

2.15. Western blotting

Equal amounts of proteins were run on 8% polyacrylamide gels at 70-90 V. Proteins were transferred to Immobilon-P PVDF membranes (Merck Millipore) for 2 h at 1000 mA and blocked at RT for 1 h in 5% non-fat milk diluted in TBS 1x (25 mM Tris-HCl, 150 mM NaCl) with 0.1% Tween-20 (TBS-T), following primary antibody incubation at 4ºC overnight. After 3 washes in TBS-T, the membranes were incubated with the appropriate secondary antibody (1:10000) at RT for 2 h. Then, the membranes were washed 3 times in TBS-T and incubated with Vistra EFC (Enhanced Chemifluorescence) substrate (Sigma) for 5 min at RT. Signal was visualized using a ChemiDoc System (Bio-Rad) and analysis was performed using the Image Lab Software (Bio-Rad). Primary antibodies used were the following: anti-CASPR2 (1:1000, Abcam ab137052), anti-Contactin-2 (1:500, R&D Systems AF4439), anti-Kv1.2 (1:200, Abcam ab192758) and anti-PGRN (1:1000, Abcam ab208777). Anti-GAPDH (1:5000, Merck Millipore MAB374) was used as loading control. Secondary antibodies used were alkaline phosphatase affinipure goat anti-mouse IgG (Jackson Immunoresearch, #115-055-146), alkaline phosphatase affinipure mouse anti-rabbit IgG (Jackson Immunoresearch, #211-055-109) and alkaline phosphatase affinipure rabbit anti-goat IgG (Jackson Immunoresearch, #305-055-003).

2.16. Slice preparation for whole-cell patch clamp and Ca^{2+} imaging

Brain organoid slices were obtained as previously described by Anca M. Paşca (Paşca et al., 2015) with some modifications. Brain organoids were removed from Maturation Medium and placed into a mold with a 3% low-melting agarose solution prepared in PBS 1x. After gelification, the agarose containing the organoid was quickly removed and glued to a vibratome support filled with ice-cold oxygenated (95%:5% O_2:CO_2 mix) N-Methyl-D-Glucamine-enriched artificial cerebrospinal fluid (NMDG-aCSF) containing 99.69 mM NMDG, 2.55 mM KCl, 30 mM $NaHCO_3$, 1.23 mM $NaH_2PO_4.H_2O$, 20 mM HEPES, 25 mM glucose, 1.97 mM thiourea, 4.99 mM Na-ascorbate, 2.99 mM Na-pyruvate, 10 mM $MgSO_4$ and 0.5 mM $CaCl_2$. Slices of 250 µm were obtained using a vibratome (Leica VT1200s, Leica Microsystems, USA) and immediately recovered in a bath at 32°C for 8 min in NMDG-aCSF. Slices were then moved to a holding chamber that contained oxygenated aCSF at 25ºC (127.48 mM NaCl, 2.55 mM KCl, 24.04 mM $NaHCO_3$, 1.23 mM $NaH_2PO_4.2H_2O$, 12.49 mM glucose, 2 mM $MgSO_4$ and 2 mM $CaCl_2$. Slices were maintained in aCSF for at least 1 h before recording.

The osmolarity of NMDG-aCSF and aCSF was adjusted to 300-310 mOsm and the pH was adjusted to 7.3-7.4 with HCl.

2.17. Whole-cell patch clamp recordings

Whole-cell patch clamp recordings were registered in a recording chamber perfused with aCSF (2–3 mL/min) at 25°C. The cells were visualized with an Axio Examiner.D1 microscope (Carl Zeiss, Germany) equipped with a Q-capture Pro7 camera (Teledyne, USA) and putative pyramidal-shaped neurons, near the surface of organoids, were identified under infrared-differential interference contrast visualization with a 40× objective. Cells were patched with borosilicate glass recording electrodes (3–7 MΩ; Science Products, Germany) filled with an internal solution of potassium-gluconate (K-int) containing: 145 mM K-gluconate, 10 mM HEPES, 1 mM EGTA, 2 mM ATP-magnesium salt, 0.3 mM GTP-sodium salt and 2 mM $MgCl_2.6H_20$, pH adjusted to 7.36 with NaOH (298-300 mOsm). The recorded neurons were voltage-clamped at -70 mV to record sEPSCs and the recording was performed for 3 minutes. The resting membrane potential (RMP) and action potential (AP) parameters were estimated under current-clamp mode. The RMP and the neuronal excitability were obtained by stepped current injection (1000 ms duration, 10 pA stepwise from -80 pA to +170 pA). The kinetics of the APs was acquired by stepped current injection (10 ms duration, 20 pA stepwise from 0 pA to +380 pA). Criteria for acceptance of cells was determined as stable access resistance under 25 MΩ, meaning an increase smaller than 30% during the recording, RMP ≤ - 40 mV and

cells firing activity upon current injection. Recordings were filtered at 2 kHz and digitized at 20 kHz. All electrophysiology data was acquired with a Multiclamp 700B amplifier and Digidata 1550A (Molecular Devices, USA). Voltage clamp data was analyzed using Clampfit software (v10.7, Molecular Devices) and current clamp data was analyzed using Easyelectrophysiology Software (v2.4.0). All electrophysiological experiments were performed between weeks 25 and 28 of *in vitro* differentiation.

2.18. Ca^{2+} imaging recordings

Slices were loaded with 4.5 μM Fluo-4 AM (acetoxymethyl ester) (Invitrogen) in aCSF solution for 30 min in an incubator at 37ºC, 5% CO_2. After 30 min, slices were washed with PBS 1x and mounted on an inverted fluorescence microscope (Zeiss Cell Observer Spinning Disk). Imaging was performed at 37ºC and 5% CO2 and the emission fluorescence was recorded at 506 nm by a highly sensitive electron multiplying camera (EM-CCD Evolve Delta). The time course of the experiments consisted of 200 ms of exposure for a total of 750 frames. Imaging processing, including background subtraction, frame alignment and bleach correction, was performed using ImageJ (Fiji). ROIs and their related activity were selected using the calcium imaging analyzer (CALIMA) software and the frequency of firing was calculated using Clampfit software (v10.7, Molecular Devices).

2.19. Statistical analysis

Data is represented as mean values ± SEM (standard error of the mean). Statistical analysis was calculated using unpaired two-tailed Student t-test, two-tailed Mann-Whitney test, one-way ANOVA, following Dunnet's multiple comparisons test, two-way ANOVA or Kolmogorov-Smirnov test. Sample normality was tested using D'Agostino-Pearson normality test. Analysis was performed using the standard statistical software GraphPad Prism 8. Differences were considered statistically significant for P values < 0.05 (*p < 0.05, **p < 0.01, ***p < 0.001, ****p < 0.0001).

CHAPTER 3

RESULTS AND DISCUSSION

BRAIN ORGANOIDS AS ROBUST MODELS TO STUDY HUMAN BRAIN DISORDERS

Part of this chapter is under preparation for submission as a research article:

Oliveira, A.R.; Cammarata, G.; Seabra, C.M.; Cardoso, A.M.; Guedes, J.; Cardoso, A.L.; Fernandes, D.; Coutinho, E.; Carvalho, A.L.; Ferreira, L.; Peça, J. Autism associated CASPR2 autoimmune antibodies modify the neuronal and network activity in human brain organoids. *(in preparation)*.

3.1. Introduction

The ability of embryonic stem cells (ESCs) and induced pluripotent stem cells (iPSCs) to differentiate and self-organize into whole tissues has allowed the generation of different models to study distinct diseases, including brain disorders. In 2001, in the presence of external cues, human ESCs (hESCs) were used to generate neuroectoderm from embryoid bodies (EBs), allowing the differentiation into mature neurons and glia (Zhang et al., 2001). More recently, Kadoshima and Lancaster developed new protocols, where no external signals are used, rather relying on the intrinsic mechanisms that drive brain development (Kadoshima et al., 2013; Lancaster et al., 2013; Lancaster and Knoblich, 2014). While Kadoshima used hESCs, Lancaster used human iPSCs (hiPSCs). Both methods allowed the rapid appearance of neuronal identity and the organization of human brain development was recapitulated (Kadoshima et al., 2013; Lancaster et al., 2013). However, Kadoshima only observed the development of human neocortex with dorsal-ventral specification, while Lancaster and colleagues observed different brain regions using their protocol. The authors termed these 3D structures as cerebral organoids (Lancaster et al., 2013). It was shown that cerebral organoids developed a variety of brain regions, mimicking the whole brain, with proper organization, expressing not only markers of dorsal cortical identity, but also of ventral cortical identity, showing the tangential migration of interneurons. Also, cerebral organoids presented markers of the hippocampus, yet without formation of the entire structure, choroid plexus, retina and meninges. Importantly, the neuronal functional ability of these cerebral organoids was determined through spontaneous calcium spikes that increased upon glutamate exposure and were blocked after tetrodotoxin (TTX) addition (Lancaster et al., 2013). Therefore, however presenting several limitations, including high batch-to-batch variability, this method offers a great potential to create different brain-like structures, recapitulating the human brain development to a great extent.

In this study, we developed whole-brain organoids following the Lancaster's protocol adaptation by Stem Cell Technologies. The generated brain organoids were characterized considering the expression of neuronal precursor markers, neuronal markers, and different cell subtypes' markers. The functional activity of the generated neurons was also assessed. The results herein achieved indicate a decrease of the expression of neuronal precursors and an increase of mature neuronal markers over time, with increased expression of voltage-gated channels. Expression of excitatory, inhibitory and dopaminergic markers was also observed. Glial cells and oligodendrocytes expression was observed at later stages of development, but no

expression of microglia was observed. Later in development, we observed, by whole-cell patch clamp, that brain organoids' neurons displayed spontaneous activity and fired action potentials upon current injection. Therefore, the implementation and characterization of this model convinced us of its usability to study the cellular and molecular mechanisms of brain disorders.

3.2. Results

3.2.1. Human brain organoids have increased expression of mature neuronal-related markers over time

hiPSCs were used for the generation of brain organoids, following the established protocol by Stem Cell Technologies, as represented in Figure 3.1A. On day 0, cells were plated on round-bottom plates, which allowed the formation of EBs in suspension. After 5 days, the medium was replaced with EB Induction Medium, which allowed the formation of neuroectoderm in the outer surface of EBs. EBs were then embedded in droplets of Matrigel to allow the formation of neuroepithelium. Neuroepithelium protruded from the EB with fluid-filled structures similar to ventricles. On day 10, Matrigel droplets containing EBs were transferred to an orbital shaker to facilitate oxygen and nutrients diffusion, improving tissue survival and development. Brain organoids were kept in suspension in Maturation Medium for up to 6 months.

We tested for the expression of markers of neuronal progenitors, mature neurons, glia and of neuronal subtypes using immunohistochemistry and qPCR between 1 and 6 months in vitro (**Fig. 3.1B-K**). Mature neurons, positive for NeuN, appeared reliably after 3 months, when there was also an increase in MAP2 expression levels (**Fig. 3.1B, H**). Additionally, we could observe an expected variety of cell types, including astrocytes, that start to show intense labeling for GFAP after 3 months in culture (**Fig. 3.1C**) and oligodendrocyte precursors (**Fig. 3.1G**), after the 5 month time-point. At later stages, excitatory and some GAD67-positive inhibitory neurons and TH-positive dopaminergic neurons, could also be observed (**Fig. 3.1D-E**). TBR1 and SATB2 showed early-born and late-born neurons, respectively, in organoids grown for 6 months *in vitro* (**Fig. 3.1F**). At this age, we observed the presence of significant number of neurons that migrated through the existing layers (**Fig. 3.1F**).

During prolonged maturation, we observed a small decrease in the expression of neuronal progenitor genes (*SOX2* and *NESTIN*), followed by an increase in the early neuronal gene *β-III TUBULIN*. However, *MAP2* and *β-III TUBULIN* expression levels were highest in brain organoids with 3 months (**Fig. 3.1H**). This may be associated with cell

death at later ages (Tanaka et al., 2020) or due to a skew in the prevalence of certain cellular populations that may appear only at later ages (e.g. astrocytes and oligodendrocytes). This dynamic change could lead to a dilution of neuronal-specific mRNAs at later timepoints.

Additionally, we evaluated the expression of sodium- and potassium-voltage gated channels, as well as markers for excitatory and inhibitory neurons (**Fig. 3.1I-J**). Again, we found a similar decrease expression at later timepoints, coinciding with the increased expression of astrocyte and oligodendrocyte markers (**Fig. 3.1I-K**). As previously reported (Renner et al., 2017), *GFAP* and *OLIG2* showed an increase in their expression over time, with little to no expression in the first months of differentiation (**Fig. 3.1K**). Together, these results suggest that in our experimental conditions, the presence of neurons and glia - which are important for proper neuronal activity - converge at the timepoint of 5-6 months in culture.

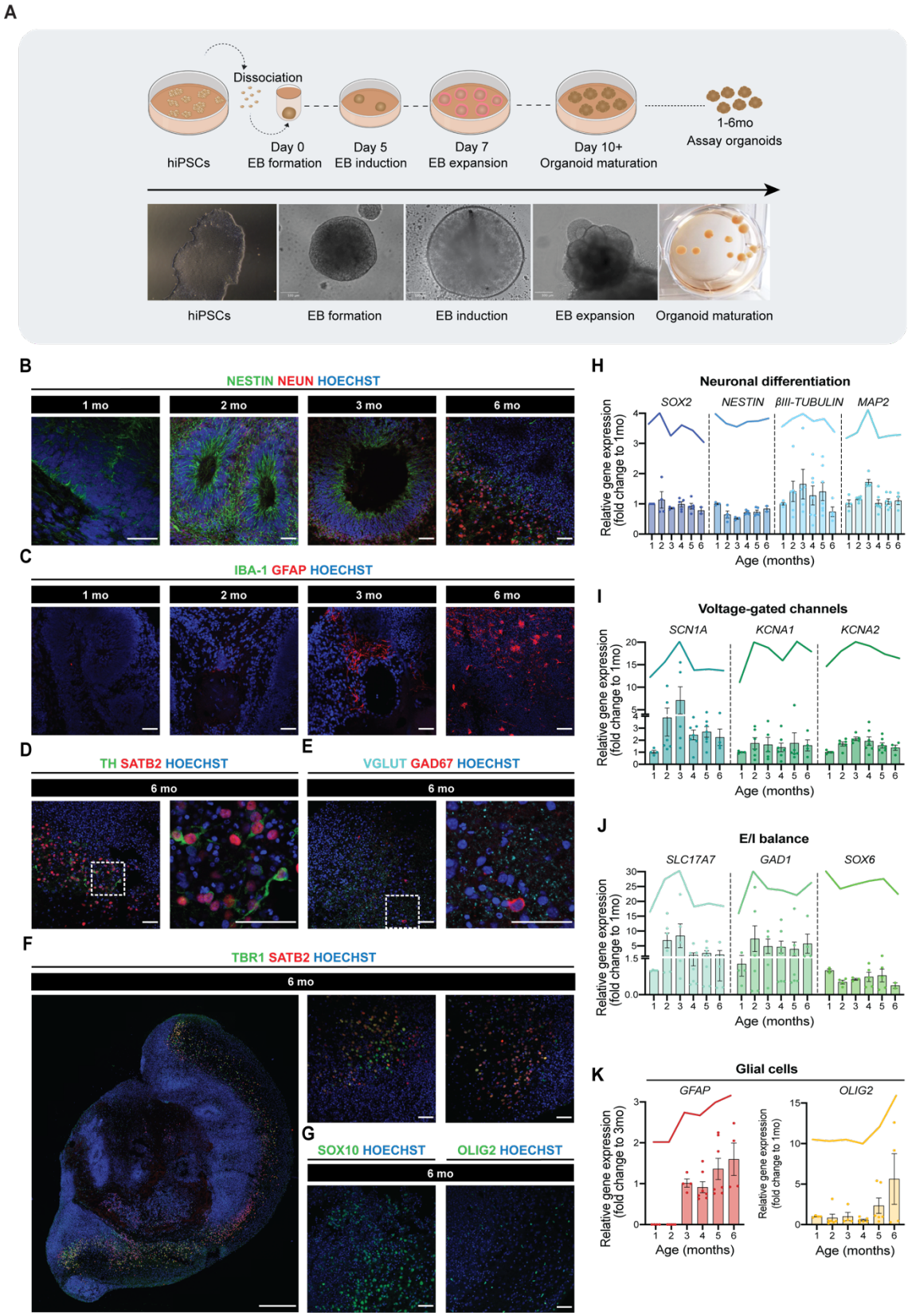

Figure 3.1. Human brain organoids show robust presence of glial cells at 6 months of culture. (A) Schematic representation of organoids generation, following the Stem Cell Technologies protocol. **(B-G)** Representative images of brain organoids maturation, pictured at different ages. **(B)** Maturation of brain organoids leads to a decrease in the levels of the neuronal progenitor marker NESTIN and an increase in the levels of the neuronal marker NEUN. **(C)** Brain organoids show the presence of glia cells, such as astrocytes

(GFAP), **(G)** oligodendrocytes precursors (SOX10 and OLIG2), **(C)** but not microglia (IBA-1). **(E)** Mature organoids express the glutamatergic marker VGLUT, the GABAergic marker GAD67 and **(D)** the dopaminergic marker TH. **(F)** Early- and late-born neurons staining reveals an inside-out migration at 6 months. Scale bars: 50 µm, except for the whole-slice: 500 µm. **(H-K)** Brain organoids maturation, showed by mRNA levels expression over time. **(H)** Maturation of brain organoids leads to a decrease in the expression of proliferative neuronal progenitors (*SOX2* and *NESTIN*) and an increase in neuronal markers (*βIII-TUBULIN* and *MAP2*), comparing to the first month of differentiation. **(I)** The expression of Na+ (*SCN1A*)- and K+ (*KCNA1* and *KCNA2*)-voltage-gated channels is substantially higher at later ages. **(J)** Brain organoids show increased expression of both excitatory glutamatergic gene (*SLC17A7*) and inhibitory gene (*GAD1*) and a decrease of the neuronal inhibitory progenitor SOX6. **(K)** Astrocytes (*GFAP*) and oligodendrocytes precursors (*OLIG2*) appear later in development. *n* = 2 – 7 organoids.
qPCRs normalized to *HPRT* and *GAPDH*; fold change to the 1st month of differentiation, except for astrocytes (fold change to 3 months). Data are presented as mean ± s.e.m.

3.2.2. Human brain organoids display neuronal activity

In addition to cell complexity, it is crucial to assess neuronal maturation to ensure that the model is accurate both from the morphologic/structural perspective but also from the functional point of view. For that, we performed whole-cell patch clamp in voltage and current clamp modes. We observed that at earlier stages of differentiation, neurons did not have spontaneous activity (**Fig. 3.2B**-3mo) and we could not observe firing of action potentials upon depolarization of patched cells (**Fig. 3.2C**). Later in development, at around 6 months of differentiation, patched neurons already displayed mature features, including spontaneous activity and action potentials upon current injections (**Fig. 3.2B**-6mo, **D**). Considering fully mature and functional neurons only at later stages, we performed our trials only after the 5-month period. The intrinsic neuronal properties, capacitance (Cm), membrane resistance (Rm) and resting membrane potential (RMP), were measured (**Fig. 3.2E-G**). The threshold potential of these neurons averaged -30 mV, while the rheobase was about 50 pA (**Fig. 3.2H-I**). We observed that neurons were capable of firing spontaneously (**Fig. 3.2J-L**), but also upon current injection, having increased action potential (AP) firing frequency with increased amounts of injected current (**Fig. 3.2M-N**). Afterwards, different parameters of the action potential kinetics were also analyzed, including latency, peak amplitude , half-amplitude, half-width, rise time and decay time (**Fig. 3.2O-U**).

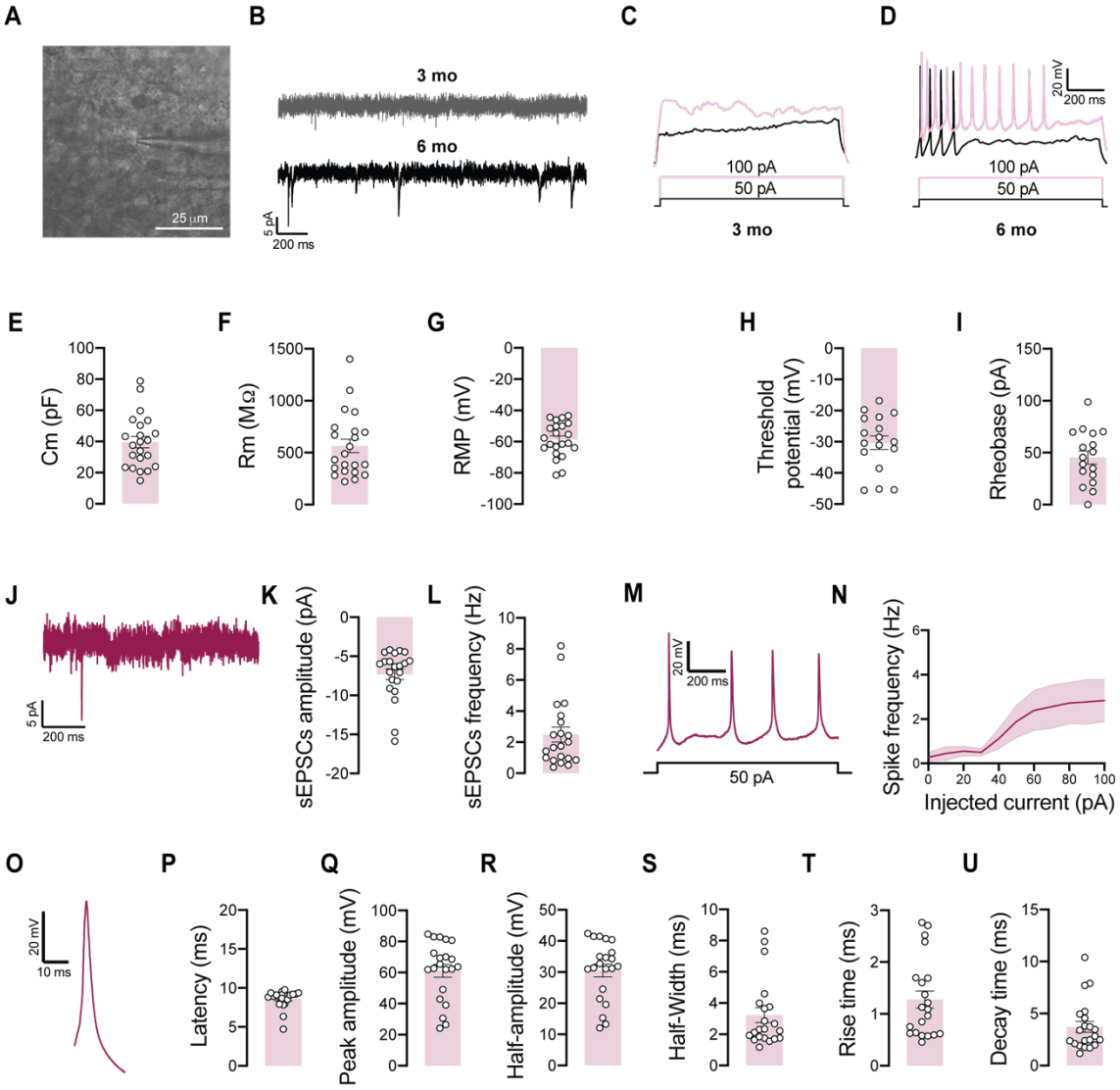

Figure 3.2. Brain organoids display neuronal activity. Upon maturation, brain organoids show an increase in synaptic activity. **(A)** Image of a recorded neuron using a 40x water immersion objective. **(B)** Representative traces of spontaneous activity at 3- and 6-months, showing mature neurons with spontaneous excitatory postsynaptic currents (sEPSCs) only at 6 months. **(C-D)** Upon injection of the same amount of current, brain organoids show action potentials at 6 months, but not at 3 months. **(E-G)** Physiological properties of the patched neurons (Cm – capacitance, Rm – membrane resistance, RMP – resting membrane potential). **(H)** Minimum voltage at which a neuron fires an action potential (threshold potential) and **(I)** amount of current needed to fire an action potential (rheobase). **(J-L)** sEPSCs amplitude and frequency. **(M-N)** Increase in the spike frequency, upon increased amounts of current injection. **(O-U)** Kinetics of a single action potential. *n* = 17 – 22 cells; 2 – 4 organoids. Data presented are as mean ± s.e.m.

3.3. Discussion

The brain is one of the most complex organs in the human body, but it is also one of the most difficult to access. This enormous limitation prevents our ability to unraveling cellular and molecular mechanisms underlying brain disorders. Implementing this model allow us to observe that neuronal progenitors are most frequent in earlier stages and are replaced by mature neurons over time. There was also a decrease in proliferative neuronal progenitors, such as SOX2 and NESTIN (**Fig. 3.1B, H**) and an increase in mature neuronal markers (**Fig. 3.1B, H**). Also, these organoids show cellular heterogeneity and different cellular types, such as astrocytes and oligodendrocytes, dopaminergic, glutamatergic and GABAergic neurons (**Fig. 3.1C-D, E, K**) (Kanton et al., 2019; Lancaster et al., 2013; Quadrato et al., 2017; Renner et al., 2017), being the glia cells and inhibitory neurons mostly expressed at later ages (**Fig. 3.1C, J, K, Supplementary Fig. 3.2-3.3**), which is consistent with *in vivo* development (Trujillo et al., 2019). It was previously shown that astrocytes with a strong positive staining only appears around 100 days (**Supplementary Fig. 3.2, 3.4**) (Renner et al., 2017). In contrast to Ormel's findings (Ormel et al., 2018), and in line with most of the literature (see previous chapter) our brain organoids do not show microglia cells (**Fig. 3.1C**).

We also noted an inside-out neuronal migration as described by Lancaster (Lancaster et al., 2013), with higher presence of early-born deep neurons and late-born superficial neurons migrating from the existing layers (**Fig. 3.1F, Supplementary Fig. 3.4**). Fully mature and functional neurons depend also on the expression of voltage-gated ion channels (Beck and Yaari, 2008; Lai and Jan, 2006). As organoids mature, an increase in the expression of Na^+-and K^+-voltage gated channels was observed (**Fig. 3.1I**). By whole-cell patch clamp (**Fig. 3.2**), we observed that brain organoids did not have spontaneous or induced APs at 3 months in culture (**Fig. 3.2B**-3mo, **C**). This matches previous findings where the authors identified different degrees of neuronal maturation: immature, developing, and mature neurons (Sivitilli et al., 2020). Sivitilli demonstrated that developing neurons have firing activity with slow kinetics and lower amplitudes, while mature neurons fire APs with fast kinetics and higher amplitudes. Moreover, our values are within the range reported by the authors. Neurons with higher peak amplitude correspond to mature cells (**Fig. 3.2Q, R**). On the other hand, neurons with higher half-width, rise time and decay time may be indicative of developing neurons (**Fig. 3.2S, T, U**).

In conclusion, we were able to reproduce Lancaster's protocol and correlate the long-term maturation of brain organoids with *in vivo* development, at the transcriptomic

and electrophysiological level, in a chronological manner, supporting the use of these *in vitro* human models to study brain development and disease.

3.4. Supplementary information

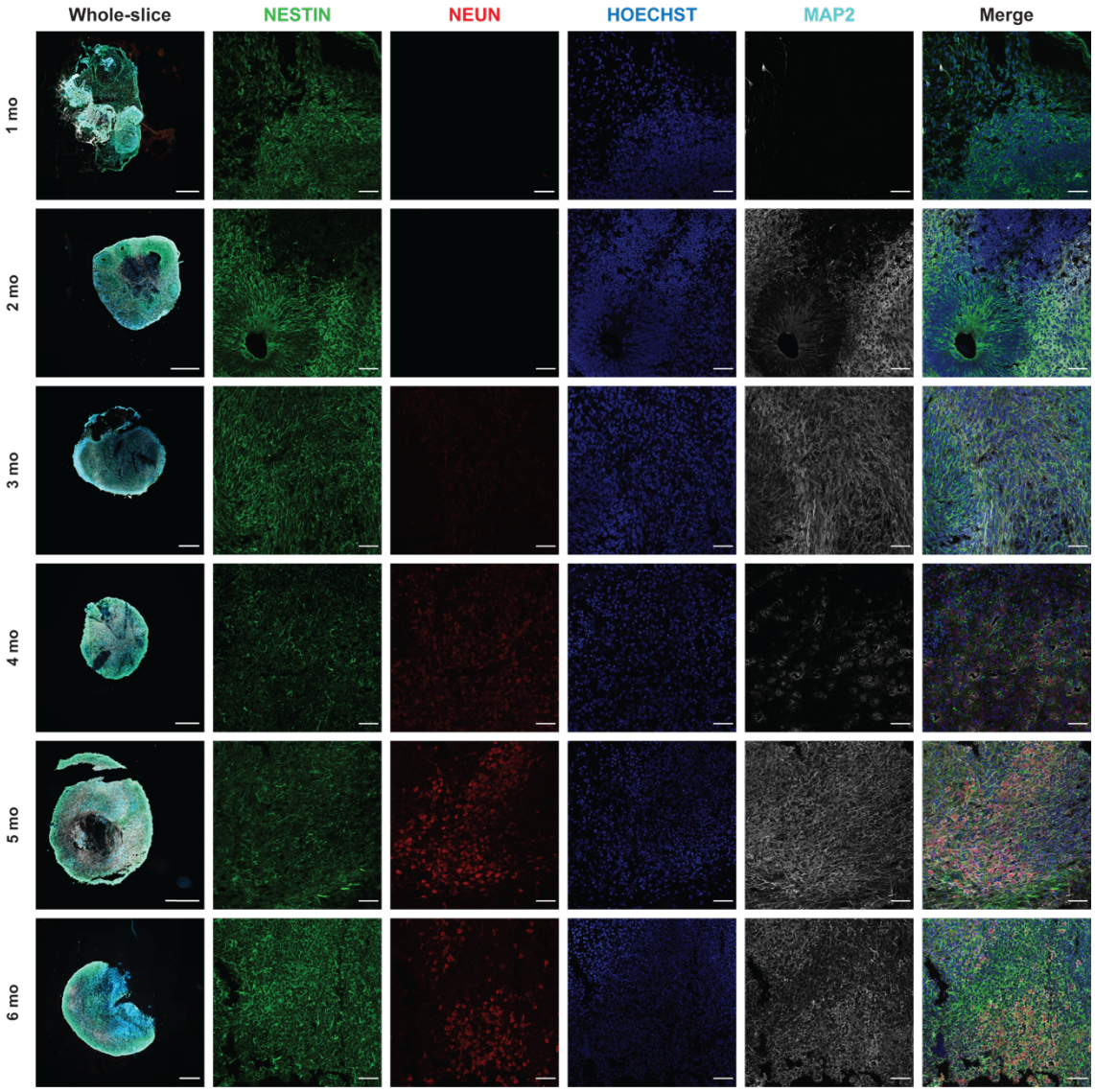

Supplementary Figure 3.1. Human brain organoids recapitulate human brain identities (NESTIN, NEUN, MAP2). Upon maturation, the expression of the neuronal progenitor NESTIN decreases, while the expression of the neuronal marker MAP2 and NEUN increases. Scale bars: 50 μm, except for the whole-slice: 500 μm.

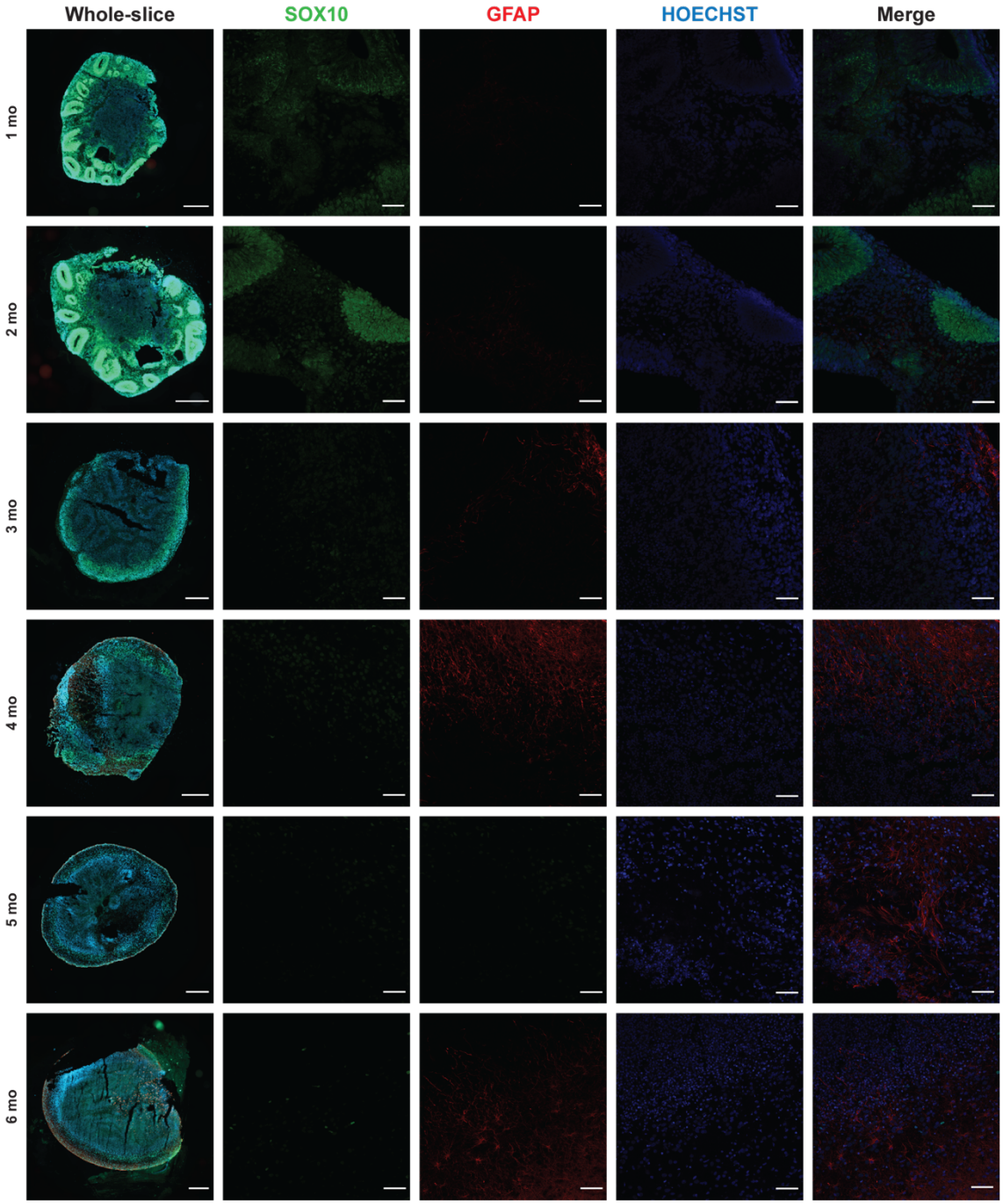

Supplementary Figure 3.2. Human brain organoids recapitulate human brain identities (SOX10, GFAP). Glial cells, such as astrocytes (GFAP) appear in a later phase of development (around 3 months). SOX10, a transcription factor involved in neural crest differentiation and modulation of oligodendrocytes production is mainly expressed in early stages. Scale bars: 50 μm, except for the whole-slice: 500 μm.

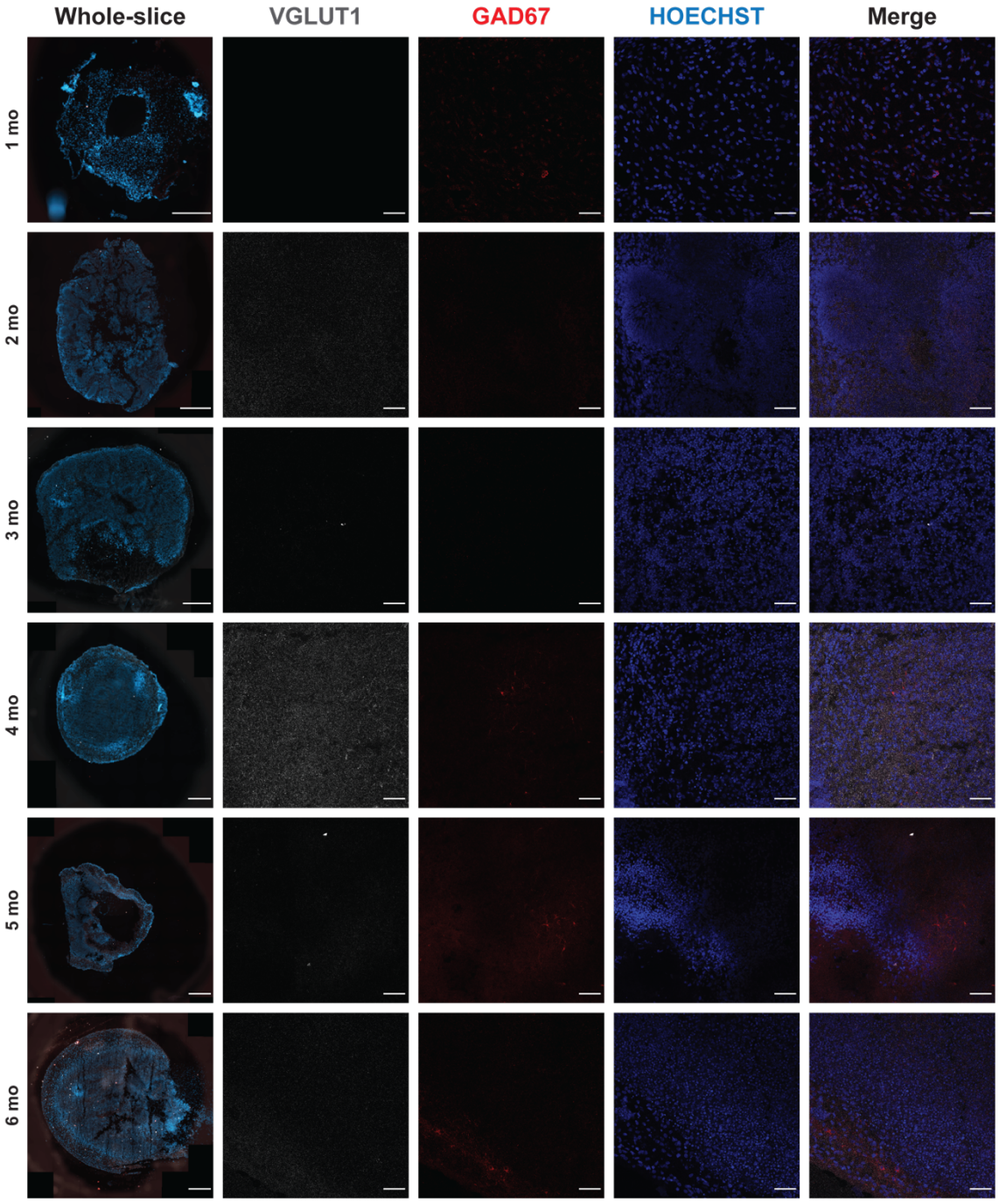

Supplementary Figure 3.3. Human brain organoids recapitulate human brain identities (VGLUT1, GAD67). Brain organoids express both excitatory (VGLUT1) and inhibitory (GAD67) markers with higher E/I ratio, being the inhibitory neurons expressed in later stages (> 3 months). Scale bars: 50 μm, except for the whole-slice: 500 μm.

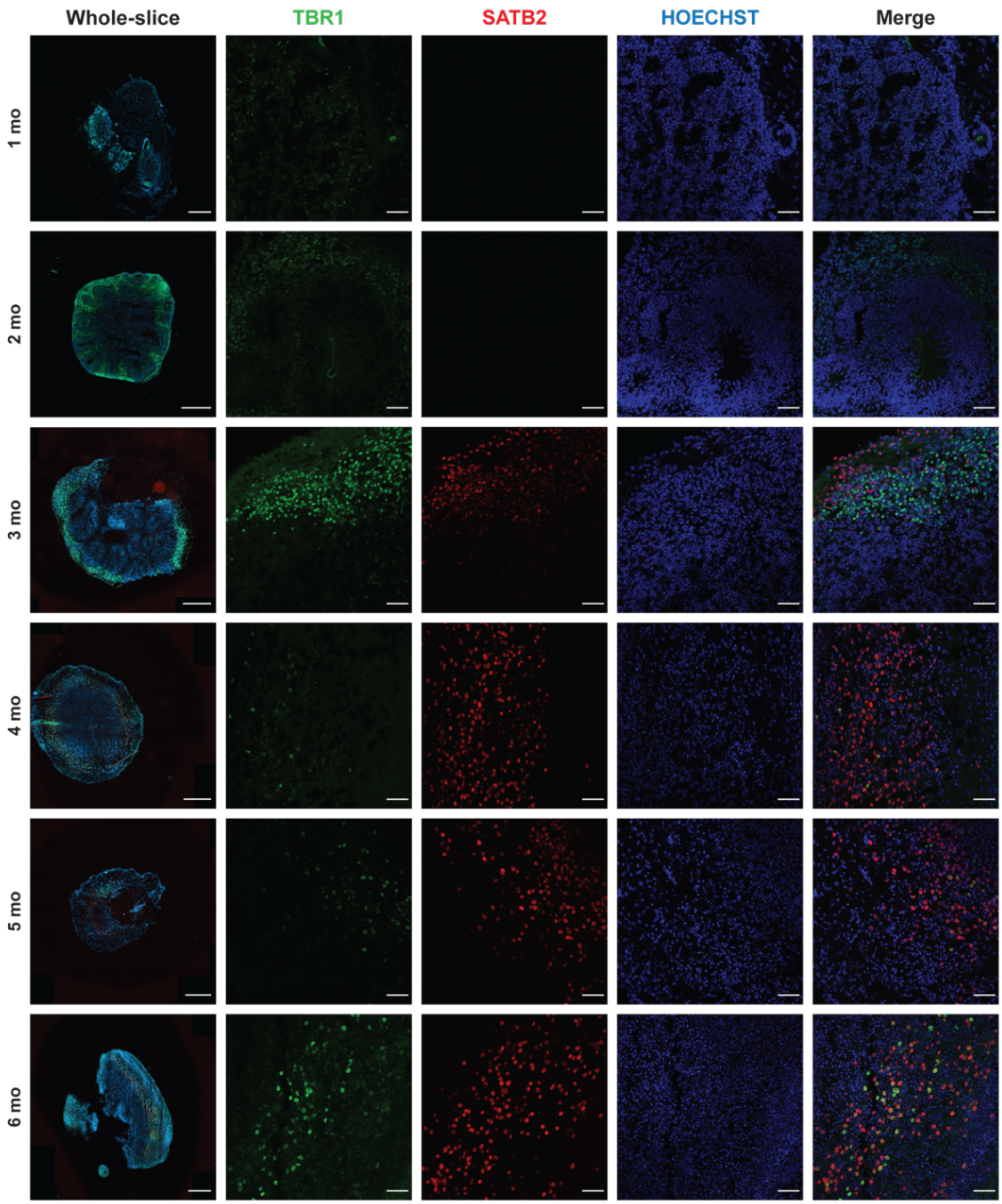

Supplementary Figure 3.4. Human brain organoids recapitulate human brain identities (TBR1, SATB2). Neurons in brain organoids show an inside-out migration firstly with expression of early-born deep neurons and later expression (> 3 months) of late-born neurons in the surface of the organoids. Scale bars: 50 μm, except for the whole-slice: 500 μm.

CHAPTER 4

RESULTS AND DISCUSSION

CASPR2 AUTOANTIBODIES MODIFY THE DEVELOPMENTAL TRAJECTORY AND NETWORK ACTIVITY IN HUMAN BRAIN ORGANOIDS

This chapter is under preparation for submission as a research article:

Oliveira, A.R.; Cammarata, G.; Seabra, C.M.; Cardoso, A.M.; Santos, H.; Guedes, J.; Sequeira D.; Marques dos Santos, J.M.; Oliveira, G.; Cardoso, A.L.; Fernandes, D.; Leite M. I.; Coutinho, E.; Carvalho, A.L.; Ferreira, L.; Peça, J. Autism associated CASPR2 autoimmune antibodies modify the neuronal and network activity in human brain organoids. *(in submission)*.

4.1. Introduction

Contactin-associated protein 2 (CASPR2), was originally identified as member of the neurexin superfamily (Poliak et al., 1999), a group of transmembrane proteins that mediate cell-cell interactions in the central nervous system. Described to colocalized with Shaker-like K^+ channels in the JXP region, this protein was hypothesized to stabilize voltage-gated potassium channels (VGKCs) in nodes of Ranvier (Poliak et al., 1999). Throughout the years, CASPR2 has been associated to many other roles, including regulation of the excitation/inhibition (E/I) balance (Jurgensen and Castillo, 2015; Vogt et al., 2018), synapse development and maintenance (Anderson et al., 2012; Fernandes et al., 2019; Gdalyahu et al., 2015; Varea et al., 2015), neuronal migration (Peñagarikano et al., 2011) and neurite outgrowth (Anderson et al., 2012; Canali et al., 2018; Varea et al., 2015). Mutations in *CNTNAP2* - the gene that encodes CASPR2 - have been associated to several neurodevelopmental and neuropsychiatric disorders (Rodenas-Cuadrado et al., 2014). CASPR2 was also identified as an antigen in autoimmune synaptic encephalitis (Irani et al., 2010; Lancaster et al., 2011), a rare CNS syndrome characterized by memory disorders, temporal lobe seizures and frontal lobe impairments. More recently, anti-CASPR2-antibodies (anti-CASPR2-Ab) have been linked to neurodevelopmental disorders due to gestational transfer from mother to fetus (Brimberg et al., 2016, 2013; Coutinho et al., 2017b, 2017a). These studies emphasize the multiple functions of CASPR2, including its involvement and importance in brain development. However, the neurobiological mechanism behind the pathogenic effects of CASPR2-abs in neurodevelopment was unknown.

VGKCs are a diverse family of K^+ channels (Kv1 to Kv12), and chief regulators of neuronal excitability due to the production of hyperpolarizing currents in response to membrane depolarization (Bertil Hille, 1992). For instance, Kv1.1. and Kv1.2 belong to the abundant Kv1 subtype and mutations in these channels have been linked to severe neurological defects (Coleman et al., 1999; Adelman et al., 1995; Xie et al., 2010). Kv1.2 mutant mice models display pronounced seizures, ultimately leading to death within weeks of birth (Brew et al., 2007). Moreover, alterations in Kv1.2 regulation and expression have been associated with cellular excitability and excitability-associated diseases (Brew et al., 2007; Dodson et al., 2003; Palani et al., 2010). Notably, in autoimmune encephalitis associated with anti-Kv1.1 and anti-Kv1.2 autoantibodies, there is increased seizure susceptibility (Kleopa et al., 2006). Considering the link between CASPR2 and VGKCs and the involvement of anti-CASPR2-Ab in

neurodevelopmental disorders, we hypothesized that these antibodies would influence human brain development.

To tackle this, we generated and characterized whole-brain organoids from human induced pluripotent stem cells (hiPSCs) (Lancaster et al., 2013; Watanabe et al., 2017). To study the impact of anti-CASPR2-Ab during early brain development, we exposed brain organoids to plasma containing anti-CASPR2 antibodies or to control plasma from a healthy individual. Our data showed that presence of human anti-CASPR2 antibodies led to decrease in protein levels of CASPR2 and Contactin-2 in 6-month-old organoids. Neuronal network dynamics showed increased spontaneous calcium transients in CASPR2-exposed organoids, increased frequency and amplitude of spontaneous excitatory postsynaptic currents (sEPSCs) and higher spiking frequency. Importantly, we observed an increase in the fast-after hyperpolarization (fAHP) voltage of the action potential, which is congruent with the neuronal excitability phenotype and supports a role for CASPR2 in regulating VGKCs.

4.2. Results

4.2.1. Autoantibodies from encephalitis patient-derived plasma bind specifically to CASPR2

We first tested the binding specificity of plasma containing anti-CASPR2-Ab to CASPR2 (**Supplementary Fig. 4.1**). For this assessment, and as previously reported (Coutinho et al., 2017b; Fernandes et al., 2019) we showed that anti-CASPR2-Ab from the patient plasma binds to the surface of both rat cortical neurons and HEK cells overexpressing CASPR2 (**Supplementary Fig. 4.1**). This same plasma did not show activity to HEK cells transfected with a control plasmid (**Supplementary Fig. 4.1**). Importantly, we also showed that the control (CTR) plasma from a healthy individual did not react with cortical neurons, nor to CASPR2- or CTR-transfected HEK cells (**Supplementary Fig. 4.1**). This indicates that the control plasma does not contain antibodies against CASPR2 or other neuronal proteins.

Additionally, we also assessed if antibodies present in the plasma would become depleted over time or if they could remain active in culture between media changes. For this experiment, “spent” media containing CTR or CASPR2 plasma (at an initial concentration of 20 μg/mL) was collected from the organoid cultures before a fresh media exchange and was then used to re-incubated HEK-transfected cells (**Supplementary Fig. 4.2**). In this experiment, we could still observe significant IgG

staining in CASPR2-transfected cells after exposure to "spent" media, suggesting anti-CASPR2-Ab are not completely depleted from the medium during 3-4 days in culture.

4.2.2. Exposure of brain organoids to anti-CASPR2 antibodies alters the expression of CASPR2

Human brain organoids were then exposed to anti-CASPR2 or CTR plasma from months 2 to 6 of differentiation, with twice weekly changes of medium containing fresh plasma (20 μg/mL) (**Fig. 4.1A**). At 6 months, brain organoids were collected and protein levels of CASPR2, Contactin-2 and Kv1.2 channels were assessed by western blot (**Fig. 4.1B-D**). We also measured mRNA expression levels of *CNTNAP2*, *KCNA2*, *GRIA1*, *GRIA2*, *GFAP*, and *OLIG2* (**Fig. 4.1E-J**). Interestingly, we found a decrease in CASPR2 and Contactin-2 protein levels, but not in total levels of Kv1.2. We also found a reduction in the mRNA of *GRIA1* and an increase in *OLIG2* expression.

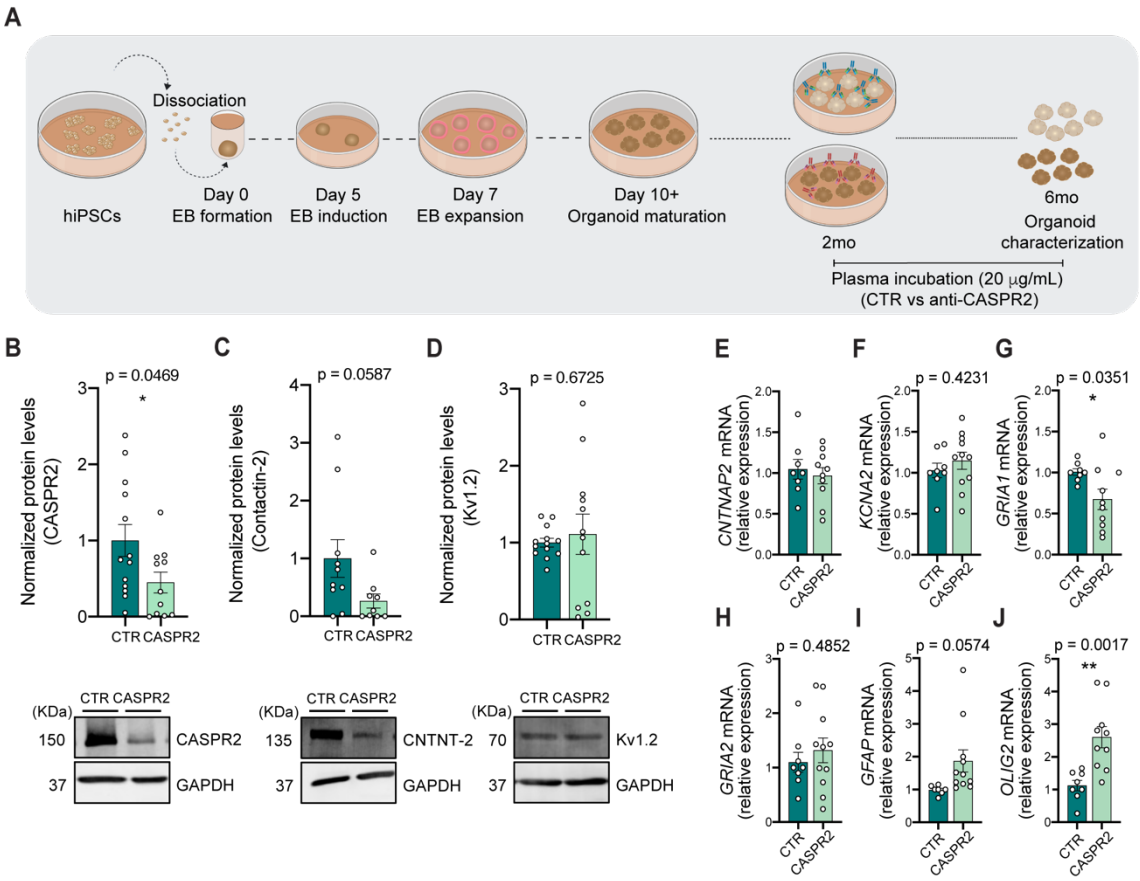

Figure 4.1. Anti-CASPR2-Ab exposed organoids present changes in CASPR2 and Contactin-2 expression. **(A)** Schematic representation of organoid generation with incubation of 20 μg/mL of control or CASPR2-encephalitis patient plasma, from 2 to 6 months of differentiation, with 2 weekly changes of medium and addition of fresh plasma. **(B-D)** CASPR2 and Contactin-2 protein levels are decreased in CASPR2-exposed organoids. *n* = 10 – 13 organoids (CTR), *n* = 9 – 12 organoids (CASPR2); **(E-J)** *CNTNAP2*, *KCNA2*, *GRIA1*, *GRIA2*, *GFAP* and *OLIG2* mRNA levels. *n* = 7 – 8 organoids (CTR), *n* = 10 – 11 organoids (CASPR2). Each dot represents an organoid. Unpaired two-tailed Student t-test. Data are presented as mean ± s.e.m. Statistical significance: **p* < 0.05, ***p* < 0.01.

4.2.3. Exposure of brain organoids to anti-CASPR2 antibodies increases neuronal excitability

Considering the role of CASPR2 in regulating voltage-gated potassium channels, we sought to determine the effect of anti-CASPR2-Ab on neuronal excitability during early brain development. For this, we performed whole-cell patch clamp in individual neurons in acute brain organoid slices (**Fig. 4.2A**). Cells were included in the analysis based on the following criteria (depicted in detail in the methods section): i) access resistance (Ra) < 25 MΩ; ii) difference between the initial Ra and the final Ra < 30 %; iii) resting membrane potential (RMP) ≤ -40 mV; iv) competency to fire APs under current clamp protocols. Therefore, from a total 62 cells in CTR condition and 75 cells in CASPR2 condition, we retained 35 cells in CTR condition and 57 cells in CASPR2 condition (56% versus 76% cells in CASPR2-exposed organoids), used across different protocols. From these, control organoids showed 71% of neurons with action potential activity, while in the CASPR2-exposed organoids condition, 79% of neurons could reliably fire action potentials (**Fig. 4.2B, D**). Moreover, not all cells responded across all current injection protocols; here, anti-CASPR2-Ab exposed neurons showed an increased ability to fire both single APs and burst APs (89% versus 60% in the CTR-exposed organoids condition) (**Fig. 4.2C, D**).

We also measured intrinsic neuronal properties, including capacitance (Cm), membrane resistance (Rm) and RMP, in both conditions and no gross differences were observed (**Fig. 4.2E-G**). We also measured spontaneous excitatory postsynaptic currents (sEPSCs) and observed an increase in amplitude and frequency of events in anti-CASPR2-Ab exposed organoids (**Fig. 4.2H-K**). We also determined neuronal excitability upon current injection and observed increased AP firing frequencies in the anti-CASPR2-Ab condition with any amount of current injection (**Fig. 4.2L-N**).

Altogether, these results suggest that exposure to anti-CASPR2-Ab impacts spontaneous synaptic activity and the spiking frequency upon current injection, indicating an increase in neuronal excitability.

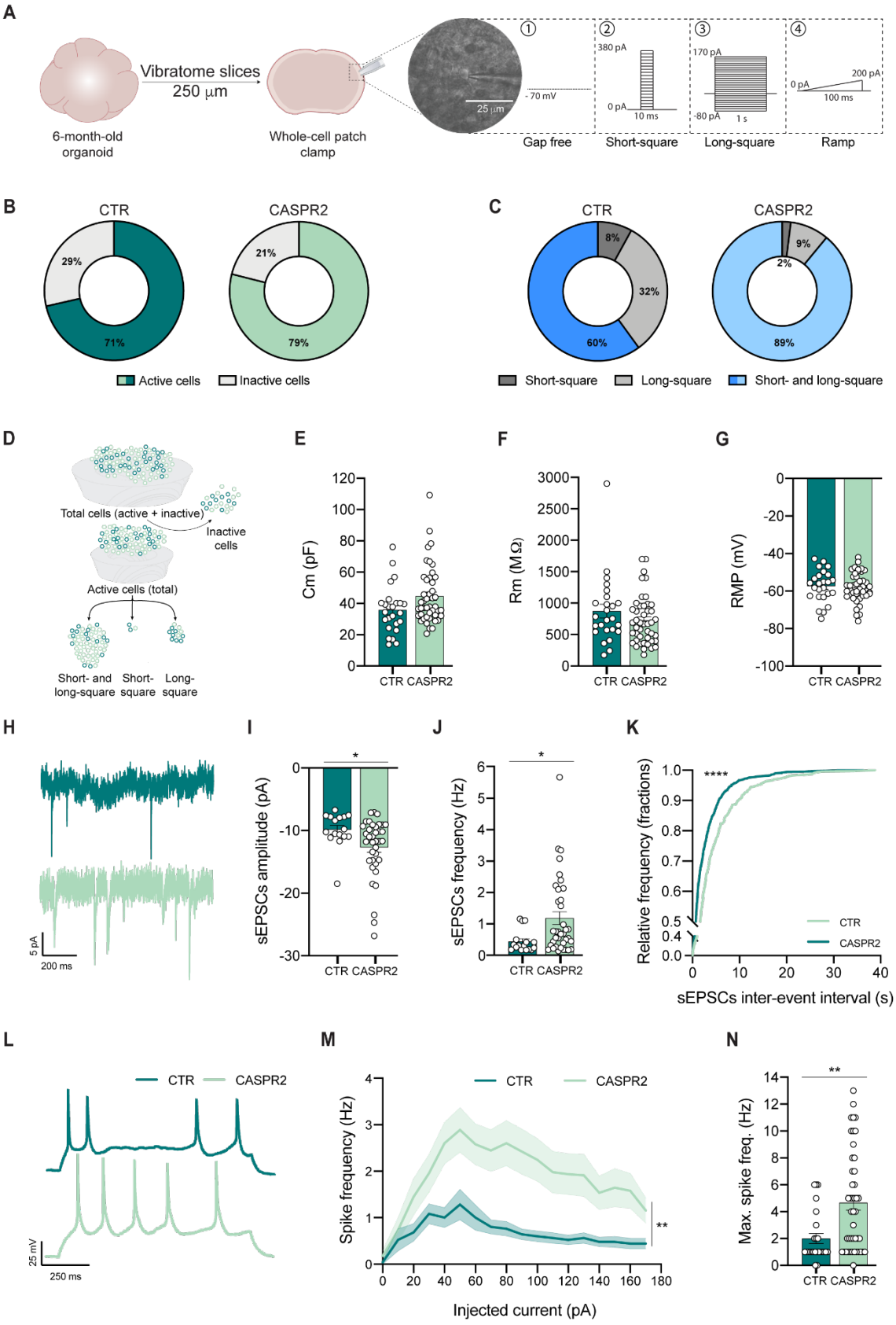

Figure 4.2. Increased neuronal excitability in human neurons following incubation with anti-CASPR2-Ab. **(A)** Whole-cell patch-clamp was performed in brain organoid slices of 250 µm and four different protocols were used: gap free (voltage-clamp), short- and long-square and ramp (current clamp). **(B)** CASPR2-exposed organoids show a higher percentage of cells presenting neuronal activity (79% CASPR2 vs 71% CTR). **(C-D)**

In CASPR2-exposed organoids, more cells fire both burst and single action potentials (89% CASPR2 vs 60% CTR). **(E-G)** The intrinsic neuronal properties are similar in both conditions (Cm – capacitance, Rm – membrane resistance, RMP – resting membrane potential). **(H-K)** CASPR2-exposed organoids display increased amplitude and frequency of spontaneous excitatory postsynaptic currents (sEPSCs). **(L-N)** Upon injection of the same amount of current, CASPR2-exposed organoids present increased frequency of action potential firing. *n* = 16 – 25 cells, 7 organoids (CTR), *n* = 37 – 45 cells, 7 organoids (CASPR2). Data in (**K**) is presented as a cumulative frequency plot, all other data are presented as mean ± s.e.m. (**K**) Student t-test, Kolmogorov-Smirnov test; (**M**) Two-way ANOVA, column factor (F (1, 68) = 9,020); all the others are two-tailed Mann-Whitney test. Statistical significance: **p* < 0.05, ***p* < 0.01, *****p* < 0.0001.

4.2.4. Exposure of brain organoids to anti-CASPR2 antibodies influences the action potential repolarization and network activity

Since changes in neuronal excitability may be a consequence of alterations in the action potential kinetics, we aimed to analyze the waveform of single action potentials. For this analysis, we determined different parameters (**Fig. 4.3A**), including AP threshold and rheobase, peak voltage, half-width, rise time, decay time and fast-afterhyperpolarization voltage (fAHP) (**Fig. 4.3C-I**). The fAHP voltage were higher in CASPR2-exposed organoids (**Fig. 4.3B, I**), which is indicative of a depolarization shift in this condition. No significant differences were observed in the other parameters **(Fig. 4.3C-H)**.

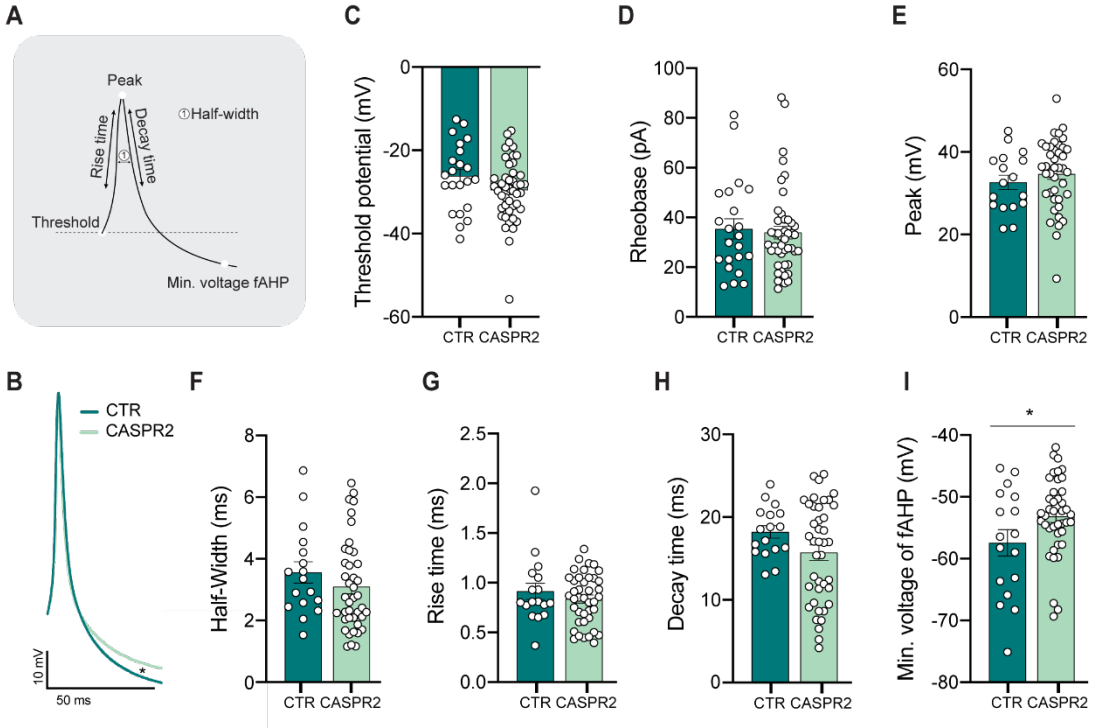

Figure 4.3. Action potential kinetics in brain organoids incubated with anti-CASPR2-Ab. **(A)** Schematic representation of the waveform parameters analyzed. **(B)** Representative traces of the action potential waveform in both conditions. **(C-H)** Brain organoids do not show differences in most parameters, including (**C**) threshold potential, (**D**) rheobase, (**E**) peak voltage, (**F**) half-width (**G**) rise time and (**H**) decay time. **(I)** CASPR2-exposed organoids present changes in the fast-afterhyperpolarization (fAHP), corroborating with the increase observed in neuronal excitability. CASPR2-exposed organoids show an increase in the voltage of the fAHP peak. *n* = 17 cells, 7 organoids (CTR), *n* = 41 cells, 7 organoids (CASPR2). (**i**) Unpaired two-tailed

Student t-test; all the others are two-tailed Mann-Whitney test. Data are presented as mean ± s.e.m. Statistical significance: *$p < 0.05$.

Finally, to determine whether increased neuronal excitability would translate to increased network dynamics in a larger population of cells, brain organoids were loaded with Fluo-4 AM and spontaneous Ca^{2+} transients were measured. Neurons in CASPR2-exposed organoids exhibited augmented frequency in Fluo-4 fluorescence dynamics (**Fig. 4.4**), suggesting an impact of anti-CASPR2-Ab in neuronal hyperexcitability and in increased network activity in 6-month-old organoids.

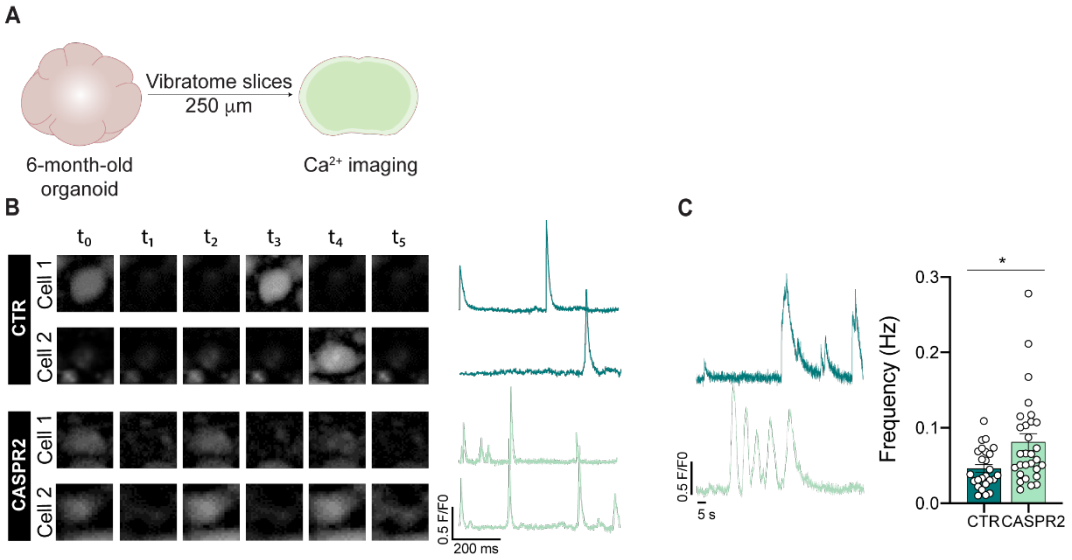

Figure 4.4. Long-term incubation with anti-CASPR2-Ab produces network hyperexcitability in human brain organoids. (A) Ca^{2+} imaging was performed in brain organoids slices of 250 µm. **(B)** Time course of live calcium imaging in neurons from CTR and CASPR2-exposed brain organoids and respective traces. **(C)** Representative traces of the frequency of firing, showing increased network activity in CASPR2-exposed organoids. Each dot represents the ROIs (region of interest) average of each video. *n* = 8 organoids (CTR), *n* = 9 organoids (CASPR2). Two-tailed Mann-Whitney test. Data are presented as mean ± s.e.m. Statistical significance: *$p < 0.05$.

4.3. Discussion

Autoimmune encephalitis is characterized by an overproduction of antibodies that target specific neuronal cell-surface or synaptic epitopes. In the case of CASPR2-encephalitis patients, they present higher levels of CASPR2 antibodies in the serum and in the cerebrospinal fluid (CSF) (Irani et al., 2010). These patients can be afflicted by several syndromes that include neuromyotonia, Morvan's syndrome and limbic encephalitis (Irani et al., 2010). In addition to these syndromes, anti-CASPR2-Ab have been associated with neurodevelopmental disorders arising from gestational maternal transfer of antibodies that attack the brain of the fetus (Braunschweig et al., 2008; Brimberg et al., 2013; Coutinho et al., 2017a; Croen et al., 2008; Singer et al., 2008). However, the alterations inflicted on neurophysiology and neuronal network activity during human brain development have not been studied. Here, using a model of early human brain development (Lancaster et al., 2013; Lancaster and Knoblich, 2014), we show that human anti-CASPR2 antibodies directly impact neuronal function and brain development.

When performing a long-term exposure of human brain organoids to anti-CASPR2-Ab, we observed a decrease in the protein levels of CASPR2 and Contactin-2, which are known to regulate VGKCs (Poliak et al., 2003). The role of CASPR2 and Contactin-2 in axonal organization is well described, with these proteins being known to cluster Kv channels at the JXP regions (Pinatel et al., 2017; Poliak et al., 2003, 1999; Traka et al., 2003). Therefore, a disruption in this complex is thought to compromise the clustering of VGKCs, namely Kv1.2 channels (Savvaki et al., 2008; Traka et al., 2003).

At the electrophysiological level, we observed a difference in the number of cells that respect neuronal criteria, as well as in the percentage of active versus inactive cells in both conditions. Brain organoids exposed to anti-CASPR2-Ab presented more cells with the ability to fire action potentials. However, within these, no differences were observed in cell capacitance, membrane resistance, resting membrane potential, action potential threshold potential or rheobase. On the other hand, we observed an increase in the amplitude and frequency of spontaneous excitatory events in CASPR2-exposed organoids. While the increased frequency in spontaneous synaptic events could be directly explained by the changes in overall network activity, the changes in amplitude of these events may be interpreted in different ways. sEPSC amplitude changes could be due to alterations in the postsynaptic site directly by i) a mechanism directly interfering with CASPR2 and glutamate receptors at the synapse; ii) be due to changes in synaptic physiology and synaptic maturation, secondary to the overall increase in neuronal activity;

or iii) a combination of both mechanisms. Mechanistically, however, this increase in neuronal and synaptic activity are most likely a consequence of membrane repolarization deficits following action potential firing, which is in line with putative alterations in Kv channel function and impaired CASPR2/Contactin-2 complex. This is in agreement with several studies showing reduced expression of Kv channels in different CASPR2 models (Dawes et al., 2018; Fernández et al., 2021; Patterson et al., 2018). Finally, our observed reduction in *GRIA1* expression, could suggest either a direct impact on AMPA receptor (Fernandes et al., 2019) or a compensatory/homeostatic plasticity mechanism aimed to tune-down the higher activity rates (Fernandes and Carvalho, 2016; Tatavarty et al., 2013; Turrigiano, 2017) present in our model. In fact, network hyperexcitability may indeed present as a key consequence of CASPR2 alterations and point also to early defects in excitation/inhibition ratio as an underlying alteration in ASDs (Manyukhina et al., 2022; Rubenstein and Merzenich, 2003; Sohal and Rubenstein, 2019). Excitatory transmission is either normal or altered in *CNTNAP2* deletion models (Anderson et al., 2012; Jurgensen and Castillo, 2015; Kim et al., 2019; Lazaro et al., 2019; Lu et al., 2021; Vogt et al., 2018). Moreover, in several studies, CASPR2 loss reduces GABAergic interneurons subpopulations, resulting in impaired GABAergic inhibitory transmission and increased excitability during postnatal development (Anderson et al., 2012; Bridi et al., 2017; Jurgensen and Castillo, 2015; Lauber et al., 2018; Lu et al., 2021; Peñagarikano et al., 2011; Vogt et al., 2018). Additionally, during early development, in a *CNTNAP2* KO mouse cortical organoid model, deficits in inhibitory neurons were also observed, contributing for E/I imbalance (Hali et al., 2020). Interestingly, by restoring the E/I balance, it was possible to rescue the hyperactivity phenotype observed in models lacking the autism candidate gene *CNTNAP2* (Hali et al., 2020; Selimbeyoglu et al., 2017), demonstrating the importance of this gene for E/I ratio and network activity (Selimbeyoglu et al., 2017).

In conclusion, our data supports the view that in early human brain development models, the presence of anti-CASPR2-Ab may disrupt the CASPR2-Contactin-2-Kv complex, resulting in the mislocalization of VGKCs, contributing to neuronal hyperexcitability and creating the early makers for future E/I imbalance, even before the maturation of the inhibitory system.

4.4. Supplementary information

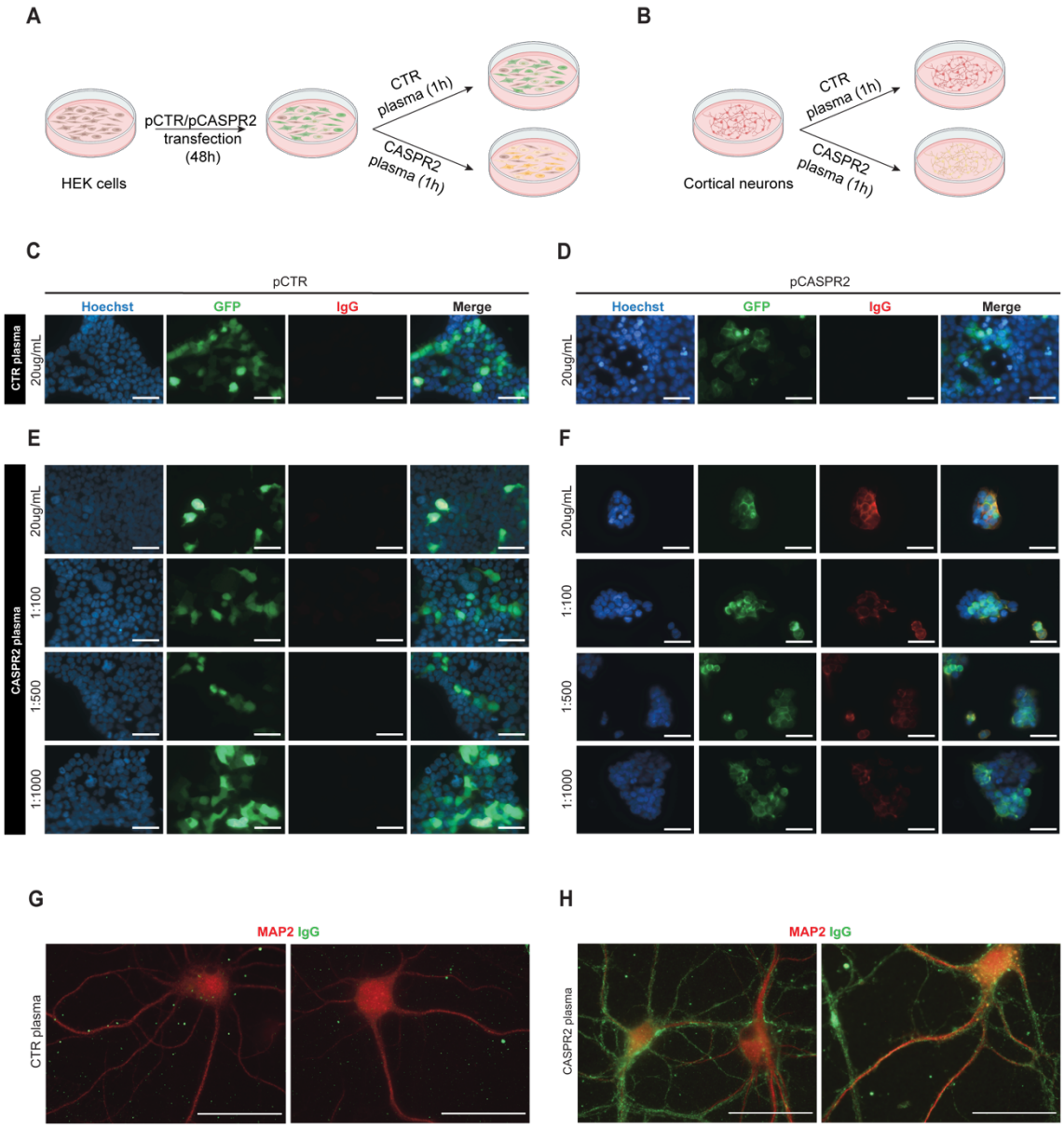

Supplementary Figure 4.1. Plasma containing anti-CASPR2-Ab specifically recognize and bind to CASPR2. (A-B) Schematic representation of the binding assay culture system. **(C-D)** Control plasma fails to bind to pCTR-transfected HEK293T cells (**C**) and to pCASPR2-transfected HEK293T cells (**D**). **(E-F)** CASPR2 plasma fails to bind to pCTR-transfected HEK293T cells (**E**) but binds specifically to pCASPR2-transfected HEK293T cells with antibodies titers > 1:1000 (**F**). **(G-H)** While control plasma fails to bind to cortical neurons (**G**), CASPR2 plasma recognizes and binds to CASPR2 in cortical neurons (**H**).

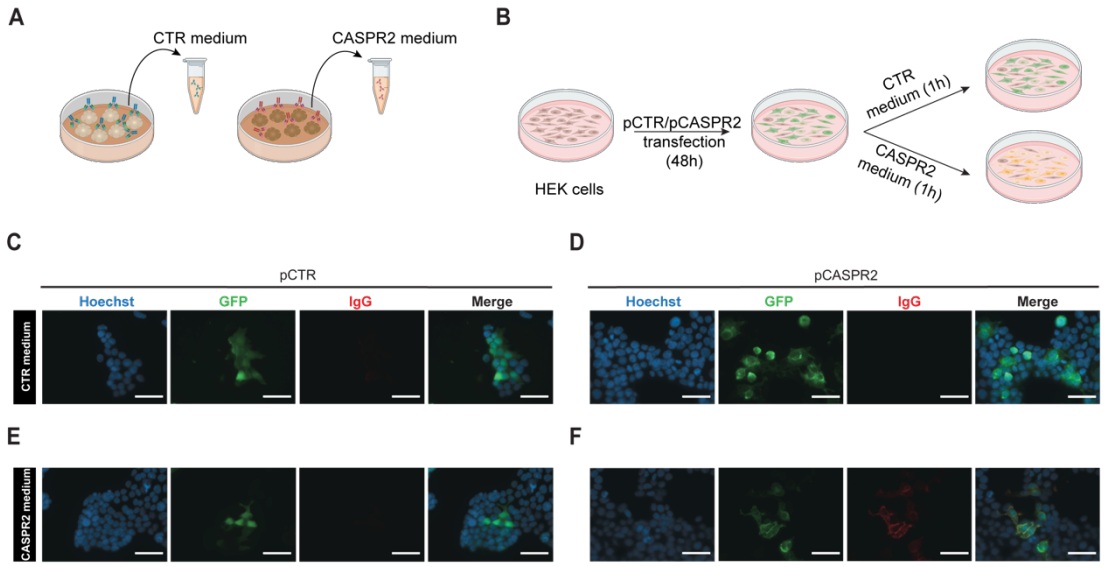

Supplementary Figure 4.2. Anti-CASPR2-Ab are not completely depleted from the medium, during the incubation time in brain organoids. (A-B) After 3-4 days of incubation in brain organoids, control and CASPR2 plasma was collected (**A**) and re-incubated in HEK293-transfected cells (**B**). **(C-D)** Re-incubated control plasma fails to bind to pCTR-transfected HEK293T cells (**C**) and to pCASPR2-transfected HEK293T cells (**D**). **(E-F)** Re-incubated CASPR2 plasma fails to bind to pCTR-transfected HEK293T cells (**E**) but binds specifically to pCASPR2-transfected HEK293T cells (**F**).

CHAPTER 5

RESULTS AND DISCUSSION

GENERATION AND CHARACTERIZATION OF NOVEL IPSC LINES FROM A PORTUGUESE FAMILY BEARING HETEROZYGOUS AND HOMOZYGOUS GRN MUTATIONS

This chapter is published as a research article:

Oliveira, A.R.; Martins, S.; Cammarata, G.; Martins, M.; Cardoso, A.M.; Almeida, M.R.; do Carmo Macário, M.; Santana, I.; Peça, J.; Cardoso, A.L. Generation and Characterization of Novel iPSC Lines from a Portuguese Family Bearing Heterozygous and Homozygous *GRN* Mutations. *Biomedicines* **2022**, *10*, 1905. https://doi.org/10.3390/biomedicines10081905.

5.1. Introduction

Frontotemporal lobar degeneration (FTLD) is the second most common form of dementia in people aged < 65 years old and comprises an heterogenous group of highly hereditable and rapid-progressing neurodegenerative diseases, mostly characterized by behavioral, language and motor impairments. In 2006, heterozygous mutations in *GRN* were identified as a cause of familial FTLD presenting with inclusions of the TAR-DNA binding protein 43 (TDP-43) (Baker et al., 2006, p. 17; Cruts et al., 2006). Mutations in *GRN*, together with mutations in microtubule-associated protein tau (MAPT) or expansion of the chromosome 9 open reading frame 72 (C9orf72) account for 5 to 10% of all FTLD cases (Greaves and Rohrer, 2019; Moore et al., 2020). In the specific case of the Portuguese population, *GRN* mutations are relatively frequent and account for around half of all genetic FTLD diagnoses (Moore et al., 2020), showing almost 100% penetrance by 80 years of age.

Progranulin, the protein encoded by the *GRN* gene, is a conserved 593 amino acid and 88-kDa protein, which includes 7.5 cysteine-rich granulin domains. In the brain, progranulin is expressed both by immune cells and by subsets of neurons and has been implicated in multiple functions required for neuronal survival (Baker et al., 2006; Cruts et al., 2006), including axonal growth, synaptogenesis (Gascon et al., 2014; Petkau et al., 2012) and neuroinflammation (Broce et al., 2018; Ferrari et al., 2014; Miller et al., 2013; Zhang et al., 2020). In addition to its extra-cellular functions, mainly mediated through interaction with the tyrosine kinase ephrin type-A receptor 2 (EphA2) and the Notch signaling pathway (Neill et al., 2016), progranulin (PGRN) has also been suggested to play an important role in autophagy and lysosomal regulation, acting as a chaperone for lysosomal enzymes involved in protein degradation (Butler et al., 2019).

In addition to FTLD, deficiencies in the *GRN* gene can cause other neurodegenerative conditions, in an allele dose-dependent manner. Clinical symptoms of patients with *GRN* mutations, including the age of disease onset, are extremely variable, even within same-family carriers of an identical pathogenic mutation (Gabryelewicz et al., 2010; van Swieten and Heutink, 2008). Interestingly, homozygous mutations in *GRN* were not initially observed, leading to the hypothesis that the loss of *GRN* in both alleles might cause embryonic death (Bruni et al., 2007). This changed in 2012, when a complete deficiency of progranulin, caused by a homozygous *GRN* loss-of-function mutation, was reported in 2 siblings diagnosed with adult-onset neuronal ceroid lipofuscinosis (NCL) type 11, presenting with visual loss, dementia and epilepsy (Canafoglia et al., 2014; Smith et al., 2012). In 2016, a c.900_901dupGT mutation in exon

9 of the *GRN* gene (p.Ser301Cysfs*61) was identified in a young Portuguese female, originating the third case of NCL due to a homozygous *GRN* mutation (Almeida et al., 2016), and the first one segregating in a family with confirmed pathology of FTD (Guerreiro et al., 2008) (**Fig. 5.1**).

The association of progranulin with a late-onset type NCL further strengthen the hypothesis of a relevant role for this protein both in lysosomal homeostasis and lipid metabolism (Evers et al., 2017; Smith et al., 2012). This was further confirmed by several studies in *GRN*$^{-/-}$ mice, which showed an abnormal accumulation of lipofuscin deposits in the brain (Ahmed et al., 2010; Moore et al., 2020), in addition to changes in lysosome size and activity, reduced activity of autophagy mediators (Chang et al., 2017) and an increase in microglia-dependent complement activation that led to abnormal synapse elimination and neuronal loss (Zhang et al., 2020).

In addition to rare loss of function *GRN* mutations, single-nucleotide polymorphisms (SNPs) in the *GRN* locus, such as rs5848, rs2269906 and rs850738, have been identified by genome-wide association studies has genetic determinants of other neurologic diseases, including Alzheimer's disease, limbic-predominant age-related TDP-43 encephalopathy (LATE), amyotrophic lateral-sclerosis (ALS) and FTLD caused by expansion of C9orf72 and Gaucher disease (Rhinn et al., 2022). All this SNPs have been related with decreased levels of circulating progranulin, which have also been reported in idiopathic Parkinson disease and autism (Al-Ayadhi and Mostafa, 2011; Yao et al., 2020). This commonality in a risk gene for neurodegeneration is almost unheard off and suggests that progranulin is a critical regulator of brain health, constituting a uniquely attractive therapeutic target (Rhinn et al., 2022).

Despite the undeniable link between pathogenic mutations in *GRN* and both FTLD and NCL, the underlying molecular and cellular pathways that explain the contribution of progranulin to the pathophysiology of these diseases, as well as the reason for brain susceptibility to progranulin loss, remain to be fully elucidated. This is partly due to the poor face validity of *GRN*$^{+/-}$ mice, as well as the lack of robust human models.

Human induced pluripotent stem cells (hiPSCs) offer remarkable opportunities to study the molecular mechanisms of this type of mutations, due to their ability to differentiate into various cell types (Takahashi et al., 2007), which enables the development and study of human neurons, while preserving the genetic background of the individuals.

Here, we describe the generation and characterization of new FTLD- and NCL-patient-specific iPSC lines, bearing the c.900_901dupGT *GRN* mutation, which we further employed to generate a human 3D model of *GRN* haploinsufficiency. We believe these

lines constitute promising new tools that will allow future studies addressing the mechanistic aspects of progranulin function and other outstanding questions regarding the impact of progranulin deficiency in the context of aging and disease.

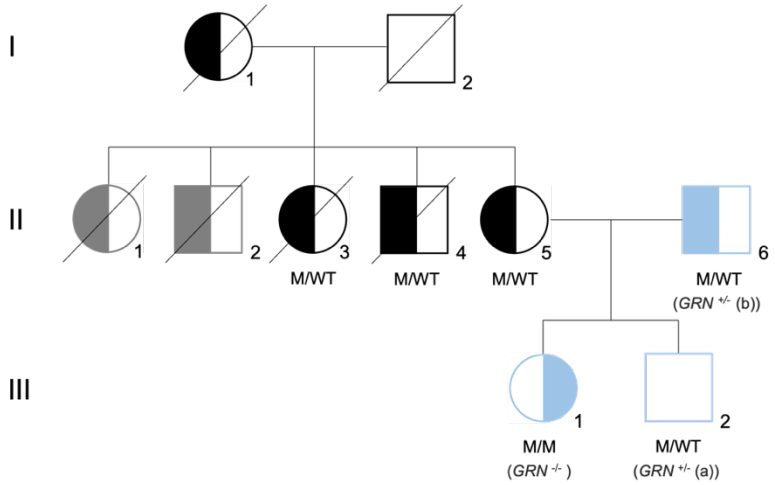

Figure 5.1. Family tree of the Portuguese family carrier of the *GRN* mutation.
Family tree representative of the mutation status for *GRN* mutation c.900_901dupGT. Both parents (II5 and II6) are heterozygous for the mutation (M/WT), presenting with the behavioral variant of FTD. The daughter (II1) is homozygous for the mutation (M/M), presenting with neuronal ceroid lipofuscinosis (CLN11). The son (II2) is heterozygous for the mutation (M/WT) and did not present symptoms at the time of the skin biopsy.
Left-side filled black/blue symbols represent individuals diagnosed with behavioral variant of FTD, while right-side filled black/blue symbols represent individuals diagnosed with neuronal ceroid lipofuscinosis. Left-side filled grey symbols represent signs of dementia plus Parkinsonism and the white square represents asymptomatic individuals. The generation is indicated by Roman numeral on the left side of the tree. The samples used in this study are represented in blue. Image adapted from *(Almeida et al., 2016; Guerreiro et al., 2008)*

5.2. Results

5.2.1. Generation and characterization of patient-derived hiPSCs

In order to study the cellular consequences of the c.900_901dupGT *GRN* mutation in human brain cells, we generated hiPSCs from primary cultures of dermal fibroblasts collected from three individuals, from the same family, which presented either a homozygous (*n* = 1) or heterozygous mutation (*n* = 2) (**Fig. 5.2A-B**). For this purpose, skin biopsies were obtained from each individual and cultured until giving rise to a stable population of dermal fibroblasts. The fibroblasts were then reprogrammed using an integration-free strategy, based on nucleofection, to overexpress OCT3/4, SOX2, KLF4, L-MYC and microRNA (miR) 302/367 cluster. For each patient, several independent hiPSC-like clones were generated and picked to Matrigel-coated plates. After several days of expansion, hiPSCs displayed the specific stem cell-like morphology (multiple round-shaped colonies with distinct borders and a high nuclear to cytoplasm

ratio) (**Fig. 2B**). Even though cell morphology is an important indicator of hiPSC status, other tests were performed to further validate the quality of the newly generated hiPSC lines. The pluripotency potential of each original hiPSC clone was confirmed by immunocytochemistry and qPCR. All hiPSC clones expressed the pluripotency markers OCT4, SSEA4 and SOX2 (**Fig. 5.2C**). Additionally, an increase in the expression of the pluripotency genes OCT4, SOX2 and NANOG, with respect to the primary cell source (fibroblasts) (**Fig. 5.2D**), was also detected by qPCR. Nevertheless, we found that the expression levels of these pluripotency markers diverged between different patient samples and, within the same patient, in different clones (**Fig. 5.2D**).

The most promising hiPSC clones (at least two for each individual) were cultured in conditions that potentiated the formation of embryoid bodies to evaluate their ability to differentiate spontaneously into each of the three-germ layers. Following 5 days in EB formation medium, EBs were transferred to Matrigel-coated plates and cultured for further 11 days in serum-containing medium. The presence of trilineage markers was determined by immunocytochemistry at the end of this period. GATA4 was used as an endodermal marker, SMA as a mesodermal marker and NESTIN and β-III TUBULIN as ectodermal markers. It was possible to observe the positive expression for markers of the three germ layers (**Fig. 5.2E**) in all clones from the three hiPSC lines. Chromosomal integrity in the newly generated hiPSCs was also examined in the two most promising hiPSC clones of each individual. Our results showed that all clones presented a normal karyotype: 46, XY (heterozygous carriers of the *GRN* mutation) or 46, XX (homozygous carrier of the *GRN* mutation) (**Fig. 5.2F**). All the hiPSCs clones were further tested for mycoplasma before clone expansion and freezing at low passage number (6-8 passages). General features of the generated cell lines are reported in **Table 5.1**.

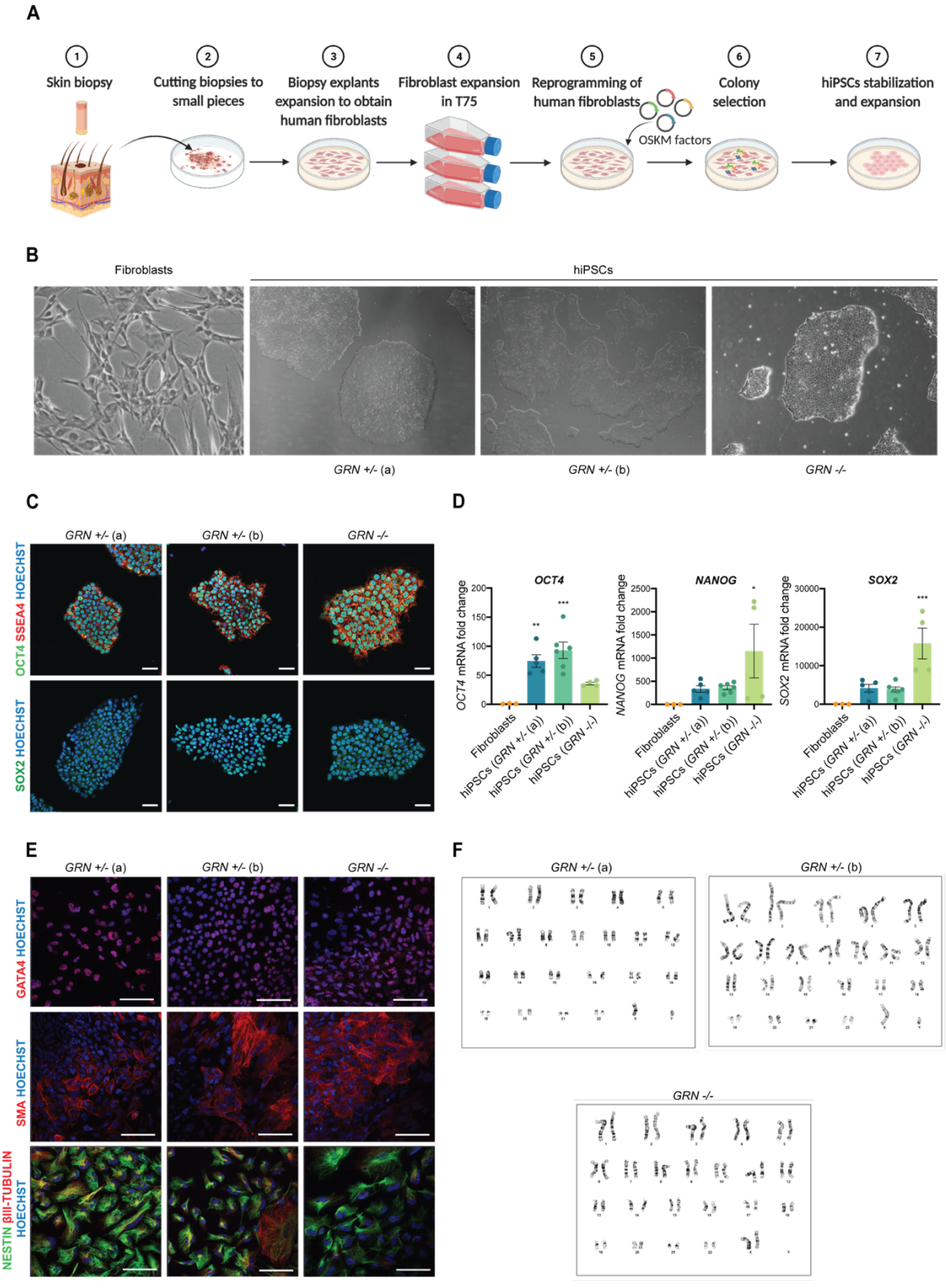

Figure 5.2. Generation and characterization of patient-derived hiPSCs.
hiPSCs were generated from skin fibroblasts of three individuals, from the same family, all carriers of the progranulin mutation c.900_901dupGT. One individual harboring a homozygous mutation and two individuals harboring a heterozygous mutation. **(A)** Schematic representation of the protocol for fibroblast isolation and reprogramming into hiPSCs. **(B)** Typical morphology of fibroblasts and hiPSCs following reprogramming. **(C)** Expression of pluripotency markers OCT4, NANOG and SOX2 was detected by

immunocytochemistry in the three hiPSCs lines (scale bar: 50 µm). **(D)** Increased expression of pluripotency genes *OCT4*, *NANOG* and *SOX2*, with respect to fibroblasts, was also observed by qPCR in at least two independent hiPSC colonies from each individual (*n* = 3 fibroblast lines; *n* = 5 *GRN* $^{+/-}$ (a); n=6 *GRN* $^{+/-}$ (b); *n* = 4 *GRN* $^{-/-}$). **(E)** Expression of trilineage markers GATA4 (endoderm), SMA (mesoderm) and NESTIN and βIII-TUBULIN (ectoderm) (scale bar: 100 µm) was determined by immunocytochemistry in all hiPSCs lines, following the three germ layer assay. **(F)** A normal karyotype, with 46 chromosomes *GRN* $^{+/-}$ (a): 46, XY, *GRN* $^{+/-}$ (b): 46, XY, *GRN* $^{-/-}$: 46, XX was identified for the three hiPSC lines; One-way ANOVA, following Dunnet's multiple comparisons test. Data are presented as mean ± s.e.m. Statistical significance: *p < 0.05, **p < 0.01, ***p < 0.001.

Table 5.1. General features of the newly generated cell lines.

Unique stem cell line identifier	NCBL1.c5	NCBL2.c11; NCBL2.c46	NCBL3.c2; NCBL3.c6	NCBL4.c27; NCBL4.c33
Alternative name of stem cell line	*GRN*$^{+/+}$	*GRN*$^{+/-}$ (a)	*GRN*$^{+/-}$ (b)	*GRN*$^{-/-}$
Institution	Center for Neuroscience and Cell Biology, University of Coimbra (CNC UC)			
Contact information of distributor	Doctor Ana Luísa Cardoso: anacardoso@cnc.uc.pt			
Type of cell line	Induced pluripotent stem cells (iPSCs)			
Origin	Dermal human fibroblasts			
Individual age and sex	36 years-old; male	29 years-old; male	63 years-old; male	34 years-old; female
Method of reprogramming	Episomal nucleofection: OSKM factors (OCT3/4, SOX2, KLF4 and MYC, together with the miR 302/367 cluster)			
Genetic modification	No	Yes	Yes	Yes
Associated disease	-	Frontotemporal lobar degeneration (FTLD)	Frontotemporal lobar degeneration (FTLD)	Neuronal ceroid lipofuscinosis (NCL11)
Gene/locus	-	Granulin (*GRN*), 17q21.31		
Date archived/stock date	2021			
Cell line repository/bank	RRID:CVCL_C0P1	RRID:CVCL_C0P2; RRID:CVCL_C0P3	RRID:CVCL_C0P4; RRID:CVCL_C0P5	RRID:CVCL_C0P6; RRID:CVCL_C0P7
Ethical approval	The study was approved by the Ethics Committee of the Faculty of Medicine, University of Coimbra (Project CE-028/2016)			

5.2.2. Patient-derived hiPSCs preserve the *GRN* genotype

After the broad characterization of the newly generated hiPSC lines, we wanted to analyze whether the genotype of each line suffered alterations due to the reprogramming process. For this purpose, the region within the *GRN* gene bearing the mutation was sequenced in each hiPSC line. As expected, the GT duplication, c.900_901dupGT (p.Ser301Cysfs*61) was identified in a single allele in the hiPSC clones

from the individuals bearing the heterozygous mutation and in both alleles in the hiPSC clones from the patient with the homozygous mutation (**Fig. 5.3A**).

It has previously been described that *GRN* loss of function mutations lead to a reduction in serum progranulin levels, that reaches more than a 50% loss in symptomatic FTLD patients, while NCL patients with homozygous mutations present a complete absence of the protein (Almeida et al., 2016). To assess if the generated hiPSC lines complied with the expected phenotype, PGRN expression levels were evaluated by western blot (**Fig. 5.3B**). We observed a significant reduction (approximately 50%) of PGRN protein levels in hiPSCs clones from one of the heterozygous patients (*GRN*$^{+/-}$ (b)), while no PGRN protein could be detected in hiPSCs clones from the homozygous patient (100% reduction). Interestingly, hiPSC clones from one of the heterozygous individuals (*GRN*$^{+/-}$ (a)) presented an increase in PGRN levels (**Fig. 5.3B**) with respect to control lines, which may be related with the fact that this individual was young and still asymptomatic at the time of the biopsy collection.

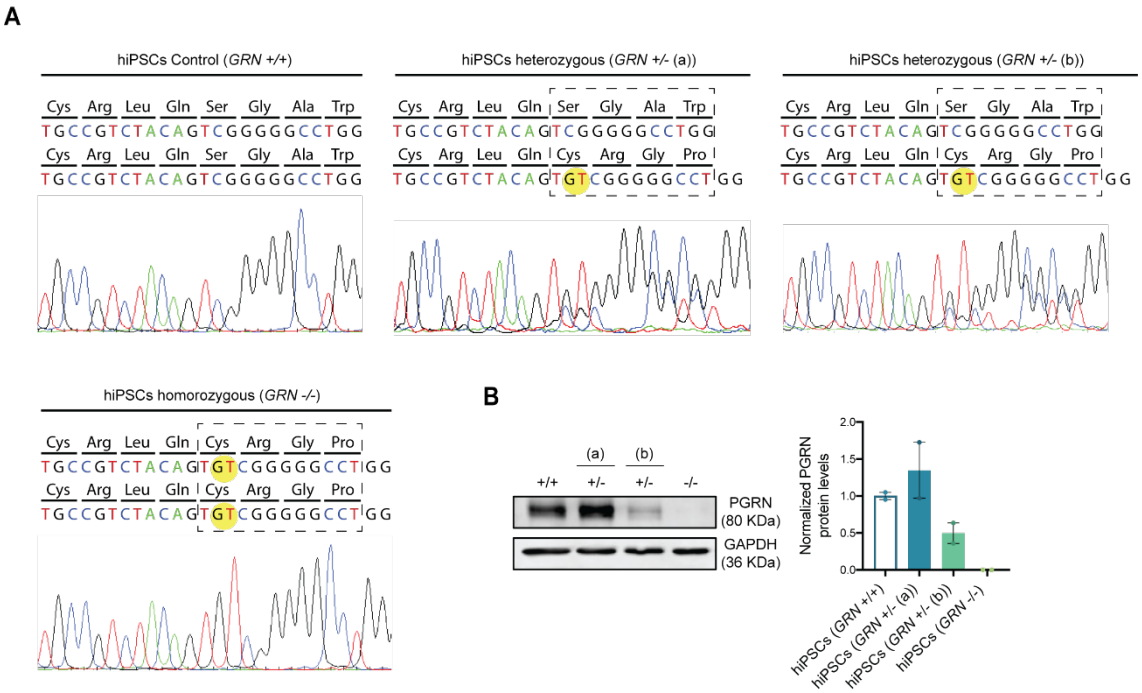

Figure 5.3. FTD patient-derived hiPSCs present different progranulin genotypes.
After reprogramming, DNA sequencing and protein expression of the newly established hiPSC lines from the three different individuals were assessed and the presence of progranulin mutation c.900_901dupGT was confirmed in all colonies generated from each of the three individuals. **(A)** Electropherogram of the regions containing the studied mutation in the generated hiPSCs shows the GT duplication in one allele from the patient harboring the heterozygous mutation and in both alleles from the patient harboring the homozygous mutation. **(B)** Western blot quantification of PGRN protein levels was performed in two independent hiPSC colonies from each individual. Representative western blot membrane and quantification of PGRN band density levels, normalized to GAPDH show a decrease in PGRN protein levels in both disease conditions, except for the asymptomatic heterozygous individual (*GRN* $^{+/-}$ (a)) that shows an increase in PGRN protein levels. Data are presented as mean ± s.e.m.

5.2.3. Patient-derived hiPSCs can generate brain organoids

Next, we wanted to understand the ability of the developed hiPSC lines to generate specific cell types from the ectodermal lineage, including neurons, in a complex 3D culture system. For this purpose, we employed the established protocol from Lancaster and colleagues (Holler et al., 2016; Lee et al., 2017) to originate brain organoids, as demonstrated in Figure 5.4A. In the first step of this process, EBs were formed from one stable hiPSC clone from each individual (at a cell passage above 20) and their size was monitored throughout the first 5 days. Interestingly, at day 5, we could observe a significant decrease in the diameter of the EBs obtained from the *GRN*$^{-/-}$ line, as well as in the *GRN*$^{+/-}$ (a) line with respect to organoids obtained from control lines (**Fig. 5.4B**). Nevertheless, we found that all three tested hiPSC lines could generate human brain organoids. At two months in culture, and similarly to controls, organoids from all three new lines presented ventricle-like structures that mimic the initial stages of cortical plate development with expression of the neuronal precursor marker NESTIN (**Fig. 5.4C**). It was also apparent the presence of the neuronal marker MAP2, more evident in the outer part of the ventricle, reflecting the inside-out neuronal migration (**Fig. 5.4C**). These findings were complemented by qPCR analysis, which revealed an increase in the expression of ectodermal genes (*NCAM1*, *NESTIN* and *β-III TUBULIN*) at this same age (**Fig. 5.4D**)

PRGN levels were also analyzed in 3-month-old brain organoids and the profile of protein expression was similar to what was previously observed in hiPSCs (**Fig. 5.4E**). We found a modest increase in PGRN in brain organoids generated from *GRN*$^{+/-}$ (a), a decrease of approximately 60% in brain organoids generated from the *GRN*$^{+/-}$ (b) hiPSC line and total loss of PGRN expression in brain organoids generated from the *GRN*$^{-/-}$ hiPSC line (**Fig. 5.4E**).

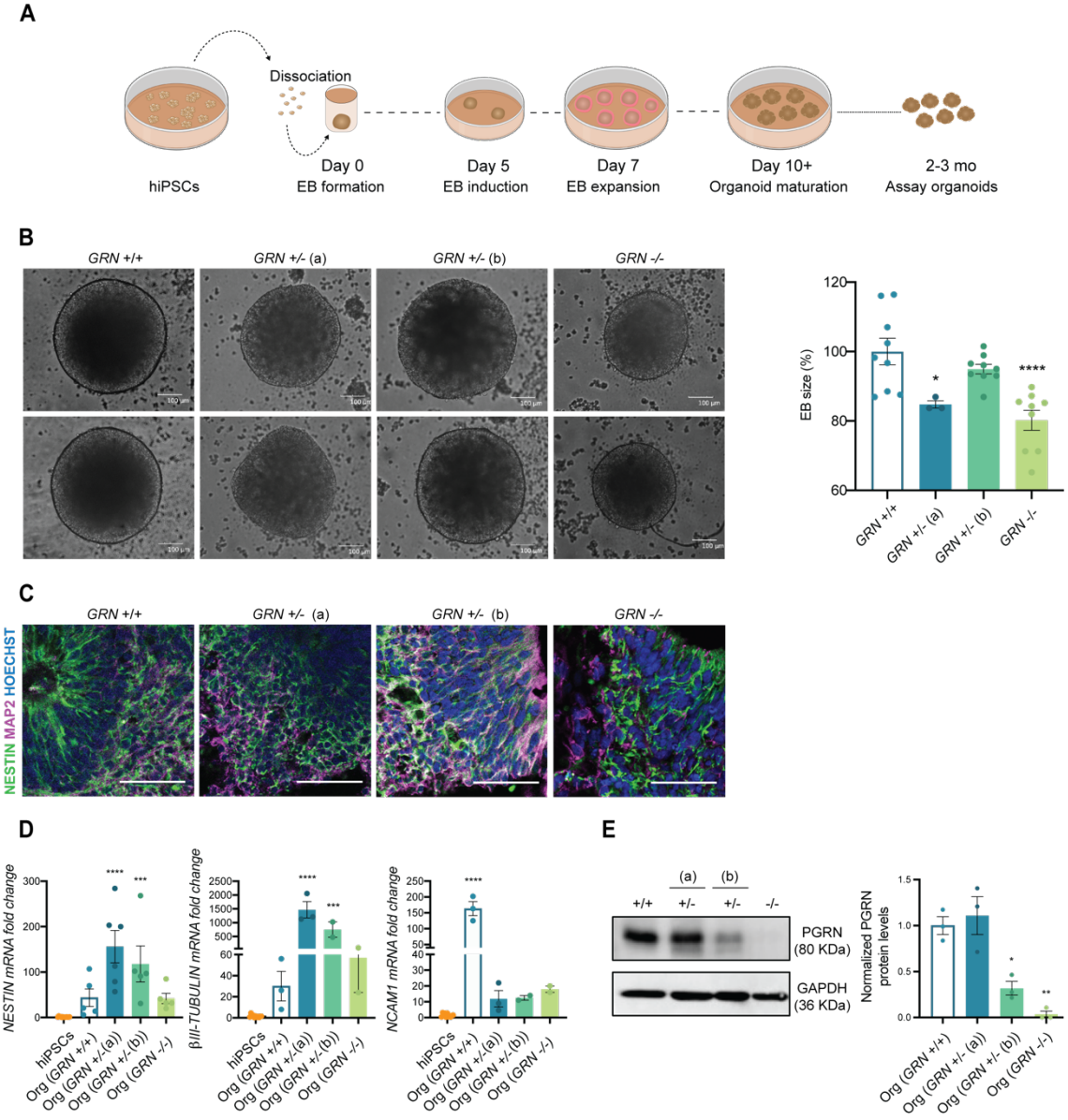

Figure 5.4. FTD patient-derived hiPSCs are capable of generating brain organoids.
Newly established hiPSCs were used to generate human 3D brain models. **(A)** Schematic representation of the organoid generation, following the protocol established by Lancaster and colleagues. **(B)** EBs size was determined at day 5 of the protocol and is presented as a % of control genotype. EBs from *GRN* $^{+/-}$ (a) and *GRN* $^{-/-}$ genotypes show a decrease in mean size. **(C)** The neuronal precursor NESTIN and neuronal marker MAP2 are expressed in 2-month-old generated brain organoids, as observed by immunohistochemistry. **(D)** Increased expression of ectodermal genes (*NESTIN*, *βIII-TUBULIN*, *NCAM1*) was also observed in the the generated brain organoids with respect to hiPSCs. **(E)** Representative western blot membrane and quantification of PGRN in 3-month-old organoids (n = 3 per genotype), normalized to GAPDH, shows a reduction in protein levels of PGRN in brain organoids of both *GRN* $^{+/-}$ (b) and *GRN* $^{-/-}$ conditions, while the *GRN* $^{+/-}$ (a) condition showed similar levels to control. One-way ANOVA following Dunnet's multiple comparisons test. Data are presented as mean ± s.e.m. Statistical significance: *p < 0.05, **p < 0.01, ***p < 0.001, ****p < 0.0001.

5.3. Discussion

GRN mutations causes a range of neurological disorders, presenting an allele dose-dependent pattern. While homozygous loss-of-function *GRN* mutations are very rare and result in a specific subtype of neuronal ceroid lipofuscinosis (CLN11), heterozygous mutations in this gene are more common and, in the case of the Portuguese population, constitute the second leading cause of genetic FTLD, a rapidly progressing type of dementia. Interestingly, while most neurodegeneration-related risk genes, such as *APP* and *SOD1*, are usually associated with a specific disease, *GRN* mutations and polymorphisms appear to be involved in a diverse group of neurological conditions, ranging from FTLD to ALS, AD, PD and even autism. This places the *GRN* gene in a unique position to regulate brain health.

Recent advances in our understanding of the cellular and molecular consequences of reduced PGRN levels have established a crucial role for this protein in lysosomal health (Butler et al., 2019), neuronal survival (Baker et al., 2006; Cruts et al., 2006), synaptic pruning and neuroinflammation (Broce et al., 2018; Ferrari et al., 2014; Miller et al., 2013; Zhang et al., 2020). Despite these insights, PGRN mechanisms of action and main signaling cascades are still poorly understood. For example, although we know that PGRN is cleaved into a set of smaller proteins named granulins inside the lysosome, little is known concerning the interplay of PGRN with its cleavage products and the role of granulins in brain homeostasis. Other relevant questions that remain unanswered include: 1) how does PGRN impact autophagy, 2) how do PGRN levels change throughout life and what epigenetic mechanisms regulate PGRN expression, 3) is there a critical period during development when PGRN is essential, 4) is restoring PGRN expression a therapeutic avenue to treat neurodegeneration and, if so, 5) how tightly do we need to control PGRN levels given its trophic properties?

In order to answer these questions, we believe that it is crucial to develop novel humanized research models that allow to simultaneously preserve the genetic background of individuals bearing *GRN* mutations and recapitulate the major pathophysiological hallmarks observed in FTLD and other *GRN*-associated diseases. With this in mind, we generated hiPSCs from dermal fibroblasts obtained from several members of a Portuguese family where cases of both FTLD-GRN and CLN11 had been previously diagnosed (Almeida et al., 2016; Guerreiro et al., 2008).

Ever since Yamanaka et al. reported that overexpressing OCT4, SOX2, KLF4 and MYC (OSKM) in mouse fibroblasts would induce the recapitulation of embryonic stem cell features and abilities (Takahashi and Yamanaka, 2006), an important ethical barrier (experimenting with human embryos) was overcome. The emerging realm of induced

pluripotent stem cells has revolutionized the ability of scientists to produce better and cheaper models of human system homeostasis and human diseases. Although the discovery of OSKM factors was a landmark for iPSC development, it was just the first step in this blooming field of science. Since then, several other reprogramming factors were identified and described to improve reprograming of different types of human and rodent cells, including fibroblasts and blood cells (Febbraro et al., 2021; K and S, 2016). In this work, human fibroblasts were effectively reprogramed by episomal nucleofection of the 4 Yamanaka factors: OCT3/4, SOX2, KLF4 and MYC, together with the miR 302/367 cluster (Yamanaka, 2007; Zaehres et al., 2005). To ensure that the newly generated cell lines were indeed iPSCs, quality control methods were used for their characterization, according to the currently accepted best practices for the characterization of iPSCs (Chen et al., 2021), including cell morphology analysis, expression of pluripotency-associated markers, ability to differentiate into the three germ layers and karyotype analysis.

Since iPSCs should be able to originate any cell type, they need to exhibit both pluripotency and the ability to differentiate into a diverse range of cells, with origin in different embryonic leaflets. In this study, both criteria were met for the cells from all PGRN mutation-carriers (**Fig. 5.2C-D, E**). However, different levels of expression of pluripotency genes were observed, which may be related to the different genetic backgrounds of the patients or due to the differences in reprogramming efficiency of each fibroblast line.

Currently, the trilineage assay is considered the standard method to evaluate iPSCs ability to generate EBs and spontaneously differentiate into the 3 germ layers: endoderm, mesoderm, and ectoderm (**Fig. 5.2E**). This assay has replaced the previously preferred teratoma assay, that consisted on the injection of iPSCs into an immune-deficient mice to assess the ability of these cells to generate a tumor (Takahashi et al., 2007; Yu et al., 2007). By replacing the teratoma assay by the trilineage assay, the same conclusion can be drawn from a less expensive and time-consuming method, while also avoiding the use of animal models. All three cell lines developed in this work were able to form EBs and express the three lineage markers SMA, GATA4, NESTIN and βIII-TUBULIN, which confirmed their iPSC status.

Since the reprogramming process is often associated with high mutation rates, which may lead to the accumulation of genomic abnormalities, karyotyping analysis is also a standard procedure in iPSC characterization. All the generated lines maintained the normal karyotype (**Fig. 5.2F**) at passage 20. However, genomic abnormalities can accumulate during long-term culturing (Ben-David et al., 2011), becoming essential to

repeat the analysis over time or restrict use to low cell passages. Additionally, it may be useful to employ other methods to detect genomic alterations not reported by karyotyping, including single nucleotide polymorphisms (SNPs) and copy number variation (CNV) arrays (Hussein et al., 2011; Närvä et al., 2010).

Considering the strong impact of *GRN* mutations in the brain, an organ that originates from the ectoderm germ layer, we decided to further test the ability of these new lines to generate ectoderm-specific cells through the formation of 3D brain organoids (**Fig. 5.4B-D**). Upon neuronal induction, we confirmed the expected increase of several ectodermal (NESTIN, βIII-TUBULIN and NCAM1) and neuronal markers (NESTIN and MAP2) (**Fig. 5.4C-D**) (Lancaster et al., 2013), as compared to the respective hiPSC line. Within the same genotype, some degree of variability was detected in the expression of these genes, which may be related to the intrinsic variability associated with the unguided organoid protocol (Lancaster and Knoblich, 2014).

Lastly, and to evaluate whether the generated cell lines presented the expected reduction in PGRN, typically observed in FTLD patients with *GRN* mutations, PGRN levels were assessed by western blot in both hiPSCs (**Fig. 3B**) and brain organoids (**Fig. 5.4E**). The profile of PGRN expression was similar in both hiPSCs and organoids, and recapitulated progranulin levels in primary fibroblasts and blood cells from the carriers (data not shown), showing that the genetic feature in study is efficiently preserved throughout the reprograming and differentiation protocols. As expected, we observed a complete loss of PGRN expression in the homozygous mutation carrier ($GRN^{-/-}$), and a significant reduction in one of the heterozygous carriers $GRN^{+/-}$ (b). Interestingly, the other heterozygous carrier ($GRN^{+/-}$ (a)) presented levels of PGRN expression similar to those of the control. Since this individual was relatively young and still asymptomatic at the time of the skin biopsy, these results may reflect a case of haplosufficiency that can later evolve to haploinsufficiency, as the organism ages and loses the ability to produce the necessary protein to preserve normal function from a single gene copy. These observations corroborate the hypothesis that PGRN levels change throughout life and tend to decrease with aging, hinting at a possible compensatory mechanism that sustains high levels of PGRN expression in *GRN* mutation carriers and that, once lost, contributes to the onset of FTLD symptoms.

In this present study, patient-derived human dermal fibroblasts bearing *GRN* mutations were successfully reprogrammed into hiPSCs. The newly generated hiPSCs can be further differentiated into cell types of the three germ layers, including neurons, as well as employed to generate complex 3D cellular models, such as brain organoids,

with the ability to recapitulate the genetic and molecular features of the original patients' cells.

CHAPTER 6

GENERAL DISCUSSION AND FUTURE DIRECTIONS

CASPR2 is one of the various cell-adhesion molecules with a central role in the central nervous system. Some of its functions are well described, but there are still significant lack of understanding on the cellular and molecular mechanisms underlying human diseases associated to *CNTNAP2* mutations. Additionally, recent findings related with an overproduction of CASPR2 antibodies in autoimmune encephalitis have reinforced the impact of CASPR2 in neurological disorders (Irani et al., 2010). Moreover, it has been reported an increased risk of neurodevelopmental/neuropsychiatric disorders in the offspring of mothers with exacerbated levels of anti-CASPR2 autoantibodies (anti-CASPR2-Ab) (Brimberg et al., 2013; Coutinho et al., 2017a). Therefore, several studies in animal models have been performed to validate and understand the impact of these antibodies in the offspring (Bagnall-Moreau et al., 2020; Brimberg et al., 2016; Coutinho et al., 2017b). In this research work, we used a human brain model to study the impact of anti-CASPR2-Ab in the developmental trajectory and network activity in an earlier phase of human brain development.

First, we generated and characterized human brain organoids regarding the expression of proliferating cells, neuronal progenitor, mature neurons and different cellular subtypes over time. The generated organoids presented a decrease in the expression of proliferating cells and neuronal progenitor markers, but an increase in mature neuron markers, showing an inside-out migration of the neuronal populations. We also observed an increased in the expression of glial cells, including astrocytes, but not in microglia. Different cellular subtypes were also observed, including dopaminergic neurons, excitatory and inhibitory neurons. Therefore, considering the protocol used, our organoids express not only dorsal markers, but also ventral markers, which is in line with the heterogenous cell populations of this whole-brain model. In addition to the different cellular populations identified, we proved that these neurons were functionally mature after a long period in culture. Hence, we can claim that whole-brain organoids are robust models to recapitulate human fetal brain development, being valuable models to study several brain disorders. Notwithstanding, improvements to this model have been achieved by others, including the use of different brain regions of interest, depending on the questions raised in the study, and addition of microglia and endothelial cells. Since microglia plays crucial roles during the early stages of brain development, particularly by helping to shape neuronal circuits, supporting neuronal survival, eliminating the excess of neuronal progenitors and guiding axonal growth, in the context of the present work it would be interesting to generate microglia from human induced pluripotent stem cells (hiPSCs) and seed it into our brain organoid model (Abud et al., 2017; Fagerlund et al., 2021; Haenseler et al., 2017; Popova et al., 2021; Sabate-Soler et al., 2022; Xu et al.,

2021). Consequently, it contributes for neuronal maturation and increased neuronal excitability in brain organoids (Popova et al., 2021; Sabate-Soler et al., 2022), allowing the generation of even more complex and realistic human models.

Following the generation of human brain models that recapitulate human fetal brain, we wanted to assess the impact of anti-CASPR2-Ab in human brain development. Brain organoids were exposed from to 2 to 6 months of differentiation to autoimmune encephalitis patient plasma, containing anti-CASPR2-Ab. As previously demonstrated (Dawes et al., 2018; Patterson et al., 2018), we observed a decrease in CASPR2, and Contactin-2 protein levels in 6-month-old organoids exposed to anti-CASPR2-Ab. These changes influenced the neuronal excitability of brain organoids, reflected in increased excitability of individual neurons and an increase in the network activity, suggesting that anti-CASPR2-Ab may modulate neuronal excitability via Kv1 channels. However, to validate this hypothesis, it would be crucial to perform pharmacological modulation of Kv1 channel currents, using for example a specific blocker of these channels (Zhao et al., 2013). Moreover, immunofluorescence experiments are essential to evaluate the kv1 channels distribution in the neurons of brain organoids, particularly along the axons. Additionally, immunoprecipitation assays could be used to validate the decrease in CASPR2-Contactin-2 interaction that later may interfere with Kv1 distribution. Importantly, considering the decrease observed in GABAergic neurons in *CNTNAP2* mutation models (Bridi et al., 2017; Hali et al., 2020; Jurgensen and Castillo, 2015; Peñagarikano et al., 2011; Vogt et al., 2018), affecting the excitation/inhibition (E/I) balance and consequently the network activity, it would be interesting to understand whether the E/I balance is compromised in this brain organoid model. However, to do so, an assembloid of dorsal and ventral organoids (Bagley et al., 2017; Birey et al., 2017) would be preferred, due to the heterogenicity in cellular populations in the whole-brain model. Another important aspect, would be to repeat these studies in the presence of microglia, since it is already known that microglia is activated in models exposed to anti-CASPR2-Ab (Coutinho et al., 2017b; Giannoccaro et al., 2019; Körtvelyessy et al., 2015).

Besides their utility as models for environmental exposure to hazards, such as those exemplified by the maternal transfer of anti-CASPR2-Ab during the gestational period, brain organoids offer a sophisticated platform to study disease-associated genetic mutations. In parallel with the present work, we generated new hiPSC from fully differentiated somatic cells of patients using an episomal-based reprogramming system that is advantageous over integrating methods, known to prevent their use for clinical applications. After several weeks of maintenance and stabilization of different clones, the generated clones presented several features of hiPSCs. The different clones

expressed several pluripotency markers and differentiated into any of the three germ layers and no chromosomal abnormalities were observed. The generated hiPSCs were able to develop into brain organoids and will be used to generate disease-specific brain organoids models to study the underlying mechanisms of those diseases in complex human 3D brain models.

Overall, this work strongly contributed for the implementation of new models, which showed to be instrumental for the understanding of the consequences of environmental insults to the developing human brain, as assessed by exposing the human brain organoid models to anti-CASPR2-Ab. Additionally, these models are expected to provide particularly useful platforms for the study of brain disease-associated genetic mutations, which can be modulated from reprogrammed and easily accessible patient somatic cells.

CHAPTER 7
REFERENCES

Abdallah, M.W., Larsen, N., Grove, J., Nørgaard-Pedersen, B., Thorsen, P., Mortensen, E.L., Hougaard, D.M., 2012. Amniotic fluid chemokines and autism spectrum disorders: an exploratory study utilizing a Danish Historic Birth Cohort. Brain. Behav. Immun. 26, 170–176. https://doi.org/10.1016/j.bbi.2011.09.003

Abrahams, B.S., Tentler, D., Perederiy, J.V., Oldham, M.C., Coppola, G., Geschwind, D.H., 2007. Genome-wide analyses of human perisylvian cerebral cortical patterning. Proc. Natl. Acad. Sci. U. S. A. 104, 17849–17854. https://doi.org/10.1073/pnas.0706128104

Abud, E.M., Ramirez, R.N., Martinez, E.S., Healy, L.M., Nguyen, C.H.H., Newman, S.A., Yeromin, A.V., Scarfone, V.M., Marsh, S.E., Fimbres, C., Caraway, C.A., Fote, G.M., Madany, A.M., Agrawal, A., Kayed, R., Gylys, K.H., Cahalan, M.D., Cummings, B.J., Antel, J.P., Mortazavi, A., Carson, M.J., Poon, W.W., Blurton-Jones, M., 2017. iPSC-Derived Human Microglia-like Cells to Study Neurological Diseases. Neuron 94, 278-293.e9. https://doi.org/10.1016/j.neuron.2017.03.042

Adelman, J.P., Bond, C.T., Pessia, M., Maylie, J., 1995. Episodic ataxia results from voltage-dependent potassium channels with altered functions. Neuron 15, 1449–1454. https://doi.org/10.1016/0896-6273(95)90022-5

Ahmed, Z., Sheng, H., Xu, Y.-F., Lin, W.-L., Innes, A.E., Gass, J., Yu, X., Wuertzer, C.A., Hou, H., Chiba, S., Yamanouchi, K., Leissring, M., Petrucelli, L., Nishihara, M., Hutton, M.L., McGowan, E., Dickson, D.W., Lewis, J., 2010. Accelerated lipofuscinosis and ubiquitination in granulin knockout mice suggest a role for progranulin in successful aging. Am. J. Pathol. 177, 311–324. https://doi.org/10.2353/ajpath.2010.090915

Akhtar, A., 2015. The flaws and human harms of animal experimentation. Camb. Q. Healthc. Ethics CQ Int. J. Healthc. Ethics Comm. 24, 407–419. https://doi.org/10.1017/S0963180115000079

Alarcón, M., Abrahams, B.S., Stone, J.L., Duvall, J.A., Perederiy, J.V., Bomar, J.M., Sebat, J., Wigler, M., Martin, C.L., Ledbetter, D.H., Nelson, S.F., Cantor, R.M., Geschwind, D.H., 2008. Linkage, association, and gene-expression analyses identify CNTNAP2 as an autism-susceptibility gene. Am. J. Hum. Genet. 82, 150–159. https://doi.org/10.1016/j.ajhg.2007.09.005

Al-Ayadhi, L.Y., Mostafa, G.A., 2011. Low plasma progranulin levels in children with autism. J. Neuroinflammation 8, 111. https://doi.org/10.1186/1742-2094-8-111

Almeida, M.R., Macário, M.C., Ramos, L., Baldeiras, I., Ribeiro, M.H., Santana, I., 2016. Portuguese family with the co-occurrence of frontotemporal lobar degeneration and neuronal ceroid lipofuscinosis phenotypes due to progranulin gene mutation. Neurobiol. Aging 41, 200.e1-200.e5. https://doi.org/10.1016/j.neurobiolaging.2016.02.019

Amiri, A., Coppola, G., Scuderi, S., Wu, F., Roychowdhury, T., Liu, F., Pochareddy, S., Shin, Y., Safi, A., Song, L., Zhu, Y., Sousa, A.M.M., PsychENCODE Consortium, Gerstein, M., Crawford, G.E., Sestan, N., Abyzov, A., Vaccarino, F.M., 2018. Transcriptome and epigenome landscape of human cortical development modeled in organoids. Science 362, eaat6720. https://doi.org/10.1126/science.aat6720

Andersen, J., Revah, O., Miura, Y., Thom, N., Amin, N.D., Kelley, K.W., Singh, M., Chen, X., Thete, M.V., Walczak, E.M., Vogel, H., Fan, H.C., Paşca, S.P., 2020. Generation of

Functional Human 3D Cortico-Motor Assembloids. Cell 183, 1913-1929.e26. https://doi.org/10.1016/j.cell.2020.11.017

Anderson, G.R., Galfin, T., Xu, W., Aoto, J., Malenka, R.C., Südhof, T.C., 2012. Candidate autism gene screen identifies critical role for cell-adhesion molecule CASPR2 in dendritic arborization and spine development. Proc. Natl. Acad. Sci. U. S. A. 109, 18120–18125. https://doi.org/10.1073/pnas.1216398109

Arking, D.E., Cutler, D.J., Brune, C.W., Teslovich, T.M., West, K., Ikeda, M., Rea, A., Guy, M., Lin, S., Cook, E.H., Chakravarti, A., 2008. A common genetic variant in the neurexin superfamily member CNTNAP2 increases familial risk of autism. Am. J. Hum. Genet. 82, 160–164. https://doi.org/10.1016/j.ajhg.2007.09.015

Atladóttir, H.Ó., Henriksen, T.B., Schendel, D.E., Parner, E.T., 2012. Autism after infection, febrile episodes, and antibiotic use during pregnancy: an exploratory study. Pediatrics 130, e1447-1454. https://doi.org/10.1542/peds.2012-1107

Bagley, J.A., Reumann, D., Bian, S., Lévi-Strauss, J., Knoblich, J.A., 2017. Fused cerebral organoids model interactions between brain regions. Nat. Methods 14, 743–751. https://doi.org/10.1038/nmeth.4304

Bagnall-Moreau, C., Huerta, P.T., Comoletti, D., La-Bella, A., Berlin, R., Zhao, C., Volpe, B.T., Diamond, B., Brimberg, L., 2020. In utero exposure to endogenous maternal polyclonal anti-Caspr2 antibody leads to behavioral abnormalities resembling autism spectrum disorder in male mice. Sci. Rep. 10, 14446. https://doi.org/10.1038/s41598-020-71201-9

Baker, M., Mackenzie, I.R., Pickering-Brown, S.M., Gass, J., Rademakers, R., Lindholm, C., Snowden, J., Adamson, J., Sadovnick, A.D., Rollinson, S., Cannon, A., Dwosh, E., Neary, D., Melquist, S., Richardson, A., Dickson, D., Berger, Z., Eriksen, J., Robinson, T., Zehr, C., Dickey, C.A., Crook, R., McGowan, E., Mann, D., Boeve, B., Feldman, H., Hutton, M., 2006. Mutations in progranulin cause tau-negative frontotemporal dementia linked to chromosome 17. Nature 442, 916–919. https://doi.org/10.1038/nature05016

Bakkaloglu, B., O'Roak, B.J., Louvi, A., Gupta, A.R., Abelson, J.F., Morgan, T.M., Chawarska, K., Klin, A., Ercan-Sencicek, A.G., Stillman, A.A., Tanriover, G., Abrahams, B.S., Duvall, J.A., Robbins, E.M., Geschwind, D.H., Biederer, T., Gunel, M., Lifton, R.P., State, M.W., 2008. Molecular cytogenetic analysis and resequencing of contactin associated protein-like 2 in autism spectrum disorders. Am. J. Hum. Genet. 82, 165–173. https://doi.org/10.1016/j.ajhg.2007.09.017

Bastiaansen, A.E.M., van Sonderen, A., Titulaer, M.J., 2017. Autoimmune encephalitis with anti-leucine-rich glioma-inactivated 1 or anti-contactin-associated protein-like 2 antibodies (formerly called voltage-gated potassium channel-complex antibodies). Curr. Opin. Neurol. 30, 302–309. https://doi.org/10.1097/WCO.0000000000000444

Bauman, M.D., Iosif, A.-M., Ashwood, P., Braunschweig, D., Lee, A., Schumann, C.M., Van de Water, J., Amaral, D.G., 2013. Maternal antibodies from mothers of children with autism alter brain growth and social behavior development in the rhesus monkey. Transl. Psychiatry 3, e278. https://doi.org/10.1038/tp.2013.47

Beck, H., Yaari, Y., 2008. Plasticity of intrinsic neuronal properties in CNS disorders. Nat. Rev. Neurosci. 9, 357–369. https://doi.org/10.1038/nrn2371

Belloso, J.M., Bache, I., Guitart, M., Caballin, M.R., Halgren, C., Kirchhoff, M., Ropers, H.-H., Tommerup, N., Tümer, Z., 2007. Disruption of the CNTNAP2 gene in a t(7;15) translocation family without symptoms of Gilles de la Tourette syndrome. Eur. J. Hum. Genet. EJHG 15, 711–713. https://doi.org/10.1038/sj.ejhg.5201824

Ben-David, U., Mayshar, Y., Benvenisty, N., 2011. Large-scale analysis reveals acquisition of lineage-specific chromosomal aberrations in human adult stem cells. Cell Stem Cell 9, 97–102. https://doi.org/10.1016/j.stem.2011.06.013

Bennett, V., Lambert, S., 1999. Physiological roles of axonal ankyrins in survival of premyelinated axons and localization of voltage-gated sodium channels. J. Neurocytol. 28, 303–318. https://doi.org/10.1023/a:1007005528505

Bertil Hille, D. k., 1992. Ionic channels of excitable membranes (second edition). Sinauer Assoc. Inc 306, 277–278. https://doi.org/10.1016/0014-5793(92)81020-M

Bhaduri, A., Andrews, M.G., Mancia, W., Jung, Diane, Shin, D., Allen, D., Jung, Dana, Schmunk, G., Haeussler, M., Salma, J., Pollen, A.A., Nowakowski, T.J., Kriegstein, A.R., 2020. Cell Stress in Cortical Organoids Impairs Molecular Subtype Specification. Nature 578, 142–148. https://doi.org/10.1038/s41586-020-1962-0

Bien, C.G., Mirzadjanova, Z., Baumgartner, C., Onugoren, M.D., Grunwald, T., Holtkamp, M., Isenmann, S., Kermer, P., Melzer, N., Naumann, M., Riepe, M., Schäbitz, W.R., von Oertzen, T.J., von Podewils, F., Rauschka, H., May, T.W., 2017. Anti-contactin-associated protein-2 encephalitis: relevance of antibody titres, presentation and outcome. Eur. J. Neurol. 24, 175–186. https://doi.org/10.1111/ene.13180

Binks, S.N.M., Klein, C.J., Waters, P., Pittock, S.J., Irani, S.R., 2018. LGI1, CASPR2 and related antibodies: a molecular evolution of the phenotypes. J. Neurol. Neurosurg. Psychiatry 89, 526–534. https://doi.org/10.1136/jnnp-2017-315720

Birey, F., Andersen, J., Makinson, C.D., Islam, S., Wei, W., Huber, N., Fan, H.C., Metzler, K.R.C., Panagiotakos, G., Thom, N., O'Rourke, N.A., Steinmetz, L.M., Bernstein, J.A., Hallmayer, J., Huguenard, J.R., Paşca, S.P., 2017. Assembly of functionally integrated human forebrain spheroids. Nature 545, 54–59. https://doi.org/10.1038/nature22330

Birey, F., Li, M.-Y., Gordon, A., Thete, M.V., Valencia, A.M., Revah, O., Paşca, A.M., Geschwind, D.H., Paşca, S.P., 2022. Dissecting the molecular basis of human interneuron migration in forebrain assembloids from Timothy syndrome. Cell Stem Cell 29, 248-264.e7. https://doi.org/10.1016/j.stem.2021.11.011

Bodnar, B., Zhang, Y., Liu, J., Lin, Y., Wang, P., Wei, Z., Saribas, S., Zhu, Y., Li, F., Wang, X., Yang, W., Li, Q., Ho, W.-Z., Hu, W., 2021. Novel Scalable and Simplified System to Generate Microglia-Containing Cerebral Organoids From Human Induced Pluripotent Stem Cells. Front. Cell. Neurosci. 15, 682272. https://doi.org/10.3389/fncel.2021.682272

Braunschweig, D., Ashwood, P., Krakowiak, P., Hertz-Picciotto, I., Hansen, R., Croen, L.A., Pessah, I.N., Van de Water, J., 2008. Autism: maternally derived antibodies

specific for fetal brain proteins. Neurotoxicology 29, 226–231. https://doi.org/10.1016/j.neuro.2007.10.010

Brennand, K.J., Simone, A., Jou, J., Gelboin-Burkhart, C., Tran, N., Sangar, S., Li, Y., Mu, Y., Chen, G., Yu, D., McCarthy, S., Sebat, J., Gage, F.H., 2011. Modelling schizophrenia using human induced pluripotent stem cells. Nature 473, 221–225. https://doi.org/10.1038/nature09915

Brew, H.M., Gittelman, J.X., Silverstein, R.S., Hanks, T.D., Demas, V.P., Robinson, L.C., Robbins, C.A., McKee-Johnson, J., Chiu, S.Y., Messing, A., Tempel, B.L., 2007. Seizures and reduced life span in mice lacking the potassium channel subunit Kv1.2, but hypoexcitability and enlarged Kv1 currents in auditory neurons. J. Neurophysiol. 98, 1501–1525. https://doi.org/10.1152/jn.00640.2006

Bridi, M.S., Park, S.M., Huang, S., 2017. Developmental Disruption of GABAAR-Meditated Inhibition in Cntnap2 KO Mice. eNeuro 4, ENEURO.0162-17.2017. https://doi.org/10.1523/ENEURO.0162-17.2017

Brimberg, L., Mader, S., Jeganathan, V., Berlin, R., Coleman, T.R., Gregersen, P.K., Huerta, P.T., Volpe, B.T., Diamond, B., 2016. Caspr2-reactive antibody cloned from a mother of an ASD child mediates an ASD-like phenotype in mice. Mol. Psychiatry 21, 1663–1671. https://doi.org/10.1038/mp.2016.165

Brimberg, L., Sadiq, A., Gregersen, P.K., Diamond, B., 2013. Brain-reactive IgG correlates with autoimmunity in mothers of a child with an autism spectrum disorder. Mol. Psychiatry 18, 1171–1177. https://doi.org/10.1038/mp.2013.101

Broce, I., Karch, C.M., Wen, N., Fan, C.C., Wang, Y., Tan, C.H., Kouri, N., Ross, O.A., Höglinger, G.U., Muller, U., Hardy, J., International FTD-Genomics Consortium, Momeni, P., Hess, C.P., Dillon, W.P., Miller, Z.A., Bonham, L.W., Rabinovici, G.D., Rosen, H.J., Schellenberg, G.D., Franke, A., Karlsen, T.H., Veldink, J.H., Ferrari, R., Yokoyama, J.S., Miller, B.L., Andreassen, O.A., Dale, A.M., Desikan, R.S., Sugrue, L.P., 2018. Immune-related genetic enrichment in frontotemporal dementia: An analysis of genome-wide association studies. PLoS Med. 15, e1002487. https://doi.org/10.1371/journal.pmed.1002487

Bruni, A.C., Momeni, P., Bernardi, L., Tomaino, C., Frangipane, F., Elder, J., Kawarai, T., Sato, C., Pradella, S., Wakutani, Y., Anfossi, M., Gallo, M., Geracitano, S., Costanzo, A., Smirne, N., Curcio, S. a. M., Mirabelli, M., Puccio, G., Colao, R., Maletta, R.G., Kertesz, A., St George-Hyslop, P., Hardy, J., Rogaeva, E., 2007. Heterogeneity within a large kindred with frontotemporal dementia: a novel progranulin mutation. Neurology 69, 140–147. https://doi.org/10.1212/01.wnl.0000265220.64396.b4

Butler, V.J., Cortopassi, W.A., Argouarch, A.R., Ivry, S.L., Craik, C.S., Jacobson, M.P., Kao, A.W., 2019. Progranulin Stimulates the In Vitro Maturation of Pro-Cathepsin D at Acidic pH. J. Mol. Biol. 431, 1038–1047. https://doi.org/10.1016/j.jmb.2019.01.027

Cakir, B., Xiang, Y., Tanaka, Y., Kural, M.H., Parent, M., Kang, Y.-J., Chapeton, K., Patterson, B., Yuan, Y., He, C.-S., Raredon, M.S.B., Dengelegi, J., Kim, K.-Y., Sun, P., Zhong, M., Lee, S., Patra, P., Hyder, F., Niklason, L.E., Lee, S.-H., Yoon, Y.-S., Park, I.-H., 2019. Engineering of human brain organoids with a functional vascular-like system. Nat. Methods 16, 1169–1175. https://doi.org/10.1038/s41592-019-0586-5

Camp, J.G., Badsha, F., Florio, M., Kanton, S., Gerber, T., Wilsch-Bräuninger, M., Lewitus, E., Sykes, A., Hevers, W., Lancaster, M., Knoblich, J.A., Lachmann, R., Pääbo, S., Huttner, W.B., Treutlein, B., 2015. Human cerebral organoids recapitulate gene expression programs of fetal neocortex development. Proc. Natl. Acad. Sci. U. S. A. 112, 15672–15677. https://doi.org/10.1073/pnas.1520760112

Canafoglia, L., Morbin, M., Scaioli, V., Pareyson, D., D'Incerti, L., Fugnanesi, V., Tagliavini, F., Berkovic, S.F., Franceschetti, S., 2014. Recurrent generalized seizures, visual loss, and palinopsia as phenotypic features of neuronal ceroid lipofuscinosis due to progranulin gene mutation. Epilepsia 55, e56-59. https://doi.org/10.1111/epi.12632

Canali, G., Garcia, M., Hivert, B., Pinatel, D., Goullancourt, A., Oguievetskaia, K., Saint-Martin, M., Girault, J.-A., Faivre-Sarrailh, C., Goutebroze, L., 2018. Genetic variants in autism-related CNTNAP2 impair axonal growth of cortical neurons. Hum. Mol. Genet. 27, 1941–1954. https://doi.org/10.1093/hmg/ddy102

Cederquist, G.Y., Asciolla, J.J., Tchieu, J., Walsh, R.M., Cornacchia, D., Resh, M.D., Studer, L., 2019. Specification of positional identity in forebrain organoids. Nat. Biotechnol. 37, 436–444. https://doi.org/10.1038/s41587-019-0085-3

Chang, M.C., Srinivasan, K., Friedman, B.A., Suto, E., Modrusan, Z., Lee, W.P., Kaminker, J.S., Hansen, D.V., Sheng, M., 2017. Progranulin deficiency causes impairment of autophagy and TDP-43 accumulation. J. Exp. Med. 214, 2611–2628. https://doi.org/10.1084/jem.20160999

Chen, C.X.-Q., Abdian, N., Maussion, G., Thomas, R.A., Demirova, I., Cai, E., Tabatabaei, M., Beitel, L.K., Karamchandani, J., Fon, E.A., Durcan, T.M., 2021. A Multistep Workflow to Evaluate Newly Generated iPSCs and Their Ability to Generate Different Cell Types. Methods Protoc. 4, 50. https://doi.org/10.3390/mps4030050

Chen, N., Koopmans, F., Gordon, A., Paliukhovich, I., Klaassen, R.V., van der Schors, R.C., Peles, E., Verhage, M., Smit, A.B., Li, K.W., 2015. Interaction proteomics of canonical Caspr2 (CNTNAP2) reveals the presence of two Caspr2 isoforms with overlapping interactomes. Biochim. Biophys. Acta 1854, 827–833. https://doi.org/10.1016/j.bbapap.2015.02.008

Chien, Y.-L., Chen, Y.-C., Gau, S.S.-F., 2021. Altered cingulate structures and the associations with social awareness deficits and CNTNAP2 gene in autism spectrum disorder. NeuroImage Clin. 31, 102729. https://doi.org/10.1016/j.nicl.2021.102729

Choi, G.B., Yim, Y.S., Wong, H., Kim, S., Kim, H., Kim, S.V., Hoeffer, C.A., Littman, D.R., Huh, J.R., 2016. The maternal interleukin-17a pathway in mice promotes autism-like phenotypes in offspring. Science 351, 933–939. https://doi.org/10.1126/science.aad0314

Coleman, S.K., Newcombe, J., Pryke, J., Dolly, J.O., 1999. Subunit Composition of Kv1 Channels in Human CNS. J. Neurochem. 73, 849–858. https://doi.org/10.1046/j.1471-4159.1999.0730849.x

Coutinho, E., Jacobson, L., Pedersen, M.G., Benros, M.E., Nørgaard-Pedersen, B., Mortensen, P.B., Harrison, P.J., Vincent, A., 2017a. CASPR2 autoantibodies are raised during pregnancy in mothers of children with mental retardation and

disorders of psychological development but not autism. J. Neurol. Neurosurg. Psychiatry 88, 718–721. https://doi.org/10.1136/jnnp-2016-315251

Coutinho, E., Menassa, D.A., Jacobson, L., West, S.J., Domingos, J., Moloney, T.C., Lang, B., Harrison, P.J., Bennett, D.L.H., Bannerman, D., Vincent, A., 2017b. Persistent microglial activation and synaptic loss with behavioral abnormalities in mouse offspring exposed to CASPR2-antibodies in utero. Acta Neuropathol. (Berl.) 134, 567–583. https://doi.org/10.1007/s00401-017-1751-5

Croen, L.A., Braunschweig, D., Haapanen, L., Yoshida, C.K., Fireman, B., Grether, J.K., Kharrazi, M., Hansen, R.L., Ashwood, P., Van de Water, J., 2008. Maternal mid-pregnancy autoantibodies to fetal brain protein: the early markers for autism study. Biol. Psychiatry 64, 583–588. https://doi.org/10.1016/j.biopsych.2008.05.006

Cruts, M., Gijselinck, I., van der Zee, J., Engelborghs, S., Wils, H., Pirici, D., Rademakers, R., Vandenberghe, R., Dermaut, B., Martin, J.-J., van Duijn, C., Peeters, K., Sciot, R., Santens, P., De Pooter, T., Mattheijssens, M., Van den Broeck, M., Cuijt, I., Vennekens, K., De Deyn, P.P., Kumar-Singh, S., Van Broeckhoven, C., 2006. Null mutations in progranulin cause ubiquitin-positive frontotemporal dementia linked to chromosome 17q21. Nature 442, 920–924. https://doi.org/10.1038/nature05017

Dalmau, J., Geis, C., Graus, F., 2017. Autoantibodies to Synaptic Receptors and Neuronal Cell Surface Proteins in Autoimmune Diseases of the Central Nervous System. Physiol. Rev. 97, 839–887. https://doi.org/10.1152/physrev.00010.2016

Dalmau, J., Tüzün, E., Wu, H., Masjuan, J., Rossi, J.E., Voloschin, A., Baehring, J.M., Shimazaki, H., Koide, R., King, D., Mason, W., Sansing, L.H., Dichter, M.A., Rosenfeld, M.R., Lynch, D.R., 2007. Paraneoplastic anti-N-methyl-D-aspartate receptor encephalitis associated with ovarian teratoma. Ann. Neurol. 61, 25–36. https://doi.org/10.1002/ana.21050

Dalton, P., Deacon, R., Blamire, A., Pike, M., McKinlay, I., Stein, J., Styles, P., Vincent, A., 2003. Maternal neuronal antibodies associated with autism and a language disorder. Ann. Neurol. 53, 533–537. https://doi.org/10.1002/ana.10557

Daviaud, N., Friedel, R.H., Zou, H., 2018. Vascularization and Engraftment of Transplanted Human Cerebral Organoids in Mouse Cortex. eNeuro 5, ENEURO.0219-18.2018. https://doi.org/10.1523/ENEURO.0219-18.2018

Dawes, J.M., Weir, G.A., Middleton, S.J., Patel, R., Chisholm, K.I., Pettingill, P., Peck, L.J., Sheridan, J., Shakir, A., Jacobson, L., Gutierrez-Mecinas, M., Galino, J., Walcher, J., Kühnemund, J., Kuehn, H., Sanna, M.D., Lang, B., Clark, A.J., Themistocleous, A.C., Iwagaki, N., West, S.J., Werynska, K., Carroll, L., Trendafilova, T., Menassa, D.A., Giannoccaro, M.P., Coutinho, E., Cervellini, I., Tewari, D., Buckley, C., Leite, M.I., Wildner, H., Zeilhofer, H.U., Peles, E., Todd, A.J., McMahon, S.B., Dickenson, A.H., Lewin, G.R., Vincent, A., Bennett, D.L., 2018. Immune or Genetic-Mediated Disruption of CASPR2 Causes Pain Hypersensitivity Due to Enhanced Primary Afferent Excitability. Neuron 97, 806-822.e10. https://doi.org/10.1016/j.neuron.2018.01.033

Debanne, D., Guérineau, N.C., Gähwiler, B.H., Thompson, S.M., 1997. Action-potential propagation gated by an axonal I(A)-like K+ conductance in hippocampus. Nature 389, 286–289. https://doi.org/10.1038/38502

Denisenko-Nehrbass, N., Goutebroze, L., Galvez, T., Bonnon, C., Stankoff, B., Ezan, P., Giovannini, M., Faivre-Sarrailh, C., Girault, J.-A., 2003a. Association of Caspr/paranodin with tumour suppressor schwannomin/merlin and beta1 integrin in the central nervous system. J. Neurochem. 84, 209–221. https://doi.org/10.1046/j.1471-4159.2003.01503.x

Denisenko-Nehrbass, N., Oguievetskaia, K., Goutebroze, L., Galvez, T., Yamakawa, H., Ohara, O., Carnaud, M., Girault, J.-A., 2003b. Protein 4.1B associates with both Caspr/paranodin and Caspr2 at paranodes and juxtaparanodes of myelinated fibres. Eur. J. Neurosci. 17, 411–416. https://doi.org/10.1046/j.1460-9568.2003.02441.x

Devaux, J., Alcaraz, G., Grinspan, J., Bennett, V., Joho, R., Crest, M., Scherer, S.S., 2003. Kv3.1b is a novel component of CNS nodes. J. Neurosci. Off. J. Soc. Neurosci. 23, 4509–4518.

Dodson, P.D., Billups, B., Rusznák, Z., Szûcs, G., Barker, M.C., Forsythe, I.D., 2003. Presynaptic rat Kv1.2 channels suppress synaptic terminal hyperexcitability following action potential invasion. J. Physiol. 550, 27–33. https://doi.org/10.1113/jphysiol.2003.046250

Eiraku, M., Takata, N., Ishibashi, H., Kawada, M., Sakakura, E., Okuda, S., Sekiguchi, K., Adachi, T., Sasai, Y., 2011. Self-organizing optic-cup morphogenesis in three-dimensional culture. Nature 472, 51–56. https://doi.org/10.1038/nature09941

Eiraku, M., Watanabe, K., Matsuo-Takasaki, M., Kawada, M., Yonemura, S., Matsumura, M., Wataya, T., Nishiyama, A., Muguruma, K., Sasai, Y., 2008. Self-organized formation of polarized cortical tissues from ESCs and its active manipulation by extrinsic signals. Cell Stem Cell 3, 519–532. https://doi.org/10.1016/j.stem.2008.09.002

Estes, M.L., McAllister, A.K., 2016. Maternal immune activation: Implications for neuropsychiatric disorders. Science 353, 772–777. https://doi.org/10.1126/science.aag3194

Evans, M.J., Kaufman, M.H., 1981. Establishment in culture of pluripotential cells from mouse embryos. Nature 292, 154–156. https://doi.org/10.1038/292154a0

Evers, B.M., Rodriguez-Navas, C., Tesla, R.J., Prange-Kiel, J., Wasser, C.R., Yoo, K.S., McDonald, J., Cenik, B., Ravenscroft, T.A., Plattner, F., Rademakers, R., Yu, G., White, C.L., Herz, J., 2017. Lipidomic and Transcriptomic Basis of Lysosomal Dysfunction in Progranulin Deficiency. Cell Rep. 20, 2565–2574. https://doi.org/10.1016/j.celrep.2017.08.056

Fagerlund, I., Dougalis, A., Shakirzyanova, A., Gómez-Budia, M., Pelkonen, A., Konttinen, H., Ohtonen, S., Fazaludeen, M.F., Koskuvi, M., Kuusisto, J., Hernández, D., Pebay, A., Koistinaho, J., Rauramaa, T., Lehtonen, Š., Korhonen, P., Malm, T., 2021. Microglia-like Cells Promote Neuronal Functions in Cerebral Organoids. Cells 11, 124. https://doi.org/10.3390/cells11010124

Fair, S.R., Julian, D., Hartlaub, A.M., Pusuluri, S.T., Malik, G., Summerfied, T.L., Zhao, G., Hester, A.B., Ackerman, W.E., Hollingsworth, E.W., Ali, M., McElroy, C.A., Buhimschi, I.A., Imitola, J., Maitre, N.L., Bedrosian, T.A., Hester, M.E., 2020. Electrophysiological Maturation of Cerebral Organoids Correlates with Dynamic Morphological and Cellular Development. Stem Cell Rep. 15, 855–868. https://doi.org/10.1016/j.stemcr.2020.08.017

Febbraro, F., Chen, M., Denham, M., 2021. Generation of Human iPSCs by Episomal Reprogramming of Skin Fibroblasts and Peripheral Blood Mononuclear Cells. Methods Mol. Biol. Clifton NJ 2239, 135–151. https://doi.org/10.1007/978-1-0716-1084-8_9

Fernandes, D., Carvalho, A.L., 2016. Mechanisms of homeostatic plasticity in the excitatory synapse. J. Neurochem. 139, 973–996. https://doi.org/10.1111/jnc.13687

Fernandes, D., Santos, S.D., Coutinho, E., Whitt, J.L., Beltrão, N., Rondão, T., Leite, M.I., Buckley, C., Lee, H.-K., Carvalho, A.L., 2019. Disrupted AMPA Receptor Function upon Genetic- or Antibody-Mediated Loss of Autism-Associated CASPR2. Cereb. Cortex N. Y. N 1991 29, 4919–4931. https://doi.org/10.1093/cercor/bhz032

Fernández, M., Sánchez-León, C.A., Llorente, J., Sierra-Arregui, T., Knafo, S., Márquez-Ruiz, J., Peñagarikano, O., 2021. Altered Cerebellar Response to Somatosensory Stimuli in the Cntnap2 Mouse Model of Autism. eNeuro 8, ENEURO.0333-21.2021. https://doi.org/10.1523/ENEURO.0333-21.2021

Ferrari, R., Hernandez, D.G., Nalls, M.A., Rohrer, J.D., Ramasamy, A., Kwok, J.B.J., Dobson-Stone, C., Brooks, W.S., Schofield, P.R., Halliday, G.M., Hodges, J.R., Piguet, O., Bartley, L., Thompson, E., Haan, E., Hernández, I., Ruiz, A., Boada, M., Borroni, B., Padovani, A., Cruchaga, C., Cairns, N.J., Benussi, L., Binetti, G., Ghidoni, R., Forloni, G., Galimberti, D., Fenoglio, C., Serpente, M., Scarpini, E., Clarimón, J., Lleó, A., Blesa, R., Waldö, M.L., Nilsson, K., Nilsson, C., Mackenzie, I.R.A., Hsiung, G.-Y.R., Mann, D.M.A., Grafman, J., Morris, C.M., Attems, J., Griffiths, T.D., McKeith, I.G., Thomas, A.J., Pietrini, P., Huey, E.D., Wassermann, E.M., Baborie, A., Jaros, E., Tierney, M.C., Pastor, P., Razquin, C., Ortega-Cubero, S., Alonso, E., Perneczky, R., Diehl-Schmid, J., Alexopoulos, P., Kurz, A., Rainero, I., Rubino, E., Pinessi, L., Rogaeva, E., St George-Hyslop, P., Rossi, G., Tagliavini, F., Giaccone, G., Rowe, J.B., Schlachetzki, J.C.M., Uphill, J., Collinge, J., Mead, S., Danek, A., Van Deerlin, V.M., Grossman, M., Trojanowski, J.Q., van der Zee, J., Deschamps, W., Van Langenhove, T., Cruts, M., Van Broeckhoven, C., Cappa, S.F., Le Ber, I., Hannequin, D., Golfier, V., Vercelletto, M., Brice, A., Nacmias, B., Sorbi, S., Bagnoli, S., Piaceri, I., Nielsen, J.E., Hjermind, L.E., Riemenschneider, M., Mayhaus, M., Ibach, B., Gasparoni, G., Pichler, S., Gu, W., Rossor, M.N., Fox, N.C., Warren, J.D., Spillantini, M.G., Morris, H.R., Rizzu, P., Heutink, P., Snowden, J.S., Rollinson, S., Richardson, A., Gerhard, A., Bruni, A.C., Maletta, R., Frangipane, F., Cupidi, C., Bernardi, L., Anfossi, M., Gallo, M., Conidi, M.E., Smirne, N., Rademakers, R., Baker, M., Dickson, D.W., Graff-Radford, N.R., Petersen, R.C., Knopman, D., Josephs, K.A., Boeve, B.F., Parisi, J.E., Seeley, W.W., Miller, B.L., Karydas, A.M., Rosen, H., van Swieten, J.C., Dopper, E.G.P., Seelaar, H., Pijnenburg, Y.A.L., Scheltens, P., Logroscino, G., Capozzo, R., Novelli, V., Puca, A.A., Franceschi, M., Postiglione, A., Milan, G., Sorrentino, P., Kristiansen, M., Chiang, H.-H., Graff, C., Pasquier, F., Rollin, A., Deramecourt, V., Lebert, F., Kapogiannis, D., Ferrucci, L., Pickering-Brown, S., Singleton, A.B., Hardy, J., Momeni, P., 2014. Frontotemporal dementia and its

subtypes: a genome-wide association study. Lancet Neurol. 13, 686–699. https://doi.org/10.1016/S1474-4422(14)70065-1

Flaherty, E., Deranieh, R.M., Artimovich, E., Lee, I.S., Siegel, A.J., Levy, D.L., Nestor, M.W., Brennand, K.J., 2017. Patient-derived hiPSC neurons with heterozygous CNTNAP2 deletions display altered neuronal gene expression and network activity. NPJ Schizophr. 3, 35. https://doi.org/10.1038/s41537-017-0033-5

Fligor, C.M., Lavekar, S.S., Harkin, J., Shields, P.K., VanderWall, K.B., Huang, K.-C., Gomes, C., Meyer, J.S., 2021. Extension of retinofugal projections in an assembled model of human pluripotent stem cell-derived organoids. Stem Cell Rep. 16, 2228–2241. https://doi.org/10.1016/j.stemcr.2021.05.009

Friedman, J.I., Vrijenhoek, T., Markx, S., Janssen, I.M., van der Vliet, W.A., Faas, B.H.W., Knoers, N.V., Cahn, W., Kahn, R.S., Edelmann, L., Davis, K.L., Silverman, J.M., Brunner, H.G., van Kessel, A.G., Wijmenga, C., Ophoff, R.A., Veltman, J.A., 2008. CNTNAP2 gene dosage variation is associated with schizophrenia and epilepsy. Mol. Psychiatry 13, 261–266. https://doi.org/10.1038/sj.mp.4002049

Gabriel, E., Albanna, W., Pasquini, G., Ramani, A., Josipovic, N., Mariappan, A., Schinzel, F., Karch, C.M., Bao, G., Gottardo, M., Suren, A.A., Hescheler, J., Nagel-Wolfrum, K., Persico, V., Rizzoli, S.O., Altmüller, J., Riparbelli, M.G., Callaini, G., Goureau, O., Papantonis, A., Busskamp, V., Schneider, T., Gopalakrishnan, J., 2021. Human brain organoids assemble functionally integrated bilateral optic vesicles. Cell Stem Cell S1934-5909(21)00295–2. https://doi.org/10.1016/j.stem.2021.07.010

Gabryelewicz, T., Masellis, M., Berdynski, M., Bilbao, J.M., Rogaeva, E., St George-Hyslop, P., Barczak, A., Czyzewski, K., Barcikowska, M., Wszolek, Z., Black, S.E., Zekanowski, C., 2010. Intra-familial clinical heterogeneity due to FTLD-U with TDP-43 proteinopathy caused by a novel deletion in progranulin gene (PGRN). J. Alzheimers Dis. JAD 22, 1123–1133. https://doi.org/10.3233/JAD-2010-101413

Gao, R., Piguel, N.H., Melendez-Zaidi, A.E., Martin-de-Saavedra, M.D., Yoon, S., Forrest, M.P., Myczek, K., Zhang, G., Russell, T.A., Csernansky, J.G., Surmeier, D.J., Penzes, P., 2018. CNTNAP2 stabilizes interneuron dendritic arbors through CASK. Mol. Psychiatry 23, 1832–1850. https://doi.org/10.1038/s41380-018-0027-3

Gascon, E., Lynch, K., Ruan, H., Almeida, S., Verheyden, J.M., Seeley, W.W., Dickson, D.W., Petrucelli, L., Sun, D., Jiao, J., Zhou, H., Jakovcevski, M., Akbarian, S., Yao, W.-D., Gao, F.-B., 2014. Alterations in microRNA-124 and AMPA receptors contribute to social behavioral deficits in frontotemporal dementia. Nat. Med. 20, 1444–1451. https://doi.org/10.1038/nm.3717

Gdalyahu, A., Lazaro, M., Penagarikano, O., Golshani, P., Trachtenberg, J.T., Geschwind, D.H., Gescwind, D.H., 2015. The Autism Related Protein Contactin-Associated Protein-Like 2 (CNTNAP2) Stabilizes New Spines: An In Vivo Mouse Study. PloS One 10, e0125633. https://doi.org/10.1371/journal.pone.0125633

Giandomenico, S.L., Mierau, S.B., Gibbons, G.M., Wenger, L.M.D., Masullo, L., Sit, T., Sutcliffe, M., Boulanger, J., Tripodi, M., Derivery, E., Paulsen, O., Lakatos, A., Lancaster, M.A., 2019. Cerebral organoids at the air-liquid interface generate

diverse nerve tracts with functional output. Nat. Neurosci. 22, 669–679. https://doi.org/10.1038/s41593-019-0350-2

Giannoccaro, M.P., Menassa, D.A., Jacobson, L., Coutinho, E., Prota, G., Lang, B., Leite, M.I., Cerundolo, V., Liguori, R., Vincent, A., 2019. Behaviour and neuropathology in mice injected with human contactin-associated protein 2 antibodies. Brain J. Neurol. 142, 2000–2012. https://doi.org/10.1093/brain/awz119

Goines, P.E., Croen, L.A., Braunschweig, D., Yoshida, C.K., Grether, J., Hansen, R., Kharrazi, M., Ashwood, P., Van de Water, J., 2011. Increased midgestational IFN-γ, IL-4 and IL-5 in women bearing a child with autism: A case-control study. Mol. Autism 2, 13. https://doi.org/10.1186/2040-2392-2-13

Gordon, A., Salomon, D., Barak, N., Pen, Y., Tsoory, M., Kimchi, T., Peles, E., 2016. Expression of Cntnap2 (Caspr2) in multiple levels of sensory systems. Mol. Cell. Neurosci. 70, 42–53. https://doi.org/10.1016/j.mcn.2015.11.012

Gordon, A., Yoon, S.-J., Tran, S.S., Makinson, C.D., Park, J.Y., Andersen, J., Valencia, A.M., Horvath, S., Xiao, X., Huguenard, J.R., Pașca, S.P., Geschwind, D.H., 2021. Long-term maturation of human cortical organoids matches key early postnatal transitions. Nat. Neurosci. 24, 331–342. https://doi.org/10.1038/s41593-021-00802-y

Greaves, C.V., Rohrer, J.D., 2019. An update on genetic frontotemporal dementia. J. Neurol. 266, 2075–2086. https://doi.org/10.1007/s00415-019-09363-4

Guedes, J.R., Ferreira, P.A., Costa, J.M., Cardoso, A.L., Peça, J., 2022. Microglia-dependent remodeling of neuronal circuits. J. Neurochem. 163, 74–93. https://doi.org/10.1111/jnc.15689

Guerreiro, R.J., Santana, I., Bras, J.M., Revesz, T., Rebelo, O., Ribeiro, M.H., Santiago, B., Oliveira, C.R., Singleton, A., Hardy, J., 2008. Novel progranulin mutation: screening for PGRN mutations in a Portuguese series of FTD/CBS cases. Mov. Disord. Off. J. Mov. Disord. Soc. 23, 1269–1273. https://doi.org/10.1002/mds.22078

Haenseler, W., Sansom, S.N., Buchrieser, J., Newey, S.E., Moore, C.S., Nicholls, F.J., Chintawar, S., Schnell, C., Antel, J.P., Allen, N.D., Cader, M.Z., Wade-Martins, R., James, W.S., Cowley, S.A., 2017. A Highly Efficient Human Pluripotent Stem Cell Microglia Model Displays a Neuronal-Co-culture-Specific Expression Profile and Inflammatory Response. Stem Cell Rep. 8, 1727–1742. https://doi.org/10.1016/j.stemcr.2017.05.017

Hali, S., Kim, J., Kwak, T.H., Lee, H., Shin, C.Y., Han, D.W., 2020. Modelling monogenic autism spectrum disorder using mouse cortical organoids. Biochem. Biophys. Res. Commun. 521, 164–171. https://doi.org/10.1016/j.bbrc.2019.10.097

Hernández, D., Rooney, L.A., Daniszewski, M., Gulluyan, L., Liang, H.H., Cook, A.L., Hewitt, A.W., Pébay, A., 2021. Culture Variabilities of Human iPSC-Derived Cerebral Organoids Are a Major Issue for the Modelling of Phenotypes Observed in Alzheimer's Disease. Stem Cell Rev. Rep. https://doi.org/10.1007/s12015-021-10147-5

Holler, C.J., Taylor, G., McEachin, Z.T., Deng, Q., Watkins, W.J., Hudson, K., Easley, C.A., Hu, W.T., Hales, C.M., Rossoll, W., Bassell, G.J., Kukar, T., 2016. Trehalose

upregulates progranulin expression in human and mouse models of GRN haploinsufficiency: a novel therapeutic lead to treat frontotemporal dementia. Mol. Neurodegener. 11, 46. https://doi.org/10.1186/s13024-016-0114-3

Horresh, I., Poliak, S., Grant, S., Bredt, D., Rasband, M.N., Peles, E., 2008. Multiple molecular interactions determine the clustering of Caspr2 and Kv1 channels in myelinated axons. J. Neurosci. Off. J. Soc. Neurosci. 28, 14213–14222. https://doi.org/10.1523/JNEUROSCI.3398-08.2008

Howden, S.E., Maufort, J.P., Duffin, B.M., Elefanty, A.G., Stanley, E.G., Thomson, J.A., 2015. Simultaneous Reprogramming and Gene Correction of Patient Fibroblasts. Stem Cell Rep. 5, 1109–1118. https://doi.org/10.1016/j.stemcr.2015.10.009

Hussein, S.M., Batada, N.N., Vuoristo, S., Ching, R.W., Autio, R., Närvä, E., Ng, S., Sourour, M., Hämäläinen, R., Olsson, C., Lundin, K., Mikkola, M., Trokovic, R., Peitz, M., Brüstle, O., Bazett-Jones, D.P., Alitalo, K., Lahesmaa, R., Nagy, A., Otonkoski, T., 2011. Copy number variation and selection during reprogramming to pluripotency. Nature 471, 58–62. https://doi.org/10.1038/nature09871

Inda, M.C., DeFelipe, J., Muñoz, A., 2006. Voltage-gated ion channels in the axon initial segment of human cortical pyramidal cells and their relationship with chandelier cells. Proc. Natl. Acad. Sci. U. S. A. 103, 2920–2925. https://doi.org/10.1073/pnas.0511197103

Irani, S.R., Alexander, S., Waters, P., Kleopa, K.A., Pettingill, P., Zuliani, L., Peles, E., Buckley, C., Lang, B., Vincent, A., 2010. Antibodies to Kv1 potassium channel-complex proteins leucine-rich, glioma inactivated 1 protein and contactin-associated protein-2 in limbic encephalitis, Morvan's syndrome and acquired neuromyotonia. Brain J. Neurol. 133, 2734–2748. https://doi.org/10.1093/brain/awq213

Jenkins, S.M., Bennett, V., 2001. Ankyrin-G coordinates assembly of the spectrin-based membrane skeleton, voltage-gated sodium channels, and L1 CAMs at Purkinje neuron initial segments. J. Cell Biol. 155, 739–746. https://doi.org/10.1083/jcb.200109026

Jo, J., Xiao, Y., Sun, A.X., Cukuroglu, E., Tran, H.-D., Göke, J., Tan, Z.Y., Saw, T.Y., Tan, C.-P., Lokman, H., Lee, Y., Kim, D., Ko, H.S., Kim, S.-O., Park, J.H., Cho, N.-J., Hyde, T.M., Kleinman, J.E., Shin, J.H., Weinberger, D.R., Tan, E.K., Je, H.S., Ng, H.-H., 2016. Midbrain-like Organoids from Human Pluripotent Stem Cells Contain Functional Dopaminergic and Neuromelanin-Producing Neurons. Cell Stem Cell 19, 248–257. https://doi.org/10.1016/j.stem.2016.07.005

Joubert, B., Saint-Martin, M., Noraz, N., Picard, G., Rogemond, V., Ducray, F., Desestret, V., Psimaras, D., Delattre, J.-Y., Antoine, J.-C., Honnorat, J., 2016. Characterization of a Subtype of Autoimmune Encephalitis With Anti-Contactin-Associated Protein-like 2 Antibodies in the Cerebrospinal Fluid, Prominent Limbic Symptoms, and Seizures. JAMA Neurol. 73, 1115–1124. https://doi.org/10.1001/jamaneurol.2016.1585

Jurgensen, S., Castillo, P.E., 2015. Selective Dysregulation of Hippocampal Inhibition in the Mouse Lacking Autism Candidate Gene CNTNAP2. J. Neurosci. Off. J. Soc. Neurosci. 35, 14681–14687. https://doi.org/10.1523/JNEUROSCI.1666-15.2015

K, T., S, Y., 2016. A decade of transcription factor-mediated reprogramming to pluripotency. Nat. Rev. Mol. Cell Biol. 17. https://doi.org/10.1038/nrm.2016.8

Kadoshima, T., Sakaguchi, H., Nakano, T., Soen, M., Ando, S., Eiraku, M., Sasai, Y., 2013. Self-organization of axial polarity, inside-out layer pattern, and species-specific progenitor dynamics in human ES cell-derived neocortex. Proc. Natl. Acad. Sci. U. S. A. 110, 20284–20289. https://doi.org/10.1073/pnas.1315710110

Kanton, S., Boyle, M.J., He, Z., Santel, M., Weigert, A., Sanchís-Calleja, F., Guijarro, P., Sidow, L., Fleck, J.S., Han, D., Qian, Z., Heide, M., Huttner, W.B., Khaitovich, P., Pääbo, S., Treutlein, B., Camp, J.G., 2019. Organoid single-cell genomic atlas uncovers human-specific features of brain development. Nature 574, 418–422. https://doi.org/10.1038/s41586-019-1654-9

Kim, J.-W., Park, K., Kang, R.J., Gonzales, E.L.T., Kim, D.G., Oh, H.A., Seung, H., Ko, M.J., Kwon, K.J., Kim, K.C., Lee, S.H., Chung, C., Shin, C.Y., 2019. Pharmacological modulation of AMPA receptor rescues social impairments in animal models of autism. Neuropsychopharmacol. Off. Publ. Am. Coll. Neuropsychopharmacol. 44, 314–323. https://doi.org/10.1038/s41386-018-0098-5

Kleopa, K.A., Elman, L.B., Lang, B., Vincent, A., Scherer, S.S., 2006. Neuromyotonia and limbic encephalitis sera target mature Shaker-type K+ channels: subunit specificity correlates with clinical manifestations. Brain J. Neurol. 129, 1570–1584. https://doi.org/10.1093/brain/awl084

Körtvelyessy, P., Bauer, J., Stoppel, C.M., Brück, W., Gerth, I., Vielhaber, S., Wiedemann, F.R., Heinze, H.J., Bartels, C., Bien, C.G., 2015. Complement-associated neuronal loss in a patient with CASPR2 antibody-associated encephalitis. Neurol. Neuroimmunol. Neuroinflammation 2, e75. https://doi.org/10.1212/NXI.0000000000000075

Lai, H.C., Jan, L.Y., 2006. The distribution and targeting of neuronal voltage-gated ion channels. Nat. Rev. Neurosci. 7, 548–562. https://doi.org/10.1038/nrn1938

Lai, M., Hughes, E.G., Peng, X., Zhou, L., Gleichman, A.J., Shu, H., Matà, S., Kremens, D., Vitaliani, R., Geschwind, M.D., Bataller, L., Kalb, R.G., Davis, R., Graus, F., Lynch, D.R., Balice-Gordon, R., Dalmau, J., 2009. AMPA receptor antibodies in limbic encephalitis alter synaptic receptor location. Ann. Neurol. 65, 424–434. https://doi.org/10.1002/ana.21589

Lai, M., Huijbers, M.G.M., Lancaster, E., Graus, F., Bataller, L., Balice-Gordon, R., Cowell, J.K., Dalmau, J., 2010. Investigation of LGI1 as the antigen in limbic encephalitis previously attributed to potassium channels: a case series. Lancet Neurol. 9, 776–785. https://doi.org/10.1016/S1474-4422(10)70137-X

Lancaster, E., Huijbers, M.G.M., Bar, V., Boronat, A., Wong, A., Martinez-Hernandez, E., Wilson, C., Jacobs, D., Lai, M., Walker, R.W., Graus, F., Bataller, L., Illa, I., Markx, S., Strauss, K.A., Peles, E., Scherer, S.S., Dalmau, J., 2011. Investigations of caspr2, an autoantigen of encephalitis and neuromyotonia. Ann. Neurol. 69, 303–311. https://doi.org/10.1002/ana.22297

Lancaster, E., Lai, M., Peng, X., Hughes, E., Constantinescu, R., Raizer, J., Friedman, D., Skeen, M.B., Grisold, W., Kimura, A., Ohta, K., Iizuka, T., Guzman, M., Graus, F., Moss, S.J., Balice-Gordon, R., Dalmau, J., 2010. Antibodies to the GABA(B) receptor in limbic encephalitis with seizures: case series and characterisation of

the antigen. Lancet Neurol. 9, 67–76. https://doi.org/10.1016/S1474-4422(09)70324-2

Lancaster, M.A., Corsini, N.S., Wolfinger, S., Gustafson, E.H., Phillips, A.W., Burkard, T.R., Otani, T., Livesey, F.J., Knoblich, J.A., 2017. Guided self-organization and cortical plate formation in human brain organoids. Nat. Biotechnol. 35, 659–666. https://doi.org/10.1038/nbt.3906

Lancaster, M.A., Knoblich, J.A., 2014. Generation of cerebral organoids from human pluripotent stem cells. Nat. Protoc. 9, 2329–2340. https://doi.org/10.1038/nprot.2014.158

Lancaster, M.A., Renner, M., Martin, C.-A., Wenzel, D., Bicknell, L.S., Hurles, M.E., Homfray, T., Penninger, J.M., Jackson, A.P., Knoblich, J.A., 2013. Cerebral organoids model human brain development and microcephaly. Nature 501, 373–379. https://doi.org/10.1038/nature12517

Lauber, E., Filice, F., Schwaller, B., 2018. Dysregulation of Parvalbumin Expression in the Cntnap2-/- Mouse Model of Autism Spectrum Disorder. Front. Mol. Neurosci. 11, 262. https://doi.org/10.3389/fnmol.2018.00262

Lazaro, M.T., Taxidis, J., Shuman, T., Bachmutsky, I., Ikrar, T., Santos, R., Marcello, G.M., Mylavarapu, A., Chandra, S., Foreman, A., Goli, R., Tran, D., Sharma, N., Azhdam, M., Dong, H., Choe, K.Y., Peñagarikano, O., Masmanidis, S.C., Rácz, B., Xu, X., Geschwind, D.H., Golshani, P., 2019. Reduced Prefrontal Synaptic Connectivity and Disturbed Oscillatory Population Dynamics in the CNTNAP2 Model of Autism. Cell Rep. 27, 2567-2578.e6. https://doi.org/10.1016/j.celrep.2019.05.006

Lee, C.W., Stankowski, J.N., Chew, J., Cook, C.N., Lam, Y.-W., Almeida, S., Carlomagno, Y., Lau, K.-F., Prudencio, M., Gao, F.-B., Bogyo, M., Dickson, D.W., Petrucelli, L., 2017. The lysosomal protein cathepsin L is a progranulin protease. Mol. Neurodegener. 12, 55. https://doi.org/10.1186/s13024-017-0196-6

Lee, I.S., Carvalho, C.M.B., Douvaras, P., Ho, S.-M., Hartley, B.J., Zuccherato, L.W., Ladran, I.G., Siegel, A.J., McCarthy, S., Malhotra, D., Sebat, J., Rapoport, J., Fossati, V., Lupski, J.R., Levy, D.L., Brennand, K.J., 2015. Characterization of molecular and cellular phenotypes associated with a heterozygous CNTNAP2 deletion using patient-derived hiPSC neural cells. NPJ Schizophr. 1, 15019. https://doi.org/10.1038/npjschz.2015.19

Li, R., Sun, L., Fang, A., Li, P., Wu, Q., Wang, X., 2017. Recapitulating cortical development with organoid culture in vitro and modeling abnormal spindle-like (ASPM related primary) microcephaly disease. Protein Cell 8, 823–833. https://doi.org/10.1007/s13238-017-0479-2

Li, Y., Muffat, J., Omer, A., Bosch, I., Lancaster, M.A., Sur, M., Gehrke, L., Knoblich, J.A., Jaenisch, R., 2017. Induction of Expansion and Folding in Human Cerebral Organoids. Cell Stem Cell 20, 385-396.e3. https://doi.org/10.1016/j.stem.2016.11.017

Lima Caldeira, G., Peça, J., Carvalho, A.L., 2019. New insights on synaptic dysfunction in neuropsychiatric disorders. Curr. Opin. Neurobiol. 57, 62–70. https://doi.org/10.1016/j.conb.2019.01.004

Liska, A., Bertero, A., Gomolka, R., Sabbioni, M., Galbusera, A., Barsotti, N., Panzeri, S., Scattoni, M.L., Pasqualetti, M., Gozzi, A., 2018. Homozygous Loss of Autism-Risk Gene CNTNAP2 Results in Reduced Local and Long-Range Prefrontal Functional Connectivity. Cereb. Cortex N. Y. N 1991 28, 1141–1153. https://doi.org/10.1093/cercor/bhx022

Liu, P., Bai, M., Ma, C., Yan, Y., Zhang, G., Wu, S., Li, Z., Zhao, D., Ren, K., Li, H., Guo, J., 2021. Case Report: Prominent Brainstem Involvement in Two Patients With Anti-CASPR2 Antibody-Associated Autoimmune Encephalitis. Front. Immunol. 12, 772763. https://doi.org/10.3389/fimmu.2021.772763

Lu, P., Wang, F., Zhou, S., Huang, X., Sun, H., Zhang, Y.-W., Yao, Y., Zheng, H., 2021. A Novel CNTNAP2 Mutation Results in Abnormal Neuronal E/I Balance. Front. Neurol. 12, 712773. https://doi.org/10.3389/fneur.2021.712773

Lu, Z., Reddy, M.V.V.V.S., Liu, Jianfang, Kalichava, A., Liu, Jiankang, Zhang, L., Chen, F., Wang, Y., Holthauzen, L.M.F., White, M.A., Seshadrinathan, S., Zhong, X., Ren, G., Rudenko, G., 2016. Molecular Architecture of Contactin-associated Protein-like 2 (CNTNAP2) and Its Interaction with Contactin 2 (CNTN2). J. Biol. Chem. 291, 24133–24147. https://doi.org/10.1074/jbc.M116.748236

Luo, C., Lancaster, M.A., Castanon, R., Nery, J.R., Knoblich, J.A., Ecker, J.R., 2016. Cerebral Organoids Recapitulate Epigenomic Signatures of the Human Fetal Brain. Cell Rep. 17, 3369–3384. https://doi.org/10.1016/j.celrep.2016.12.001

Mansour, A.A., Gonçalves, J.T., Bloyd, C.W., Li, H., Fernandes, S., Quang, D., Johnston, S., Parylak, S.L., Jin, X., Gage, F.H., 2018. An in vivo model of functional and vascularized human brain organoids. Nat. Biotechnol. 36, 432–441. https://doi.org/10.1038/nbt.4127

Manyukhina, V.O., Prokofyev, A.O., Galuta, I.A., Goiaeva, D.E., Obukhova, T.S., Schneiderman, J.F., Altukhov, D.I., Stroganova, T.A., Orekhova, E.V., 2022. Globally elevated excitation-inhibition ratio in children with autism spectrum disorder and below-average intelligence. Mol. Autism 13, 20. https://doi.org/10.1186/s13229-022-00498-2

Mariani, J., Simonini, M.V., Palejev, D., Tomasini, L., Coppola, G., Szekely, A.M., Horvath, T.L., Vaccarino, F.M., 2012. Modeling human cortical development in vitro using induced pluripotent stem cells. Proc. Natl. Acad. Sci. U. S. A. 109, 12770–12775. https://doi.org/10.1073/pnas.1202944109

Mazina, V., Gerdts, J., Trinh, S., Ankenman, K., Ward, T., Dennis, M.Y., Girirajan, S., Eichler, E.E., Bernier, R., 2015. Epigenetics of autism-related impairment: copy number variation and maternal infection. J. Dev. Behav. Pediatr. JDBP 36, 61–67. https://doi.org/10.1097/DBP.0000000000000126

Mikhail, F.M., Lose, E.J., Robin, N.H., Descartes, M.D., Rutledge, K.D., Rutledge, S.L., Korf, B.R., Carroll, A.J., 2011. Clinically relevant single gene or intragenic deletions encompassing critical neurodevelopmental genes in patients with developmental delay, mental retardation, and/or autism spectrum disorders. Am. J. Med. Genet. A. 155A, 2386–2396. https://doi.org/10.1002/ajmg.a.34177

Miller, Z.A., Rankin, K.P., Graff-Radford, N.R., Takada, L.T., Sturm, V.E., Cleveland, C.M., Criswell, L.A., Jaeger, P.A., Stan, T., Heggeli, K.A., Hsu, S.C., Karydas, A., Khan, B.K., Grinberg, L.T., Gorno-Tempini, M.L., Boxer, A.L., Rosen, H.J., Kramer, J.H.,

Coppola, G., Geschwind, D.H., Rademakers, R., Seeley, W.W., Wyss-Coray, T., Miller, B.L., 2013. TDP-43 frontotemporal lobar degeneration and autoimmune disease. J. Neurol. Neurosurg. Psychiatry 84, 956–962. https://doi.org/10.1136/jnnp-2012-304644

Miura, Y., Li, M.-Y., Birey, F., Ikeda, K., Revah, O., Thete, M.V., Park, J.-Y., Puno, A., Lee, S.H., Porteus, M.H., Pașca, S.P., 2020. Generation of human striatal organoids and cortico-striatal assembloids from human pluripotent stem cells. Nat. Biotechnol. 38, 1421–1430. https://doi.org/10.1038/s41587-020-00763-w

Monzel, A.S., Smits, L.M., Hemmer, K., Hachi, S., Moreno, E.L., van Wuellen, T., Jarazo, J., Walter, J., Brüggemann, I., Boussaad, I., Berger, E., Fleming, R.M.T., Bolognin, S., Schwamborn, J.C., 2017. Derivation of Human Midbrain-Specific Organoids from Neuroepithelial Stem Cells. Stem Cell Rep. 8, 1144–1154. https://doi.org/10.1016/j.stemcr.2017.03.010

Moore, K.M., Nicholas, J., Grossman, M., McMillan, C.T., Irwin, D.J., Massimo, L., Deerlin, V.M.V., Warren, J.D., Fox, N.C., Rossor, M.N., Mead, S., Bocchetta, M., Boeve, B.F., Knopman, D.S., Graff-Radford, N.R., Forsberg, L.K., Rademakers, R., Wszolek, Z.K., Swieten, J.C. van, Jiskoot, L.C., Meeter, L.H., Dopper, E.G., Papma, J.M., Snowden, J.S., Saxon, J., Jones, M., Pickering-Brown, S., Ber, I.L., Camuzat, A., Brice, A., Caroppo, P., Ghidoni, R., Pievani, M., Benussi, L., Binetti, G., Dickerson, B.C., Lucente, D., Krivensky, S., Graff, C., Öijerstedt, L., Fallström, M., Thonberg, H., Ghoshal, N., Morris, J.C., Borroni, B., Benussi, A., Padovani, A., Galimberti, D., Scarpini, E., Fumagalli, G.G., Mackenzie, I.R., Hsiung, G.-Y.R., Sengdy, P., Boxer, A.L., Rosen, H., Taylor, J.B., Synofzik, M., Wilke, C., Sulzer, P., Hodges, J.R., Halliday, G., Kwok, J., Sanchez-Valle, R., Lladó, A., Borrego-Ecija, S., Santana, I., Almeida, M.R., Tábuas-Pereira, M., Moreno, F., Barandiaran, M., Indakoetxea, B., Levin, J., Danek, A., Rowe, J.B., Cope, T.E., Otto, M., Anderl-Straub, S., Mendonça, A. de, Maruta, C., Masellis, M., Black, S.E., Couratier, P., Lautrette, G., Huey, E.D., Sorbi, S., Nacmias, B., Laforce, R., Tremblay, M.-P.L., Vandenberghe, R., Damme, P.V., Rogalski, E.J., Weintraub, S., Gerhard, A., Onyike, C.U., Ducharme, S., Papageorgiou, S.G., Ng, A.S.L., Brodtmann, A., Finger, E., Guerreiro, R., Bras, J., Rohrer, J.D., Heller, C., Convery, R.S., Woollacott, I.O., Shafei, R.M., Graff-Radford, J., Jones, D.T., Dheel, C.M., Savica, R., Lapid, M.I., Baker, M., Fields, J.A., Gavrilova, R., Domoto-Reilly, K., Poos, J.M., Ende, E.L.V. der, Panman, J.L., Kaat, L.D., Seelaar, H., Richardson, A., Frisoni, G., Mega, A., Fostinelli, S., Chiang, H.-H., Alberici, A., Arighi, A., Fenoglio, C., Heuer, H., Miller, B., Karydas, A., Fong, J., Leitão, M.J., Santiago, B., Duro, D., Ferreira, Carlos, Gabilondo, A., Arriba, M.D., Tainta, M., Zulaica, M., Ferreira, Catarina, Semler, E., Ludolph, A., Landwehrmeyer, B., Volk, A.E., Miltenberger, G., Verdelho, A., Afonso, S., Tartaglia, M.C., Freedman, M., Rogaeva, E., Ferrari, C., Piaceri, I., Bessi, V., Lombardi, G., St-Onge, F., Doré, M.-C., Bruffaerts, R., Vandenbulcke, M., Stock, J.V. den, Mesulam, M.M., Bigio, E., Koros, C., Papatriantafyllou, J., Kroupis, C., Stefanis, L., Shoesmith, C., Robertson, E., Coppola, G., Ramos, E.M.D.S., Geschwind, D., 2020. Age at symptom onset and death and disease duration in genetic frontotemporal dementia: an international retrospective cohort study. Lancet Neurol. 19, 145–156. https://doi.org/10.1016/S1474-4422(19)30394-1

Muguruma, K., Nishiyama, A., Kawakami, H., Hashimoto, K., Sasai, Y., 2015. Self-organization of polarized cerebellar tissue in 3D culture of human pluripotent stem cells. Cell Rep. 10, 537–550. https://doi.org/10.1016/j.celrep.2014.12.051

Närvä, E., Autio, R., Rahkonen, N., Kong, L., Harrison, N., Kitsberg, D., Borghese, L., Itskovitz-Eldor, J., Rasool, O., Dvorak, P., Hovatta, O., Otonkoski, T., Tuuri, T., Cui, W., Brüstle, O., Baker, D., Maltby, E., Moore, H.D., Benvenisty, N., Andrews, P.W., Yli-Harja, O., Lahesmaa, R., 2010. High-resolution DNA analysis of human embryonic stem cell lines reveals culture-induced copy number changes and loss of heterozygosity. Nat. Biotechnol. 28, 371–377. https://doi.org/10.1038/nbt.1615

Nascimento, J.M., Saia-Cereda, V.M., Sartore, R.C., da Costa, R.M., Schitine, C.S., Freitas, H.R., Murgu, M., de Melo Reis, R.A., Rehen, S.K., Martins-de-Souza, D., 2019. Human Cerebral Organoids and Fetal Brain Tissue Share Proteomic Similarities. Front. Cell Dev. Biol. 7, 303. https://doi.org/10.3389/fcell.2019.00303

Neill, T., Buraschi, S., Goyal, A., Sharpe, C., Natkanski, E., Schaefer, L., Morrione, A., Iozzo, R.V., 2016. EphA2 is a functional receptor for the growth factor progranulin. J. Cell Biol. 215, 687–703. https://doi.org/10.1083/jcb.201603079

O'Dushlaine, C., Kenny, E., Heron, E., Donohoe, G., Gill, M., Morris, D., International Schizophrenia Consortium, Corvin, A., 2011. Molecular pathways involved in neuronal cell adhesion and membrane scaffolding contribute to schizophrenia and bipolar disorder susceptibility. Mol. Psychiatry 16, 286–292. https://doi.org/10.1038/mp.2010.7

Ogawa, Y., Horresh, I., Trimmer, J.S., Bredt, D.S., Peles, E., Rasband, M.N., 2008. Postsynaptic density-93 clusters Kv1 channels at axon initial segments independently of Caspr2. J. Neurosci. Off. J. Soc. Neurosci. 28, 5731–5739. https://doi.org/10.1523/JNEUROSCI.4431-07.2008

Oiso, S., Takeda, Y., Futagawa, T., Miura, T., Kuchiiwa, S., Nishida, K., Ikeda, R., Kariyazono, H., Watanabe, K., Yamada, K., 2009. Contactin-associated protein (Caspr) 2 interacts with carboxypeptidase E in the CNS. J. Neurochem. 109, 158–167. https://doi.org/10.1111/j.1471-4159.2009.05928.x

Olsen, A.L., Lai, Y., Dalmau, J., Scherer, S.S., Lancaster, E., 2015. Caspr2 autoantibodies target multiple epitopes. Neurol. Neuroimmunol. Neuroinflammation 2, e127. https://doi.org/10.1212/NXI.0000000000000127

Ormel, P.R., Vieira de Sá, R., van Bodegraven, E.J., Karst, H., Harschnitz, O., Sneeboer, M.A.M., Johansen, L.E., van Dijk, R.E., Scheefhals, N., Berdenis van Berlekom, A., Ribes Martínez, E., Kling, S., MacGillavry, H.D., van den Berg, L.H., Kahn, R.S., Hol, E.M., de Witte, L.D., Pasterkamp, R.J., 2018. Microglia innately develop within cerebral organoids. Nat. Commun. 9, 4167. https://doi.org/10.1038/s41467-018-06684-2

Palani, D., Baginskas, A., Raastad, M., 2010. Bursts and hyperexcitability in non-myelinated axons of the rat hippocampus. Neuroscience 167, 1004–1013. https://doi.org/10.1016/j.neuroscience.2010.03.021

Park, I.-H., Arora, N., Huo, H., Maherali, N., Ahfeldt, T., Shimamura, A., Lensch, M.W., Cowan, C., Hochedlinger, K., Daley, G.Q., 2008. Disease-specific induced pluripotent stem cells. Cell 134, 877–886. https://doi.org/10.1016/j.cell.2008.07.041

Paşca, A.M., Sloan, S.A., Clarke, L.E., Tian, Y., Makinson, C.D., Huber, N., Kim, C.H., Park, J.-Y., O'Rourke, N.A., Nguyen, K.D., Smith, S.J., Huguenard, J.R., Geschwind, D.H.,

Barres, B.A., Paşca, S.P., 2015. Functional cortical neurons and astrocytes from human pluripotent stem cells in 3D culture. Nat. Methods 12, 671–678. https://doi.org/10.1038/nmeth.3415

Patterson, K.R., Dalmau, J., Lancaster, E., 2018. Mechanisms of Caspr2 antibodies in autoimmune encephalitis and neuromyotonia. Ann. Neurol. 83, 40–51. https://doi.org/10.1002/ana.25120

Peça, J., Feng, G., 2012. Cellular and synaptic network defects in autism. Curr. Opin. Neurobiol. 22, 866–872. https://doi.org/10.1016/j.conb.2012.02.015

Peñagarikano, O., Abrahams, B.S., Herman, E.I., Winden, K.C., Gdalyahu, A., Dong, H., Sonnenblick, L.I., Gruver, R., Almajano, J., Bragin, A., Golshani, P., Trachtenberg, J.T., Peles, E., Geschwind, D.H., 2011. Absence of CNTNAP2 leads to epilepsy, neuronal migration abnormalities and core autism-related deficits. Cell 147, 235–246. https://doi.org/10.1016/j.cell.2011.08.040

Petit-Pedrol, M., Armangue, T., Peng, X., Bataller, L., Cellucci, T., Davis, R., McCracken, L., Martinez-Hernandez, E., Mason, W.P., Kruer, M.C., Ritacco, D.G., Grisold, W., Meaney, B.F., Alcalá, C., Sillevis-Smitt, P., Titulaer, M.J., Balice-Gordon, R., Graus, F., Dalmau, J., 2014. Encephalitis with refractory seizures, status epilepticus, and antibodies to the GABAA receptor: a case series, characterisation of the antigen, and analysis of the effects of antibodies. Lancet Neurol. 13, 276–286. https://doi.org/10.1016/S1474-4422(13)70299-0

Petkau, T.L., Neal, S.J., Milnerwood, A., Mew, A., Hill, A.M., Orban, P., Gregg, J., Lu, G., Feldman, H.H., Mackenzie, I.R.A., Raymond, L.A., Leavitt, B.R., 2012. Synaptic dysfunction in progranulin-deficient mice. Neurobiol. Dis. 45, 711–722. https://doi.org/10.1016/j.nbd.2011.10.016

Pfaffl, M.W., 2001. A new mathematical model for relative quantification in real-time RT-PCR. Nucleic Acids Res. 29. https://doi.org/10.1093/nar/29.9.e45

Pham, M.T., Pollock, K.M., Rose, M.D., Cary, W.A., Stewart, H.R., Zhou, P., Nolta, J.A., Waldau, B., 2018. Generation of human vascularized brain organoids. Neuroreport 29, 588–593. https://doi.org/10.1097/WNR.0000000000001014

Pinatel, D., Hivert, B., Boucraut, J., Saint-Martin, M., Rogemond, V., Zoupi, L., Karagogeos, D., Honnorat, J., Faivre-Sarrailh, C., 2015. Inhibitory axons are targeted in hippocampal cell culture by anti-Caspr2 autoantibodies associated with limbic encephalitis. Front. Cell. Neurosci. 9, 265. https://doi.org/10.3389/fncel.2015.00265

Pinatel, D., Hivert, B., Saint-Martin, M., Noraz, N., Savvaki, M., Karagogeos, D., Faivre-Sarrailh, C., 2017. The Kv1-associated molecules TAG-1 and Caspr2 are selectively targeted to the axon initial segment in hippocampal neurons. J. Cell Sci. 130, 2209–2220. https://doi.org/10.1242/jcs.202267

Poliak, S., Gollan, L., Martinez, R., Custer, A., Einheber, S., Salzer, J.L., Trimmer, J.S., Shrager, P., Peles, E., 1999. Caspr2, a new member of the neurexin superfamily, is localized at the juxtaparanodes of myelinated axons and associates with K+ channels. Neuron 24, 1037–1047. https://doi.org/10.1016/s0896-6273(00)81049-1

Poliak, S., Salomon, D., Elhanany, H., Sabanay, H., Kiernan, B., Pevny, L., Stewart, C.L., Xu, X., Chiu, S.-Y., Shrager, P., Furley, A.J.W., Peles, E., 2003. Juxtaparanodal clustering of Shaker-like K+ channels in myelinated axons depends on Caspr2 and TAG-1. J. Cell Biol. 162, 1149–1160. https://doi.org/10.1083/jcb.200305018

Pollen, A.A., Bhaduri, A., Andrews, M.G., Nowakowski, T.J., Meyerson, O.S., Mostajo-Radji, M.A., Di Lullo, E., Alvarado, B., Bedolli, M., Dougherty, M.L., Fiddes, I.T., Kronenberg, Z.N., Shuga, J., Leyrat, A.A., West, J.A., Bershteyn, M., Lowe, C.B., Pavlovic, B.J., Salama, S.R., Haussler, D., Eichler, E.E., Kriegstein, A.R., 2019. Establishing Cerebral Organoids as Models of Human-Specific Brain Evolution. Cell 176, 743-756.e17. https://doi.org/10.1016/j.cell.2019.01.017

Popova, G., Soliman, S.S., Kim, C.N., Keefe, M.G., Hennick, K.M., Jain, S., Li, T., Tejera, D., Shin, D., Chhun, B.B., McGinnis, C.S., Speir, M., Gartner, Z.J., Mehta, S.B., Haeussler, M., Hengen, K.B., Ransohoff, R.R., Piao, X., Nowakowski, T.J., 2021. Human microglia states are conserved across experimental models and regulate neural stem cell responses in chimeric organoids. Cell Stem Cell 28, 2153-2166.e6. https://doi.org/10.1016/j.stem.2021.08.015

Qian, X., Nguyen, H.N., Song, M.M., Hadiono, C., Ogden, S.C., Hammack, C., Yao, B., Hamersky, G.R., Jacob, F., Zhong, C., Yoon, K.-J., Jeang, W., Lin, L., Li, Y., Thakor, J., Berg, D.A., Zhang, C., Kang, E., Chickering, M., Nauen, D., Ho, C.-Y., Wen, Z., Christian, K.M., Shi, P.-Y., Maher, B.J., Wu, H., Jin, P., Tang, H., Song, H., Ming, G.-L., 2016. Brain-Region-Specific Organoids Using Mini-bioreactors for Modeling ZIKV Exposure. Cell 165, 1238–1254. https://doi.org/10.1016/j.cell.2016.04.032

Quadrato, G., Nguyen, T., Macosko, E.Z., Sherwood, J.L., Yang, S.M., Berger, D., Maria, N., Scholvin, J., Goldman, M., Kinney, J., Boyden, E.S., Lichtman, J., Williams, Z.M., McCarroll, S.A., Arlotta, P., 2017. Cell diversity and network dynamics in photosensitive human brain organoids. Nature 545, 48–53. https://doi.org/10.1038/nature22047

Rasband, M.N., Park, E.W., Zhen, D., Arbuckle, M.I., Poliak, S., Peles, E., Grant, S.G.N., Trimmer, J.S., 2002. Clustering of neuronal potassium channels is independent of their interaction with PSD-95. J. Cell Biol. 159, 663–672. https://doi.org/10.1083/jcb.200206024

Rasband, M.N., Peles, E., 2015. The Nodes of Ranvier: Molecular Assembly and Maintenance. Cold Spring Harb. Perspect. Biol. 8, a020495. https://doi.org/10.1101/cshperspect.a020495

Renner, M., Lancaster, M.A., Bian, S., Choi, H., Ku, T., Peer, A., Chung, K., Knoblich, J.A., 2017. Self-organized developmental patterning and differentiation in cerebral organoids. EMBO J. 36, 1316–1329. https://doi.org/10.15252/embj.201694700

Reubinoff, B.E., Pera, M.F., Fong, C.Y., Trounson, A., Bongso, A., 2000. Embryonic stem cell lines from human blastocysts: somatic differentiation in vitro. Nat. Biotechnol. 18, 399–404. https://doi.org/10.1038/74447

Rhinn, H., Tatton, N., McCaughey, S., Kurnellas, M., Rosenthal, A., 2022. Progranulin as a therapeutic target in neurodegenerative diseases. Trends Pharmacol. Sci. S0165-6147(21)00232–7. https://doi.org/10.1016/j.tips.2021.11.015

Rodenas-Cuadrado, P., Ho, J., Vernes, S.C., 2014. Shining a light on CNTNAP2: complex functions to complex disorders. Eur. J. Hum. Genet. EJHG 22, 171–178. https://doi.org/10.1038/ejhg.2013.100

Rubenstein, J.L.R., Merzenich, M.M., 2003. Model of autism: increased ratio of excitation/inhibition in key neural systems. Genes Brain Behav. 2, 255–267. https://doi.org/10.1034/j.1601-183x.2003.00037.x

Sabate-Soler, S., Nickels, S.L., Saraiva, C., Berger, E., Dubonyte, U., Barmpa, K., Lan, Y.J., Kouno, T., Jarazo, J., Robertson, G., Sharif, J., Koseki, H., Thome, C., Shin, J.W., Cowley, S.A., Schwamborn, J.C., 2022. Microglia integration into human midbrain organoids leads to increased neuronal maturation and functionality. Glia. https://doi.org/10.1002/glia.24167

Sacai, H., Sakoori, K., Konno, K., Nagahama, K., Suzuki, H., Watanabe, T., Watanabe, M., Uesaka, N., Kano, M., 2020. Autism spectrum disorder-like behavior caused by reduced excitatory synaptic transmission in pyramidal neurons of mouse prefrontal cortex. Nat. Commun. 11, 5140. https://doi.org/10.1038/s41467-020-18861-3

Saint-Martin, M., Joubert, B., Pellier-Monnin, V., Pascual, O., Noraz, N., Honnorat, J., 2018. Contactin-associated protein-like 2, a protein of the neurexin family involved in several human diseases. Eur. J. Neurosci. 48, 1906–1923. https://doi.org/10.1111/ejn.14081

Saint-Martin, M., Pieters, A., Déchelotte, B., Malleval, C., Pinatel, D., Pascual, O., Karagogeos, D., Honnorat, J., Pellier-Monnin, V., Noraz, N., 2019. Impact of anti-CASPR2 autoantibodies from patients with autoimmune encephalitis on CASPR2/TAG-1 interaction and Kv1 expression. J. Autoimmun. 103, 102284. https://doi.org/10.1016/j.jaut.2019.05.012

Sakaguchi, H., Kadoshima, T., Soen, M., Narii, N., Ishida, Y., Ohgushi, M., Takahashi, J., Eiraku, M., Sasai, Y., 2015. Generation of functional hippocampal neurons from self-organizing human embryonic stem cell-derived dorsomedial telencephalic tissue. Nat. Commun. 6, 8896. https://doi.org/10.1038/ncomms9896

Sakaguchi, H., Ozaki, Y., Ashida, T., Matsubara, T., Oishi, N., Kihara, S., Takahashi, J., 2019. Self-Organized Synchronous Calcium Transients in a Cultured Human Neural Network Derived from Cerebral Organoids. Stem Cell Rep. 13, 458–473. https://doi.org/10.1016/j.stemcr.2019.05.029

Savvaki, M., Panagiotaropoulos, T., Stamatakis, A., Sargiannidou, I., Karatzioula, P., Watanabe, K., Stylianopoulou, F., Karagogeos, D., Kleopa, K.A., 2008. Impairment of learning and memory in TAG-1 deficient mice associated with shorter CNS internodes and disrupted juxtaparanodes. Mol. Cell. Neurosci. 39, 478–490. https://doi.org/10.1016/j.mcn.2008.07.025

Schou, M.B., Sæther, S.G., Drange, O.K., Brenner, E., Crespi, J., Eikenes, L., Mykland, M.S., Pintzka, C., Håberg, A.K., Sand, T., Vaaler, A., Kondziella, D., 2019. A prospective three-year follow-up study on the clinical significance of anti-neuronal antibodies in acute psychiatric disorders. Sci. Rep. 10, 35. https://doi.org/10.1038/s41598-019-56934-6

Scott, K.E., Mann, R.S., Schormans, A.L., Schmid, S., Allman, B.L., 2022. Hyperexcitable and Immature-Like Neuronal Activity in the Auditory Cortex of Adult Rats Lacking

the Language-Linked CNTNAP2 Gene. Cereb. Cortex N. Y. N 1991 bhab517. https://doi.org/10.1093/cercor/bhab517

Scott, R., Sánchez-Aguilera, A., van Elst, K., Lim, L., Dehorter, N., Bae, S.E., Bartolini, G., Peles, E., Kas, M.J.H., Bruining, H., Marín, O., 2019. Loss of Cntnap2 Causes Axonal Excitability Deficits, Developmental Delay in Cortical Myelination, and Abnormal Stereotyped Motor Behavior. Cereb. Cortex N. Y. N 1991 29, 586–597. https://doi.org/10.1093/cercor/bhx341

Sehested, L.T., Møller, R.S., Bache, I., Andersen, N.B., Ullmann, R., Tommerup, N., Tümer, Z., 2010. Deletion of 7q34-q36.2 in two siblings with mental retardation, language delay, primary amenorrhea, and dysmorphic features. Am. J. Med. Genet. A. 152A, 3115–3119. https://doi.org/10.1002/ajmg.a.33476

Selimbeyoglu, A., Kim, C.K., Inoue, M., Lee, S.Y., Hong, A.S.O., Kauvar, I., Ramakrishnan, C., Fenno, L.E., Davidson, T.J., Wright, M., Deisseroth, K., 2017. Modulation of prefrontal cortex excitation/inhibition balance rescues social behavior in CNTNAP2-deficient mice. Sci. Transl. Med. 9, eaah6733. https://doi.org/10.1126/scitranslmed.aah6733

Seok, J., Warren, H.S., Cuenca, A.G., Mindrinos, M.N., Baker, H.V., Xu, W., Richards, D.R., McDonald-Smith, G.P., Gao, H., Hennessy, L., Finnerty, C.C., López, C.M., Honari, S., Moore, E.E., Minei, J.P., Cuschieri, J., Bankey, P.E., Johnson, J.L., Sperry, J., Nathens, A.B., Billiar, T.R., West, M.A., Jeschke, M.G., Klein, M.B., Gamelli, R.L., Gibran, N.S., Brownstein, B.H., Miller-Graziano, C., Calvano, S.E., Mason, P.H., Cobb, J.P., Rahme, L.G., Lowry, S.F., Maier, R.V., Moldawer, L.L., Herndon, D.N., Davis, R.W., Xiao, W., Tompkins, R.G., Inflammation and Host Response to Injury, Large Scale Collaborative Research Program, 2013. Genomic responses in mouse models poorly mimic human inflammatory diseases. Proc. Natl. Acad. Sci. U. S. A. 110, 3507–3512. https://doi.org/10.1073/pnas.1222878110

Shepherd, G.M.G., 2013. Corticostriatal connectivity and its role in disease. Nat. Rev. Neurosci. 14, 278–291. https://doi.org/10.1038/nrn3469

Shi, Y., Sun, L., Wang, M., Liu, J., Zhong, S., Li, R., Li, P., Guo, L., Fang, A., Chen, R., Ge, W.-P., Wu, Q., Wang, X., 2020. Vascularized human cortical organoids (vOrganoids) model cortical development in vivo. PLoS Biol. 18, e3000705. https://doi.org/10.1371/journal.pbio.3000705

Silverstein, A.M., 1996. Paul Ehrlich: the founding of pediatric immunology. Cell. Immunol. 174, 1–6. https://doi.org/10.1006/cimm.1996.0286

Simister, N.E., Mostov, K.E., 1989. An Fc receptor structurally related to MHC class I antigens. Nature 337, 184–187. https://doi.org/10.1038/337184a0

Simons, M., Trajkovic, K., 2006. Neuron-glia communication in the control of oligodendrocyte function and myelin biogenesis. J. Cell Sci. 119, 4381–4389. https://doi.org/10.1242/jcs.03242

Singer, H.S., Morris, C., Gause, C., Pollard, M., Zimmerman, A.W., Pletnikov, M., 2009. Prenatal exposure to antibodies from mothers of children with autism produces neurobehavioral alterations: A pregnant dam mouse model. J. Neuroimmunol. 211, 39–48. https://doi.org/10.1016/j.jneuroim.2009.03.011

Singer, H.S., Morris, C.M., Gause, C.D., Gillin, P.K., Crawford, S., Zimmerman, A.W., 2008. Antibodies against fetal brain in sera of mothers with autistic children. J. Neuroimmunol. 194, 165–172. https://doi.org/10.1016/j.jneuroim.2007.11.004

Sivitilli, A.A., Gosio, J.T., Ghoshal, B., Evstratova, A., Trcka, D., Ghiasi, P., Hernandez, J.J., Beaulieu, J.M., Wrana, J.L., Attisano, L., 2020. Robust production of uniform human cerebral organoids from pluripotent stem cells. Life Sci. Alliance 3, e202000707. https://doi.org/10.26508/lsa.202000707

Sloan, S.A., Andersen, J., Paşca, A.M., Birey, F., Paşca, S.P., 2018. Generation and assembly of human brain region-specific three-dimensional cultures. Nat. Protoc. 13, 2062–2085. https://doi.org/10.1038/s41596-018-0032-7

Smith, K.R., Damiano, J., Franceschetti, S., Carpenter, S., Canafoglia, L., Morbin, M., Rossi, G., Pareyson, D., Mole, S.E., Staropoli, J.F., Sims, K.B., Lewis, J., Lin, W.-L., Dickson, D.W., Dahl, H.-H., Bahlo, M., Berkovic, S.F., 2012. Strikingly different clinicopathological phenotypes determined by progranulin-mutation dosage. Am. J. Hum. Genet. 90, 1102–1107. https://doi.org/10.1016/j.ajhg.2012.04.021

Sohal, V.S., Rubenstein, J.L.R., 2019. Excitation-inhibition balance as a framework for investigating mechanisms in neuropsychiatric disorders. Mol. Psychiatry 24, 1248–1257. https://doi.org/10.1038/s41380-019-0426-0

Song, L., Yuan, X., Jones, Z., Griffin, K., Zhou, Y., Ma, T., Li, Y., 2019a. Assembly of Human Stem Cell-Derived Cortical Spheroids and Vascular Spheroids to Model 3-D Brain-like Tissues. Sci. Rep. 9, 5977. https://doi.org/10.1038/s41598-019-42439-9

Song, L., Yuan, X., Jones, Z., Vied, C., Miao, Y., Marzano, M., Hua, T., Sang, Q.-X.A., Guan, J., Ma, T., Zhou, Y., Li, Y., 2019b. Functionalization of Brain Region-specific Spheroids with Isogenic Microglia-like Cells. Sci. Rep. 9, 11055. https://doi.org/10.1038/s41598-019-47444-6

Strauss, K.A., Puffenberger, E.G., Huentelman, M.J., Gottlieb, S., Dobrin, S.E., Parod, J.M., Stephan, D.A., Morton, D.H., 2006. Recessive symptomatic focal epilepsy and mutant contactin-associated protein-like 2. N. Engl. J. Med. 354, 1370–1377. https://doi.org/10.1056/NEJMoa052773

Takahashi, K., Tanabe, K., Ohnuki, M., Narita, M., Ichisaka, T., Tomoda, K., Yamanaka, S., 2007. Induction of pluripotent stem cells from adult human fibroblasts by defined factors. Cell 131, 861–872. https://doi.org/10.1016/j.cell.2007.11.019

Takahashi, K., Yamanaka, S., 2006. Induction of pluripotent stem cells from mouse embryonic and adult fibroblast cultures by defined factors. Cell 126, 663–676. https://doi.org/10.1016/j.cell.2006.07.024

Tanabe, Y., Fujita-Jimbo, E., Momoi, M.Y., Momoi, T., 2015. CASPR2 forms a complex with GPR37 via MUPP1 but not with GPR37(R558Q), an autism spectrum disorder-related mutation. J. Neurochem. 134, 783–793. https://doi.org/10.1111/jnc.13168

Tanaka, Y., Cakir, B., Xiang, Y., Sullivan, G.J., Park, I.-H., 2020. Synthetic Analyses of Single-Cell Transcriptomes from Multiple Brain Organoids and Fetal Brain. Cell Rep. 30, 1682-1689.e3. https://doi.org/10.1016/j.celrep.2020.01.038

Tatavarty, V., Sun, Q., Turrigiano, G.G., 2013. How to Scale Down Postsynaptic Strength. J. Neurosci. 33, 13179–13189. https://doi.org/10.1523/JNEUROSCI.1676-13.2013

Thomson, J.A., Itskovitz-Eldor, J., Shapiro, S.S., Waknitz, M.A., Swiergiel, J.J., Marshall, V.S., Jones, J.M., 1998. Embryonic stem cell lines derived from human blastocysts. Science 282, 1145–1147. https://doi.org/10.1126/science.282.5391.1145

Ting, J.T., Peça, J., Feng, G., 2012. Functional consequences of mutations in postsynaptic scaffolding proteins and relevance to psychiatric disorders. Annu. Rev. Neurosci. 35, 49–71. https://doi.org/10.1146/annurev-neuro-062111-150442

Traka, M., Goutebroze, L., Denisenko, N., Bessa, M., Nifli, A., Havaki, S., Iwakura, Y., Fukamauchi, F., Watanabe, K., Soliven, B., Girault, J.-A., Karagogeos, D., 2003. Association of TAG-1 with Caspr2 is essential for the molecular organization of juxtaparanodal regions of myelinated fibers. J. Cell Biol. 162, 1161–1172. https://doi.org/10.1083/jcb.200305078

Trujillo, C.A., Gao, R., Negraes, P.D., Gu, J., Buchanan, J., Preissl, S., Wang, A., Wu, W., Haddad, G.G., Chaim, I.A., Domissy, A., Vandenberghe, M., Devor, A., Yeo, G.W., Voytek, B., Muotri, A.R., 2019. Complex Oscillatory Waves Emerging from Cortical Organoids Model Early Human Brain Network Development. Cell Stem Cell 25, 558-569.e7. https://doi.org/10.1016/j.stem.2019.08.002

Turrigiano, G.G., 2017. The dialectic of Hebb and homeostasis. Philos. Trans. R. Soc. Lond. B. Biol. Sci. 372, 20160258. https://doi.org/10.1098/rstb.2016.0258

van Sonderen, A., Ariño, H., Petit-Pedrol, M., Leypoldt, F., Körtvélyessy, P., Wandinger, K.-P., Lancaster, E., Wirtz, P.W., Schreurs, M.W.J., Sillevis Smitt, P.A.E., Graus, F., Dalmau, J., Titulaer, M.J., 2016. The clinical spectrum of Caspr2 antibody-associated disease. Neurology 87, 521–528. https://doi.org/10.1212/WNL.0000000000002917

van Swieten, J.C., Heutink, P., 2008. Mutations in progranulin (GRN) within the spectrum of clinical and pathological phenotypes of frontotemporal dementia. Lancet Neurol. 7, 965–974. https://doi.org/10.1016/S1474-4422(08)70194-7

Vangipuram, M., Ting, D., Kim, S., Diaz, R., Schüle, B., 2013. Skin punch biopsy explant culture for derivation of primary human fibroblasts. J. Vis. Exp. JoVE e3779. https://doi.org/10.3791/3779

Varea, O., Martin-de-Saavedra, M.D., Kopeikina, K.J., Schürmann, B., Fleming, H.J., Fawcett-Patel, J.M., Bach, A., Jang, S., Peles, E., Kim, E., Penzes, P., 2015. Synaptic abnormalities and cytoplasmic glutamate receptor aggregates in contactin associated protein-like 2/Caspr2 knockout neurons. Proc. Natl. Acad. Sci. U. S. A. 112, 6176–6181. https://doi.org/10.1073/pnas.1423205112

Varga, E., Nemes, C., Bock, I., Táncos, Z., Berzsenyi, S., Lévay, G., Román, V., Kobolák, J., Dinnyés, A., 2017. Establishment of an induced pluripotent stem cell (iPSC) line from a 9-year old male with autism spectrum disorder (ASD). Stem Cell Res. 21, 19–22. https://doi.org/10.1016/j.scr.2017.03.013

Velasco, S., Kedaigle, A.J., Simmons, S.K., Nash, A., Rocha, M., Quadrato, G., Paulsen, B., Nguyen, L., Adiconis, X., Regev, A., Levin, J.Z., Arlotta, P., 2019. Individual brain organoids reproducibly form cell diversity of the human cerebral cortex. Nature 570, 523–527. https://doi.org/10.1038/s41586-019-1289-x

Verkerk, A.J.M.H., Mathews, C.A., Joosse, M., Eussen, B.H.J., Heutink, P., Oostra, B.A., Tourette Syndrome Association International Consortium for Genetics, 2003. CNTNAP2 is disrupted in a family with Gilles de la Tourette syndrome and obsessive compulsive disorder. Genomics 82, 1–9. https://doi.org/10.1016/s0888-7543(03)00097-1

Vernes, S.C., Newbury, D.F., Abrahams, B.S., Winchester, L., Nicod, J., Groszer, M., Alarcón, M., Oliver, P.L., Davies, K.E., Geschwind, D.H., Monaco, A.P., Fisher, S.E., 2008. A functional genetic link between distinct developmental language disorders. N. Engl. J. Med. 359, 2337–2345. https://doi.org/10.1056/NEJMoa0802828

Vogt, D., Cho, K.K.A., Shelton, S.M., Paul, A., Huang, Z.J., Sohal, V.S., Rubenstein, J.L.R., 2018. Mouse Cntnap2 and Human CNTNAP2 ASD Alleles Cell Autonomously Regulate PV+ Cortical Interneurons. Cereb. Cortex N. Y. N 1991 28, 3868–3879. https://doi.org/10.1093/cercor/bhx248

Watanabe, K., Kamiya, D., Nishiyama, A., Katayama, T., Nozaki, S., Kawasaki, H., Watanabe, Y., Mizuseki, K., Sasai, Y., 2005. Directed differentiation of telencephalic precursors from embryonic stem cells. Nat. Neurosci. 8, 288–296. https://doi.org/10.1038/nn1402

Watanabe, K., Ueno, M., Kamiya, D., Nishiyama, A., Matsumura, M., Wataya, T., Takahashi, J.B., Nishikawa, Satomi, Nishikawa, Shin-ichi, Muguruma, K., Sasai, Y., 2007. A ROCK inhibitor permits survival of dissociated human embryonic stem cells. Nat. Biotechnol. 25, 681–686. https://doi.org/10.1038/nbt1310

Watanabe, M., Buth, J.E., Vishlaghi, N., de la Torre-Ubieta, L., Taxidis, J., Khakh, B.S., Coppola, G., Pearson, C.A., Yamauchi, K., Gong, D., Dai, X., Damoiseaux, R., Aliyari, R., Liebscher, S., Schenke-Layland, K., Caneda, C., Huang, E.J., Zhang, Y., Cheng, G., Geschwind, D.H., Golshani, P., Sun, R., Novitch, B.G., 2017. Self-Organized Cerebral Organoids with Human-Specific Features Predict Effective Drugs to Combat Zika Virus Infection. Cell Rep. 21, 517–532. https://doi.org/10.1016/j.celrep.2017.09.047

Weiss, P., Taylor, A.C., 1960. RECONSTITUTION OF COMPLETE ORGANS FROM SINGLE-CELL SUSPENSIONS OF CHICK EMBRYOS IN ADVANCED STAGES OF DIFFERENTIATION. Proc. Natl. Acad. Sci. U. S. A. 46, 1177–1185.

Wen, Z., Nguyen, H.N., Guo, Z., Lalli, M.A., Wang, X., Su, Y., Kim, N.-S., Yoon, K.-J., Shin, J., Zhang, C., Makri, G., Nauen, D., Yu, H., Guzman, E., Chiang, C.-H., Yoritomo, N., Kaibuchi, K., Zou, J., Christian, K.M., Cheng, L., Ross, C.A., Margolis, R.L., Chen, G., Kosik, K.S., Song, H., Ming, G., 2014. Synaptic dysregulation in a human iPS cell model of mental disorders. Nature 515, 414–418. https://doi.org/10.1038/nature13716

Wilson, H.V., 1907. A NEW METHOD BY WHICH SPONGES MAY BE ARTIFICIALLY REARED. Science 25, 912–915. https://doi.org/10.1126/science.25.649.912

Xiang, Y., Tanaka, Y., Cakir, B., Patterson, B., Kim, K.-Y., Sun, P., Kang, Y.-J., Zhong, M., Liu, X., Patra, P., Lee, S.-H., Weissman, S.M., Park, I.-H., 2019. hESC-Derived Thalamic Organoids Form Reciprocal Projections When Fused with Cortical Organoids. Cell Stem Cell 24, 487-497.e7. https://doi.org/10.1016/j.stem.2018.12.015

Xiang, Y., Tanaka, Y., Patterson, B., Kang, Y.-J., Govindaiah, G., Roselaar, N., Cakir, B., Kim, K.-Y., Lombroso, A.P., Hwang, S.-M., Zhong, M., Stanley, E.G., Elefanty, A.G., Naegele, J.R., Lee, S.-H., Weissman, S.M., Park, I.-H., 2017. Fusion of Regionally Specified hPSC-Derived Organoids Models Human Brain Development and Interneuron Migration. Cell Stem Cell 21, 383-398.e7. https://doi.org/10.1016/j.stem.2017.07.007

Xie, G., Harrison, J., Clapcote, S.J., Huang, Y., Zhang, J.-Y., Wang, L.-Y., Roder, J.C., 2010. A new Kv1.2 channelopathy underlying cerebellar ataxia. J. Biol. Chem. 285, 32160–32173. https://doi.org/10.1074/jbc.M110.153676

Xu, R., Boreland, A.J., Li, X., Erickson, C., Jin, M., Atkins, C., Pang, Z.P., Daniels, B.P., Jiang, P., 2021. Developing human pluripotent stem cell-based cerebral organoids with a controllable microglia ratio for modeling brain development and pathology. Stem Cell Rep. 16, 1923–1937. https://doi.org/10.1016/j.stemcr.2021.06.011

Yamanaka, S., 2007. Strategies and new developments in the generation of patient-specific pluripotent stem cells. Cell Stem Cell 1, 39–49. https://doi.org/10.1016/j.stem.2007.05.012

Yao, Y.-N., Wang, M.-D., Tang, X.-C., Wu, B., Sun, H.-M., 2020. Reduced plasma progranulin levels are associated with the severity of Parkinson's disease. Neurosci. Lett. 725, 134873. https://doi.org/10.1016/j.neulet.2020.134873

Yoon, S.-J., Elahi, L.S., Paşca, A.M., Marton, R.M., Gordon, A., Revah, O., Miura, Y., Walczak, E.M., Holdgate, G.M., Fan, H.C., Huguenard, J.R., Geschwind, D.H., Pașca, S.P., 2019. Reliability of human cortical organoid generation. Nat. Methods 16, 75–78. https://doi.org/10.1038/s41592-018-0255-0

Yu, J., Vodyanik, M.A., Smuga-Otto, K., Antosiewicz-Bourget, J., Frane, J.L., Tian, S., Nie, J., Jonsdottir, G.A., Ruotti, V., Stewart, R., Slukvin, I.I., Thomson, J.A., 2007. Induced pluripotent stem cell lines derived from human somatic cells. Science 318, 1917–1920. https://doi.org/10.1126/science.1151526

Zaehres, H., Lensch, M.W., Daheron, L., Stewart, S.A., Itskovitz-Eldor, J., Daley, G.Q., 2005. High-efficiency RNA interference in human embryonic stem cells. Stem Cells Dayt. Ohio 23, 299–305. https://doi.org/10.1634/stemcells.2004-0252

Zafeiriou, M.-P., Bao, G., Hudson, J., Halder, R., Blenkle, A., Schreiber, M.-K., Fischer, A., Schild, D., Zimmermann, W.-H., 2020. Developmental GABA polarity switch and neuronal plasticity in Bioengineered Neuronal Organoids. Nat. Commun. 11, 3791. https://doi.org/10.1038/s41467-020-17521-w

Zhang, J., Velmeshev, D., Hashimoto, K., Huang, Y.-H., Hofmann, J.W., Shi, X., Chen, J., Leidal, A.M., Dishart, J.G., Cahill, M.K., Kelley, K.W., Liddelow, S.A., Seeley, W.W., Miller, B.L., Walther, T.C., Farese, R.V., Taylor, J.P., Ullian, E.M., Huang, B., Debnath, J., Wittmann, T., Kriegstein, A.R., Huang, E.J., 2020. Neurotoxic microglia promote TDP-43 proteinopathy in progranulin deficiency. Nature 588, 459–465. https://doi.org/10.1038/s41586-020-2709-7

Zhang, S.C., Wernig, M., Duncan, I.D., Brüstle, O., Thomson, J.A., 2001. In vitro differentiation of transplantable neural precursors from human embryonic stem cells. Nat. Biotechnol. 19, 1129–1133. https://doi.org/10.1038/nbt1201-1129

Zhao, X., Bhattacharyya, A., 2018. Human Models Are Needed for Studying Human Neurodevelopmental Disorders. Am. J. Hum. Genet. 103, 829–857. https://doi.org/10.1016/j.ajhg.2018.10.009

Zhao, X., Tang, Z., Zhang, H., Atianjoh, F.E., Zhao, J.-Y., Liang, L., Wang, W., Guan, X., Kao, S.-C., Tiwari, V., Gao, Y.-J., Hoffman, P.N., Cui, H., Li, M., Dong, X., Tao, Y.-X., 2013. A long noncoding RNA contributes to neuropathic pain by silencing Kcna2 in primary afferent neurons. Nat. Neurosci. 16, 1024–1031. https://doi.org/10.1038/nn.3438

Zhong, X., Gutierrez, C., Xue, T., Hampton, C., Vergara, M.N., Cao, L.-H., Peters, A., Park, T.S., Zambidis, E.T., Meyer, J.S., Gamm, D.M., Yau, K.-W., Canto-Soler, M.V., 2014. Generation of three-dimensional retinal tissue with functional photoreceptors from human iPSCs. Nat. Commun. 5, 4047. https://doi.org/10.1038/ncomms5047